

ANALYSIS OF GENES INVOLVED IN DEVELOPMENTAL PATHWAYS IN TWO
BASIDIOMYCETOUS FUNGI, *USTILAGO MAYDIS* AND *SCLEROTIUM ROLFSII*

by

JOHANNA ELISE TAKACH

(Under the Direction of Scott Gold)

ABSTRACT

Fungi rely on complex molecular pathways to orchestrate the physical changes necessary to survive and reproduce. In pathogenic fungi, these pathways can also mediate host infection. Identification of the factors that coordinate these changes in morphology is critical for improved management of fungal pathogens. To this end, genetic factors involved in developmental and morphological change in *Ustilago maydis* and *Sclerotium rolfsii* were investigated.

In the model system *U. maydis*, the well-characterized cAMP/PKA signaling pathways mediates filamentation in response to environmental cues. Genome analysis identified two potential additional components of the signal cascade. An adenylate cyclase-associated protein (CAP) homolog was detected. Yeast 2-hybrid analysis indicates that the *U. maydis* Cap1 interacts with adenylate cyclase (Uac1). Deletion of *cap1* results in abnormal colony morphology and filamentous cells that revert to budding when treated with exogenous cAMP, similar to *U. maydis* strains with low cAMP production. $\Delta cap1$ strains are reduced in mating ability and pathogenicity. These results suggest that Cap1 positively regulates cAMP production by adenylate cyclase and is required for budding growth.

A genome search also revealed the presence of a second cAMP binding domain, in addition to Ubc1, the only previously identified target of cAMP in *U. maydis*. The gene encoding the domain, *cab1*, was deleted, but no morphological, mating, or pathogenicity phenotypes were observed. $\Delta cab1$ strains had a severe growth defect in medium enriched with yeast extract. These results indicate that *cab1* has little to no role in the cAMP signaling cascade.

S. rolfssii produces small sclerotia that serve as overwintering structures and inocula. Little is known about the genetic factors involved in sclerotial development. To this end, two cDNA libraries were created using Suppressive Subtractive Hybridization PCR (SSH) and screened to identify genes differentially expressed during sclerotium formation and development. Of the 53 unique sequences identified, 31 were homologous to expressed sequences in fungal systems, including a lectin, cytochrome P450, and two ribosomal proteins. Relative gene expression was measured using quantitative real-time PCR, with a subset further verified by northern blot analysis. The results from this study will provide a foundation for future genetic studies in *S. rolfssii*.

INDEX WORDS: *Ustilago maydis*, Dimorphic transition, cAMP signaling pathway, Adenylate Cyclase-Associated Protein (CAP), *Sclerotium rolfssii*, Differential gene expression, Sclerotia, Suppressive Subtractive Hybridization PCR (SSH)

ANALYSIS OF GENES INVOLVED IN DEVELOPMENTAL PATHWAYS IN TWO
BASIDIOMYCETOUS FUNGI, *USTILAGO MAYDIS* AND *SCLEROTIUM ROLFSSII*

by

JOHANNA ELISE TAKACH

B.S., The University of Kentucky, 2002

A Dissertation Submitted to the Graduate Faculty of The University of Georgia in Partial
Fulfillment of the Requirements for the Degree

DOCTOR OF PHILOSOPHY

ATHENS, GEORGIA

2009

© 2009

Johanna Elise Takach

All Rights Reserved

ANALYSIS OF GENES INVOLVED IN DEVELOPMENTAL PATHWAYS IN TWO
BASIDIOMYCETOUS FUNGI, *USTILAGO MAYDIS* AND *SCLEROTIUM ROLFII*

by

JOHANNA ELISE TAKACH

Major Professor: Scott Gold

Committee: Timothy Brenneman
Sarah Covert
Michelle Momany

Electronic Version Approved:

Maureen Grasso
Dean of the Graduate School
The University of Georgia
December 2009

DEDICATION

To my parents. Thanks for everything. This “three-lip” is for you!

ACKNOWLEDGEMENTS

As with the Academy Awards, there are too many people to thank and not enough time or space to do so. Many people have been instrumental in the creation of this dissertation and research described herein. My committee members, Dr. Scott Gold, Dr. Sarah Covert, Dr. Michelle Momany, Dr. Tim Brenneman, provided critical insight into my research questions, methods, and manuscripts as well as kind words when the going got tough. I am indebted to my current (and forever) major adviser Scott Gold for his guidance, personal support, and sense of humor throughout my graduate education. Many thanks also go to the members of the Gold lab, Dr. Dave Andrews, Dr. Zahi Paz, Dr. Emir Islamovic, Dr. Mariola Garcia-Pedrajas, Dr. Steve Klosterman, the newly-minted Dr. Marina Nadal, Nadia Chacko and Angelino, who gave me advice and supplies when I needed them, as well as ice cream, coffee, and occasional language lessons.

I also need to thank my friends and fellow grad students. The newly-minted Dr. Joe Lowery, Dr. Lorna Putnam, the soon-to-be Dr. Caitlin Powell, and the soon-to-be Dr. Katherine Mills-Lujan all gave me an outlet for my frustrations and kind calm words to motivate me to finish—I am proud of all of us! I am also grateful to my fellow Plant Path graduate students and members of SAPPS who have been incredibly supportive throughout the years.

Although I have dedicated this entire work to my parents, I'd be remiss to not mention them again for their unflagging support, even when they didn't know what my research entailed. I also need to thank my 'little' brother Jackson for being supportive and just outright awesome during my times of need.

And last but not least, my friends who have grown into family. Without your unfailing support and encouragement, I would have been a total mess...like Britney Spears. So to Jen, Jessie, Josh, Mel, Sarah, Amy, Heather, Les, Fievel, Courtney, Lorna, Jas, Hank, Dave, both Kevins, Kameka, Steph, Donna, Andrew, Elizabeth, Ginny, Jeremy and Erika...Thanks.

TABLE OF CONTENTS

	Page
ACKNOWLEDGEMENTS	v
CHAPTER	
1 INTRODUCTION	1
Literature Cited.....	4
2 LITERATURE REVIEW	5
<i>Ustilago maydis</i>	5
<i>Sclerotium rolfsii</i>	12
Literature Cited.....	16
3 IDENTIFICATION AND CHARACTERIZATION OF CAP1, THE ADENYLATE CYCLASE-ASSOCIATED PROTEIN HOMOLOG IN <i>USTILAGO MAYDIS</i>	23
Abstract	24
Introduction	24
Results	27
Discussion	30
Experimental Procedures.....	32
References	35
4 IDENTIFICATION OF CAB1, A POTENTIAL cAMP BINDING PROTEIN AND NEUROPATHY TARGET ESTERASE (NTE) HOMOLOG IN <i>USTILAGO MAYDIS</i>	48

Introduction	48
Results	50
Discussion	52
Materials and Methods	54
Literature Cited.....	58
5 IDENTIFICATION AND CHARACTERIZATION OF GENES DIFFERENTIALLY EXPRESSED DURING SCLEROTIUM FORMATION IN <i>SCLEROTIUM</i> <i>ROLFSII</i>	70
Abstract	71
Introduction	72
Materials and Methods	73
Results	79
Discussion	82
Literature Cited.....	85
6 CONCLUSIONS	96
APPENDIX.....	99
A GENBANK ACCESSION NUMBERS FOR SEQUENCES IDENTIFIED IN CHAPTER 5.....	100

CHAPTER 1

INTRODUCTION

Ustilago maydis and *Sclerotium rolfii* are two distantly related basidiomycete fungi that cause economically important crop diseases in the United States. *Ustilago maydis*, the causal agent of corn smut, is a model organism for the study of genetics, fungal mating determinants, fungal dimorphism, signaling pathways and pathogenesis. Although not well characterized genetically, *Sclerotium rolfii* is a potentially devastating plant pathogen that infects a large number of economically important crops. Although these organisms differ in growth pattern, host range, and habitat, both rely upon complex molecular pathways to alter their morphology during development. Identification of the genes and pathways that govern these changes and their consequences will give further insight into fungal cellular processes.

U. maydis has emerged as a basidiomycete model system for the study of signaling pathways affecting dimorphism and disease development (for review, see Klosterman et al, 2007). Two interconnected signaling pathways mediate the filamentation process: the pheromone responsive MAP kinase cascade and the environment-responsive cAMP/PKA pathway. Proper regulation and function of the cAMP/PKA pathway are required for virulence and pathogenicity of *U. maydis*.

Components of the cAMP/PKA pathway include Gpa3, a G-protein α subunit; Uac1, adenylate cyclase; Ubc1, the PKA regulatory subunit; and Adr1, the PKA catalytic subunit. Mutation of genes upstream of the cAMP signal (*gpa3* or *uac1*) results in a filamentous phenotype that can be rescued by addition of exogenous cAMP (Gold et al, 1994; Krüger et al,

1998). Inactivation of the PKA regulatory subunit, effectively simulating a high level of cAMP by allowing constitutive activation of the PKA catalytic subunit, results in a multiple budding yeast phenotype (Gold et al, 1994). Collectively, these results indicate that the absence of the cAMP signal results in filamentous growth and presence of cAMP promotes budding and suppresses filamentous growth in *U. maydis*.

Currently, Gpa3 is the only identified cAMP/PKA pathway component upstream of adenylate cyclase. However, in yeast and other fungal systems, cAMP signaling is mediated by multiple proteins, including an adenylate cyclase-associated protein (CAP). CAP homologs play a significant role in the cAMP-mediated dimorphic switch required for pathogenesis in two human pathogens, *Candida albicans* and *Cryptococcus neoformans* (Bahn and Sundstrom, 2001; Bahn et al, 2004). Although no previous reports have identified a CAP homolog in *U. maydis*, the identification and characterization of such a protein would result in a more complete understanding of cAMP signal production and its roles in morphology and cellular development.

Just as Gpa3 is the only previously identified upstream activator of adenylate cyclase in *U. maydis*, Ubc1 is the only identified target of cAMP. However, two lines of evidence suggest that additional components of the *U. maydis* cAMP pathway exist and can influence cellular morphology. Wild type strains of *U. maydis* induce pheromone gene transcription in the presence of 6 mM cAMP and reduce pheromone gene expression in the presence of 15 mM cAMP (Krüger et al, 1998). This dose-dependent effect of cAMP on *mfa* transcription was also observed in a $\Delta ubc1$ strain (Hartmann et al, 1999). The second line of evidence involves the pH-mediated filamentation pathway. Haploid cells grow as filaments when introduced to acidic medium, but the addition of 25 mM exogenous cAMP results in a reversion to the budding phenotype (Martinez-Espinoza et al, 2004). $\Delta ubc1$ mutants also filament when grown in acidic

conditions and, although lacking the only known protein to interact with cAMP, are restored to budding growth with the addition of 25 mM cAMP. These results suggest the existence of an alternate rPKA subunit or the presence of another factor that interacts with cAMP.

Unlike the *U. maydis* system, *S. rolfisii* does not have a wide range of molecular tools available for study. It is, however, an exceedingly important pathogen of peanut. *S. rolfisii* is a soil-born basidiomycete that caused a 10% reduction in crop value and cost Georgia farmers \$44.4 million in 2007 (Martinez, 2008). Current management strategies include crop rotation with grasses and cotton, planting resistant peanut varieties, and chemical control. These strategies have limited effectiveness due to the wide host range of the pathogen and the costs associated with fungicide applications.

S. rolfisii spreads primarily in the form of small melanized sclerotia. These resistant structures germinate midseason under wet or humid conditions, producing fluffy white mycelia on aboveground portions of plant hosts. The mycelium grows until it exhausts the nutrient supply and then produces copious sclerotia, which serve as both primary and secondary inoculum. The sclerotia allow the pathogen to overwinter in the soil, thus playing a crucial role in the persistence of disease potential. Although many studies have been devoted to identifying factors that stimulate production of sclerotia, little is known about the genetic factors involved in sclerotium formation and development.

The goal of this study was to fill gaps in knowledge of the genetic basis of developmental and morphological changes in *U. maydis* and *S. rolfisii*. The specific objectives were to:

1. Identify and characterize a *U. maydis* CAP homolog, a potential modulator of cAMP production by adenylate cyclase.
2. Identify and characterize genes that encode cAMP binding domains in *U. maydis*.

3. Identify genes differentially regulated in *S. rolfsii* during sclerotium formation and development.

LITERATURE CITED

1. Bahn, Y. S., and P. Sundstrom. 2001. CAP1, an adenylate cyclase-associated protein gene, regulates bud-hypha transitions, filamentous growth, and cyclic AMP levels and is required for virulence of *Candida albicans*. *J. Bacteriol.* 183 (10):3211-3223.
2. Bahn, Y. S., J. K. Hicks, S. S. Giles, G. M. Cox, and J. Heitman. 2004. Adenylyl cyclase-associated protein Aca1 regulates virulence and differentiation of *Cryptococcus neoformans* via the cyclic AMP-protein kinase A cascade. *Eukaryot. Cell.* 3 (6):1476-1491.
3. Gold, S., G. Duncan, K. Barrett, and J. Kronstad. 1994. cAMP regulates morphogenesis in the fungal pathogen *Ustilago maydis*. *Genes Dev.* 8 (23):2805-2816.
4. Hartmann, H. A., J. Krüger, F. Lottspeich, and R. Kahmann. 1999. Environmental signals controlling sexual development of the corn smut fungus *Ustilago maydis* through the transcriptional regulator prf1. *Plant Cell.* 11 (7):1293-1305.
5. Klosterman, SJ, MH Perlin, M Garcia-Pedrajas, SF Covert, and SE Gold. 2007. Genetics of morphogenesis and pathogenic development of *Ustilago maydis*. In *Fungal Genomics*, edited by J. C. Dunlap. St. Louis, MO: Academic Press.
6. Krüger, J., G. Loubradou, E. Regenfelder, A. Hartmann, and R. Kahmann. 1998. Crosstalk between cAMP and pheromone signalling pathways in *Ustilago maydis*. *Mol. Gen. Genet.* 260 (2-3):193-198.
7. Martinez, A. 2008. Georgia plant disease lost estimates. Coop. Ext. Ser. Bull. 41-10, University of Georgia, Athens.
8. Martinez-Espinoza, A. D., J. Ruiz-Herrera, C. G. Leon, and S. E. Gold. 2004. MAP kinase and cAMP signaling pathways modulate the pH-induced yeast-to-mycelium dimorphic transition in the corn smut fungus *Ustilago maydis*. *Curr. Microbiol.* 49 (4):274-281.

CHAPTER 2

LITERATURE REVIEW

The phylum Basidiomycota in the kingdom Fungi includes a wide variety of plant pathogens, including smuts (order Ustilaginales), rusts (order Uredinales), and assorted root/stem rotting fungi. *Ustilago maydis*, the causal agent of corn smut, has emerged as a basidiomycete model system for the study of signaling pathways affecting filamentation and disease development (for review, see Klosterman et al, 2007). In contrast, very little is known about genetic determinants involved in disease development of the filamentous fungus *Sclerotium rolfsii*, a plant pathogen that causes millions of dollars annually in damage to economically important crops in the southeastern United States. The two organisms are similar, however, in that both require significant morphological changes to complete their life and disease cycles. This chapter will address the current knowledge regarding the biology of these pathogens.

Ustilago maydis

***U. maydis* biology.** The complex life cycle of *U. maydis* includes a haploid budding phase, a dikaryotic filamentous phase, and a brief diploid phase. In spring or early summer, diploid teliospores germinate to produce basidia that in turn produce haploid sporidia. The cigar-shaped sporidia are saprobic and can reproduce asexually by budding (Banuett, 1995). Two compatible sporidia (i.e. containing different alleles at the *a* and *b* mating type locus) fuse to produce a dikaryotic hypha that can invade host cells (Christensen, 1963). Although cellular

fusion events can be observed on laboratory media or the surface of host tissues, the filamentous dikaryon grows well only within host tissues, suggesting that host signaling is essential for dikaryon stability (Banuett, 1995). The dikaryon directly penetrates host tissues and grows intra- and intercellularly (Snetselaar and Mims, 1992; Snetselaar and Mims, 1994; Banuett and Herskowitz, 1996). The host-pathogen interactions trigger hyperplasia and hypertrophy of host cells, resulting in gall formation. As the galls mature, hyphae proliferate within the tissues and nuclei fuse during the formation of diploid teliospores (Banuett and Herskowitz, 1996). Teliospores overwinter within plant detritus until the following spring or summer.

The transition from haploid budding cells to dikaryotic hyphae is required for disease development. The fusion of two compatible sporidia and subsequent filament formation can be observed on specialized media in the laboratory, allowing the fusion event to be a morphological indicator for the study of genetic factors involved in mating and pathogenic development. Additionally, the *U. maydis* genome became publicly available in 2003, further enhancing the usefulness of this system as a model for the study of signaling pathways involved in morphological development (Kamper et al, 2006).

Dimorphism and signaling pathways in *U. maydis*. Morphogenesis in *U. maydis* is coordinated by both genetic and environmental inputs. Fusion of haploid budding cells and subsequent dikaryon formation is controlled genetically by the *a* and *b* mating type loci (Holliday, 1961; Banuett, 1995; Rowell, 1955). Filamentous growth of haploid cells can also be triggered by environmental signals that include nutrient and nitrogen deprivation (Kernkamp, 1939; Banuett and Herskowitz, 1994) or exposure to air, acidic pH, or lipids (Gold et al, 1994; Ruiz-Herrera et al, 1995; Klose et al, 2004). Collectively, these factors coordinate cellular morphology through interconnected signaling pathways.

Genetic control of filamentation is mediated by two mating type loci, termed *a* and *b* (Banuett and Herskowitz 1994). The biallelic *a* locus regulates the process of cell fusion and contains genes encoding a pheromone precursor (*mfa*) and a pheromone receptor (*pra*) that binds pheromone molecules secreted by the opposite mating type (Bölker et al, 1992). Pheromone-receptor recognition activates a mitogen-activated protein kinase (MAPK) cascade, resulting in the activation of the transcription factor Prf1 (Hartmann et al, 1996). MAPK phosphorylation of Prf1 is required for differential expression of 57 genes, including the upregulation of the *b* locus genes (Zarnack et al, 2008). The multiallelic *b* locus controls events occurring post-cell fusion, including the establishment of a stable dikaryon and pathogenicity (Puhalla, 1970) as well as inhibition of further mating (Laity et al, 1995). The *b* locus contains genes (*bE* and *bW*) that encode homeodomain proteins that interact when produced from different alleles (Gillissen et al, 1992; Kamper et al, 1995). Haploid strains engineered to express different *bE* and *bW* alleles are able to infect host plants without a mating partner, indicating the fundamental role of the *bE/bW* heterodimer in pathogenic development (Bölker et al, 1995). The *b* protein complex has been demonstrated to bind a *b*-specific promoter element identified in *b*-responsive genes (Romeis et al, 2000; Brachmann et al, 2001). The *bE/bW* heterodimer represses transcription of the pheromone and pheromone receptor genes (*mfa* and *pra*) but increases transcription of genes related to pathogenicity and dikaryon stability (Urban et al, 1996; Scherer et al, 2006).

In addition to the pheromone/receptor signaling pathways, environmental signals also modulate the morphology of *U. maydis* cells. Filamentation of haploid cells due to environmental stimuli is independent of the *b* locus, involves downregulation of the cAMP/PKA pathway, and requires the activity of the pheromone responsive MAP kinase cascade (Gold et al, 1994; Gold et al, 1997; Martinez-Espinoza et al, 2004). Components of the cAMP/PKA

signaling cascade include the $G\alpha$ subunit Gpa3 (Regenfelder et al, 1997; Krüger et al, 1998); adenylate cyclase, Uac1, which catalyzes the formation of cAMP (Barrett et al, 1993; Gold et al, 1994); and the regulatory and catalytic subunits of PKA, Ubc1 and Adr1, respectively (Gold et al, 1994; Gold et al, 1997). The catalytic subunit of PKA phosphorylates Prf1 in a site-specific manner, resulting in increased transcription of *a* and *b* genes (Hartmann et al, 1999; Kaffarnik et al, 2003; Zarnack et al, 2008).

Disruption of the cAMP/PKA pathway in *U. maydis* results in abnormal cellular morphology. Disruption of genes upstream of the cAMP signal (caused by deletion or disruption of *gpa3* or *uac1*) results in a filamentous phenotype that can be rescued by addition of exogenous cAMP (Gold et al, 1994; Krüger et al, 1998). Disruption of the *adr1* gene encoding the catalytic subunit of PKA results in a similar filamentous phenotype but is not remedied by addition of cAMP (Dürrenberger et al, 1998). Inactivation of the PKA regulatory subunit, effectively simulating a high level of cAMP by allowing constitutive activation of the PKA catalytic subunit, results in a multiple budding phenotype (Gold et al, 1994). Collectively, these results indicate that the absence of the cAMP signal results in filamentous growth and presence of cAMP promotes budding and suppresses filamentous growth in *U. maydis*.

Proper regulation and function of the cAMP/PKA pathway are also required for virulence and pathogenicity. Strains downregulated for cAMP signaling, including $\Delta gpa3$, $uac1^-$, and $\Delta adr1$ mutants, do not produce tumors in infected plant tissues (Kronstad, 1997). Strains with constitutively activated cAMP signaling are also defective in disease development. $\Delta ubc1$ mutants produce early symptoms of infection (chlorosis and anthocyanin production), but do not produce tumors (Gold et al, 1997). Strains with a constitutively active $G\alpha$ allele (*gpa3*_{Q206L}) can form tumors *in planta*; however, the fungal development in these plants is severely compromised

(Krüger et al, 2000). These results collectively indicate the integral role of cAMP signaling in fungal proliferation and teliospore formation within galls.

Although much is known about the cAMP signaling cascade in *U. maydis*, there are still significant gaps in knowledge. In other fungal systems, multiple effectors regulate adenylate cyclase activity, including G-proteins and adenylate cyclase-associated proteins (CAPs). Currently, Gpa3 is the only identified cAMP/PKA pathway component upstream of Uac1 in *U. maydis*, and no previous reports have identified additional mediators of cAMP production. Additionally, experimental evidence in the *U. maydis* system suggests that cAMP plays a role independent of Ubc1. Identification of additional components of the cAMP signaling cascade is critical for a full understanding of pathway and its roles in morphology and cellular development.

Adenylate cyclase-associated protein (CAP) as an upstream effector of adenylate cyclase. In *Saccharomyces cerevisiae*, cAMP production is stimulated by both the G-protein Gpa3 and Ras2 (Colombo et al, 1998; Toda et al, 1985). Ras2 activation of adenylate cyclase is mediated by Srv2, an adenylate cyclase-associated protein (CAP) (Fedor-Chaiken et al, 1990; Field et al, 1990). CAP/Srv2 homologs have been identified in all eukaryotic species, although not all family members have been demonstrated to bind adenylate cyclase (Hubberstey and Mottillo, 2002). However, CAP/Srv2 homologs have been demonstrated to bind adenylate cyclase and affect cAMP production in several fungal species, including the dimorphic pathogens *Cryptococcus neoformans* and *Candida albicans*.

CAP/Srv2 function. The CAP/Srv2 protein was identified in *S. cerevisiae* as an adenylate cyclase binding protein and a mediator of RAS2 activation of adenylate cyclase

(Fedor-Chaiken et al, 1990; Field et al, 1990). Disruption of the gene resulted in abnormal cellular morphology (enlarged, fragile cells), temperature sensitivity when grown on synthetic media, inability to grow on a rich medium, sensitivity to nitrogen starvation, and a blocked ability to accumulate cAMP. Constitutive activation of the Ras2/cAMP/PKA pathway suppressed the temperature and nitrogen sensitivity phenotypes but did not affect the morphological changes and inability to grow on rich medium, indicating that CAP/Srv2 has a function unrelated to the Ras2/adenylate cyclase pathway (Field et al, 1990). Gerst and colleagues further explored the bifunctional nature of this protein by showing that expression of the C-terminal region of the protein was sufficient to suppress the abnormal cellular morphology and nutrient sensitivity phenotype and that expression of the N-terminal region alone was necessary to restore the cellular response to Ras2 activation (1991). The C-terminal region was subsequently found to bind monomeric actin *in vitro* and *in vivo*, although this interaction is not required for the cAMP signal transduction function of the N-terminus (Freeman et al, 1995; Yu et al, 1999; Uetz et al, 2000).

Since the initial discovery of this protein in yeast, homologs of CAP/Srv2 have been identified in the genome of all eukaryotic organisms (Hubberstey and Mottillo 2002). Disruption of this gene in other organisms yields varying phenotypes. Deletion or disruption of the CAP/Srv2 gene homologs in *Drosophila* and mammalian cells results in abnormal actin polymerization and defects in actin-dependent processes, including motility and endocytosis (Baum et al, 2000; Bertling et al, 2004). *Dictyostelium discoideum* mutants that produce <5% of the wildtype CAP protein have abnormally large and multinucleate cells that lack polarity and display defects in phototaxis, growth, and endocytosis (Noegel et al, 1999; Noegel et al, 2004). In fungi, deletion mutants have altered cellular morphologies related to disruptions in cAMP

signaling. In *Schizosaccharomyces pombe*, CAP deletion mutants are abnormally large, temperature sensitive cells with abnormal ascus production and overexpression of CAP results in increased cellular cAMP levels (Kawamukai et al, 1992). *C. albicans cap1/cap1* strains bud normally, but are unable to produce the spike of cellular cAMP that precedes germ tube emergence and are defective in bud-hypha transitions, filamentous growth, and virulence (Bahn and Sundstrom, 2001). The *C. neoformans* homolog Aca1 is a positive regulator of adenylate cyclase (Cac1) and required for cAMP-mediated capsule formation and virulence (Bahn et al, 2004).

CAP/Srv2 structure. Members of the CAP protein family contain two conserved regions. The C-terminal domain associates with actin monomers and plays a role in cofilin-mediated actin turnover (Moriyama and Yahara 2002; Bertling et al, 2004; Mattila et al, 2004; Bertling et al, 2007; Quintero-Monzon et al, 2009). Specifically, *S. cerevisiae* Srv2 binds monomeric G-actin with a binding coefficient similar to that of another actin-sequestering protein, thymosin β -4 (Freeman et al, 1995; Weber et al, 1992). CAP/Srv2 proteins also have conserved polyproline regions that are required to bind components of actin-turnover machinery, including Abp1 and profilin in yeast (Bertling et al, 2007; Freeman et al, 1996; Lila and Drubin, 1997; Paunola et al, 2002; Vojtek and Cooper, 1993). This complex promotes cofilin-mediated actin turnover (Mattila et al, 2004; Bertling et al, 2007; Quintero-Monzon et al, 2009).

The N-terminal region is more variable within the CAP/Srv2 family. This portion of the protein has been shown to interact with adenylate cyclase in some fungi (including *S. cerevisiae*, *S. pombe*, and *C. neoformans*) and the cellular slime mold *D. discoideum* but not in animals (Bahn et al, 2004; Gerst et al, 1991; Kawamukai et al, 1992; Hubberstey and Mottillo, 2002; Noegel et al, 2004).

cAMP influence on cellular morphology in the absence of Ubc1. Two lines of evidence suggest that additional components of the *U. maydis* cAMP pathway exist and can influence cellular morphology. Wild type strains of *U. maydis* induce pheromone gene transcription in the presence of 6 mM cAMP and reduce pheromone gene expression in the presence of 15 mM cAMP (Krüger et al, 1998). This dose-dependent effect of cAMP on *mfa* transcription was also observed in a strain of *U. maydis* lacking Ubc1, the only protein known to interact directly with cAMP (Hartmann et al, 1999). These results suggest that a second cAMP pathway, independent of Ubc1, mediates this transcriptional repression. A second line of evidence involves the pH-mediated filamentation pathway. Haploid cells grow as filaments when introduced to acidic medium, but the addition of 25 mM exogenous cAMP results in a reversion to the budding phenotype (Martinez-Espinoza et al, 2004). $\Delta ubc1$ mutants also filament when grown in acidic conditions and, although lacking the only known target of cAMP, are restored to budding growth with the addition of 25 mM cAMP. These results suggest the existence of an alternate rPKA subunit or the presence of another factor that interacts with cAMP.

Sclerotium rolfsii

***S. rolfsii* biology.** *S. rolfsii*, also referred to as white mold or southern blight, is a soil-borne basidiomycete fungus with an extremely wide host range that includes at least 500 plant species in 100 families. Susceptible crop hosts include tomato, pepper, peanut, corn (maize), soybeans, cotton, alfalfa, wheat, and apple. This pathogen also infects many genera of ornamentals, including *Chrysanthemum*, *Dianthus*, *Iris*, *Lilium*, *Narcissus*, *Hosta*, *Hemerocallis*, and *Viola*. Cool season turfgrasses, such as bentgrass, fescue, perennial ryegrass, and bluegrass

may also be infected. The fungus has a worldwide distribution, but occurs most frequently in tropical or subtropical locations, where the warm, humid conditions promote fungal growth.

Sclerotium rolfsii is a particularly problematic pathogen of peanut plants. Average losses in peanut crops due to white mold in the United States are typically 7-10% annually, but can be as high as 25-80%. White mold causes major losses in Georgia peanut production; in 2007 *S. rolfsii* alone caused a 10% reduction in crop value and cost farmers \$44.4 million (Kemerait, 2008). An early season epidemic of white mold in 1998 resulted in a loss of \$50.7 million (Brenneman and Culbreath, 1999). Current management strategies include crop rotation with grasses and cotton, planting resistant peanut varieties, and chemical control. Crop rotation is not a fully effective management strategy due to the wide host range of the pathogen. Chemical control with tebuconazole (Folicur), azoxystrobin (Abound), flutolanil (Moncut or Artisan), Pyraclostrobin (Headline), or the insecticide Lorsban 15G can be partially effective, but it is costly and requires the chemicals to penetrate the canopy and reach the crown and limbs. Rotation of these chemicals is also suggested to avoid developing fungicide resistance.

White mold spreads from season to season by movement of small, mustard-seed sized balls of fungal tissue called sclerotia. Sclerotia germinate midseason under wet or humid conditions to grow as white fluffy mycelia on peanut stems, pegs, and pods. The mycelium typically grows until it exhausts the nutrient supply, then produces copious sclerotia, which serve as primary and secondary inoculum. These structures allow the pathogen to overwinter in the soil and are critical to the persistence of disease potential. Although the sexual stage of this pathogen has been produced under laboratory conditions, it is rarely seen in the field.

Sclerotium formation. Sclerotial development occurs in three discrete stages, beginning as sclerotial initials (I), followed by the developmental (D) and maturation (M) stages (Henis and Chet, 1968). Young sclerotia in the first stage of development are referred to as “initials” until they reach the second stage of development. Initials arise from local regions of hyphal proliferation and branching as a loose association of several mycelial strands, becoming visible to the naked eye as the number and density of hyphae increase (Zarani and Christias, 1997). Initials lack pigment and are easily deformed by physical pressure. Sclerotia in the second (developmental) stage are more structured, with a distinctively spherical shape and light pigmentation. Developmental sclerotia produce droplets of protein-rich exudate within a membranous hyphal layer that is shed by the end of the stage (Christias, 1980; Zarani and Christias, 1997). Fully mature sclerotia are hard, compact spheres that have shed any remaining attachments to the mycelium. Mature sclerotia are approximately 1.0 mm in diameter, although reported measurements range from 0.25 to 10 mm; however, the largest measurements may be the result of the coalescence of several smaller sclerotia prior to melanization (Aycock, 1966). Mature sclerotia are composed of four structural layers: an outer skin, rind, cortex, and medulla (Townsend and Willetts, 1954; Chet et al, 1969). Melanin is deposited in the rind, making the mature structures dark and resistant to UV light.

Because sclerotia are the primary means of disease spread, several studies have investigated factors that stimulate or suppress the production these structures by *S. rolfsii*. Sclerotium formation can be stimulated by restriction of hyphal growth through physical manipulation or cold treatment (Chet and Henis, 1968; Rawn, 1991). The presence of EDTA, iron, oxygen, or 10 mM L-threonine also promotes sclerotium formation (Chet and Henis, 1968; Griffin and Nair, 1968; Henis et al, 1973; Kritzman et al, 1977). Glucose depletion also triggers

the formation of sclerotia, but the reintroduction of glucose to the depleted medium results in suppression of initiation, although it does not affect the development of sclerotial initials formed prior to the addition of glucose (Hadar et al, 1983). These results suggest that *S. rolf sii* may utilize different pathways to regulate sclerotium initiation and subsequent development. In addition to glucose availability, sclerotium formation is also suppressed by disruption of protein synthesis or metabolite translocation (Okon et al, 1973). Exogenous application of antioxidant compounds beta-carotene and ascorbate cause a concentration-dependent reduction in both sclerotium formation and development (Georgiou et al, 2001; Georgiou et al, 2003).

Genetic factors of sclerotium formation. Although many studies have examined what factors trigger sclerotium formation in *S. rolf sii*, little attention has been paid to the genetic basis of these events. Studies in other sclerogenic fungi have begun to identify genetic factors involved in the induction or suppression of sclerotium formation. In *Aspergillus flavus* and *A. paraciticus*, sclerotium formation is linked to secondary metabolite formation (Calvo et al, 2002), with the *veA* and *laeA* genes required for both sclerotium formation and mycotoxin production in *A. flavus* (Calvo et al, 2004; Duran et al, 2007). In *Botrytis cinerea*, the MAPK homologs BcSAK1 and Bmp3 are required for sclerotium production (Segmüller et al, 2007; Rui and Hahn, 2007). Deletion of the *B. cinerea* Gα-subunit *bcg3* results in a decreased ability to monitor nutrient availability and increased sclerotium formation, suggesting that the MAPK and cAMP/PKA pathways both coordinate sclerotium formation (Doehlemann et al, 2006). The *Sclerotinia sclerotiorum* MAPK homolog Smk1 is required for sclerotial initiation and maturation and functions in a cAMP-dependent signaling pathway (Chen et al, 2004). *S. sclerotiorum* transcription factor Pac1 is required for sclerotial development and growth at high pH (Rollins, 2003). More studies are necessary in *S. rolf sii* to allow comparison of proteins and

pathways necessary to regulate sclerotium formation and development in these evolutionarily divergent fungi.

LITERATURE CITED

1. Aycock, R. 1966. *Stem rot and other diseases caused by Sclerotium rolfsii*. Vol. 174. Raleigh: North Carolina Agricultural Experiment Station.
2. Bahn, Y. S., and P. Sundstrom. 2001. CAP1, an adenylate cyclase-associated protein gene, regulates bud-hypha transitions, filamentous growth, and cyclic AMP levels and is required for virulence of *Candida albicans*. *J. Bacteriol.* 183:3211-3223.
3. Bahn, Y. S., J. K. Hicks, S. S. Giles, G. M. Cox, and J. Heitman. 2004. Adenylyl cyclase-associated protein Aca1 regulates virulence and differentiation of *Cryptococcus neoformans* via the cyclic AMP-protein kinase A cascade. *Eukaryot. Cell.* 3:1476-1491.
4. Banuett, F. 1995. Genetics of *Ustilago maydis*, a fungal pathogen that induces tumors in maize. *Annu. Rev. Genet.* 29:179-208.
5. Banuett, F., and I. Herskowitz. 1994. Morphological transitions in the life cycle of *Ustilago maydis* and their genetic control by the *a* and *b* loci. *Exp. Mycol.* 18: 247-266.
6. Banuett, F., and I. Herskowitz. 1996. Discrete developmental stages during teliospore formation in the corn smut fungus, *Ustilago maydis*. *Development.* 122:2965-2976.
7. Barrett, K. J., S. E. Gold, and J. W. Kronstad. 1993. Identification and complementation of a mutation to constitutive filamentous growth in *Ustilago maydis*. *Mol. Plant Microbe Interact.* 6:274-283.
8. Baum, B., W. Li, and N. Perrimon. 2000. A cyclase-associated protein regulates actin and cell polarity during *Drosophila* oogenesis and in yeast. *Curr. Biol.* 10:964-973.
9. Bertling, E., P. Hotulainen, P. K. Mattila, T. Matilainen, M. Salminen, and P. Lappalainen. 2004. Cyclase-associated protein 1 (CAP1) promotes cofilin-induced actin dynamics in mammalian nonmuscle cells. *Mol. Biol. Cell.* 15:2324-2334.
10. Bertling, E., O. Quintero-Monzon, P. K. Mattila, B. L. Goode, and P. Lappalainen. 2007. Mechanism and biological role of profilin-Srv2/CAP interaction. *J. Cell Sci.* 120:1225-1234.

11. Bölker, M., S. Genin, C. Lehmler, and R. Kahmann. 1995. Genetic regulation of mating and dimorphism in *Ustilago maydis*. *Can. J. Bot.* 73:320-325.
12. Bölker, M., M. Urban, and R. Kahmann. 1992. The *a* mating type locus of *Ustilago maydis* specifies cell signaling components. *Cell.* 68:441-450.
13. Brachmann, A., G. Weinzierl, J. Kamper, and R. Kahmann. 2001. Identification of genes in the bW/bE regulatory cascade in *Ustilago maydis*. *Mol. Microbiol.* 42:1047-1063.
14. Brenneman, T., and A. Culbreath. 1999. Georgia Plant Disease Loss Estimate. In *Cooperative Extension Service Bulletin* 41-01, edited by J. L. Williams-Woodward. University of Georgia, Athens.
15. Calvo, A.M., R.A. Wilson, J.W. Bok, and N.P. Keller. 2002. Relationship between secondary metabolism and fungal development. *Microbiol. Mol. Biol. Rev.* 66:447-459.
16. Calvo, A.M., J.W. Bok, W. Brooks, and N.P. Keller. 2004. *veA* is required for toxin and sclerotial production in *Aspergillus parasiticus*. *Appl. Environ. Microbiol.* 70:4733-4739.
17. Chen, C. B., A. Harel, R. Gorovoits, O. Yarden, and M. B. Dickman. 2004. MAPK regulation of sclerotial development in *Sclerotinia sclerotiorum* is linked with pH and cAMP sensing. *Mol. Plant Microbe Interact.* 17:404-413.
18. Chet I., and Y. Henis. 1968. Control mechanism of sclerotial formation in *Sclerotium rolfsii* Sacc. *J. Gen. Microbiol.* 54:231-7.
19. Chet, I., Y. Henis, and N. Kislev. 1969. Ultrastructure of sclerotia and hyphae of *Sclerotium rolfsii* Sacc. *J. Gen. Microbiol.* 57:143-7.
20. Christensen, J.J. 1963. *Corn smut caused by Ustilago maydis*, Monograph No. 2. St. Paul: American Phytopathological Society.
21. Christias, C. 1980. Nature of the sclerotial exudate of *Sclerotium rolfsii* Sacc. *Soil Biol. Biochem.* 12:199-201.
22. Colombo, S., P. Ma, L. Cauwenberg, J. Winderickx, M. Crauwels, A. Teunissen, D. Nauwelaers, J.H. De Winde, M.F. Gorwa, and D. Colavizza. 1998. Involvement of distinct G-proteins, Gpa2 and Ras, in glucose- and intracellular acidification-induced cAMP signalling in the yeast *Saccharomyces cerevisiae*. *EMBO J.* 17:3326.
23. Doehlemann, G., P. Berndt, and M. Hahn. 2006. Different signalling pathways involving a *Gα* protein, cAMP and a MAP kinase control germination of *Botrytis cinerea* conidia. *Mol. Microbiol.* 59:821-835.

24. Duran, R.M., J.W. Cary, and A.M. Calvo. 2007. Production of cyclopiazonic acid, aflatrem, and aflatoxin by *Aspergillus flavus* is regulated by *veA*, a gene necessary for sclerotial formation. *Appl. Environ. Microbiol.* 73:1158-1168.
25. Dürrenberger, F., K. Wong, and J. W. Kronstad. 1998. Identification of a cAMP-dependent protein kinase catalytic subunit required for virulence and morphogenesis in *Ustilago maydis*. *Proc. Natl. Acad. Sci. USA.* 95:5684-5689.
26. Fedor-Chaiken, M., R. J. Deschenes, and J. R. Broach. 1990. SRV2, a gene required for RAS activation of adenylate cyclase in yeast. *Cell.* 61:329-340.
27. Field, J., A. Vojtek, R. Ballester, G. Bolger, J. Colicelli, K. Ferguson, J. Gerst, T. Kataoka, T. Michaeli, and S. Powers. 1990. Cloning and characterization of CAP, the *Saccharomyces cerevisiae* gene encoding the 70 kd adenylyl cyclase-associated protein. *Cell.* 61:319-327.
28. Freeman, N. L., Z. Chen, J. Horenstein, A. Weber, and J. Field. 1995. An actin monomer binding activity localizes to the carboxyl-terminal half of the *Saccharomyces cerevisiae* cyclase-associated protein. *J. Biol. Chem.* 270:5680-5685.
29. Freeman, N.L., T. Lila, K.A. Mintzer, Z. Chen, A.J. Pahk, R. Ren, D.G. Drubin, and J. Field. 1996. A conserved proline-rich region of the *Saccharomyces cerevisiae* cyclase-associated protein binds SH3 domains and modulates cytoskeletal localization. *Mol. Cell Biol.* 16:548-556.
30. Gerst, J. E., K. Ferguson, A. Vojtek, M. Wigler, and J. Field. 1991. Cap is a bifunctional component of the *Saccharomyces cerevisiae* adenylyl cyclase complex. *Mol. Cell Biol.* 11:1248-1257.
31. Georgiou CD, G. Zervoudakis, and P.K. Petropoulou. 2003. Ascorbic acid may play a role in sclerotial differentiation of *Sclerotium rolfsii*. *Mycologia.* 95:308-16.
32. Gerogiou CD, Zervoudakis G, Tairis N, Kornaros M. 2001. β -Carotene production and its role in sclerotial differentiation of *Sclerotium rolfsii*. *Fungal Genet. Biol.* 34:11-20.
33. Gillissen, B., J. Bergemann, C. Sandmann, B. Schroeer, M. Bölker, and R. Kahmann. 1992. A two-component regulatory system for self/non-self recognition in *Ustilago maydis*. *Cell.* 68:647-657.
34. Gold, S. E., S. M. Brogdon, M. E. Mayorga, and J. W. Kronstad. 1997. The *Ustilago maydis* regulatory subunit of a cAMP-dependent protein kinase is required for gall formation in maize. *Plant Cell.* 9:1585-1594.
35. Gold, S.E., G. Duncan, K.J. Barrett, and J.W. Kronstad. 1994. cAMP regulates morphogenesis in the fungal pathogen *Ustilago maydis*. *Genes Dev.* 8:2805-2816.
36. Griffin, D.M. and G.N. Nair. 1968. Growth of *Sclerotium rolfsii* at different concentrations of oxygen and carbon dioxide. *J. Exp. Bot.* 19:812-6.

37. Hadar Y, Pines M, Chet I, Henis Y. 1983. The regulation of sclerotium initiation in *Sclerotium rolfsii* by glucose and cyclic AMP. *Can. J. Microbiol.* 29:21-26.
38. Hartmann, H. A., R. Kahmann, and M. Bölker. 1996. The pheromone response factor coordinates filamentous growth and pathogenicity in *Ustilago maydis*. *EMBO J.* 15:1632-1641.
39. Hartmann, H. A., J. Krüger, F. Lottspeich, and R. Kahmann. 1999. Environmental signals controlling sexual development of the corn smut fungus *Ustilago maydis* through the transcriptional regulator prf1. *Plant Cell* 11:1293-1305.
40. Henis, Y., and I. Chet. 1968. Developmental biology of sclerotia of *Sclerotium rolfsii*. *Can. J. Bot.* 46:947-50.
41. Henis, Y., Y. Okon, and I. Chet. 1973. Relationship between early hyphal branching and formation of sclerotia in *Sclerotium rolfsii*. *J. Gen Microbiol.* 79:147-50.
42. Holliday, R. 1961. Induced mitotic crossing-over in *Ustilago maydis*. *Genet. Res.* 2:231-248.
43. Hubberstey, A. V., and E. P. Mottillo. 2002. Cyclase-associated proteins: CAPacity for linking signal transduction and actin polymerization. *FASEB J.* 16:487-499.
44. Kaffarnik, F., P. Muller, M. Leibundgut, R. Kahmann, and M. Feldbrugge. 2003. PKA and MAPK phosphorylation of Prf1 allows promoter discrimination in *Ustilago maydis*. *EMBO J.* 22:5817-5826.
45. Kamper, J., R. Kahmann, M. Bölker, L.J. Ma, T. Brefort, B.J. Saville, F. Banuett, J.W. Kronstad, S.E. Gold, O. Muller, et al. 2006. Insights from the genome of the biotrophic fungal plant pathogen *Ustilago maydis*. *Nature.* 444:97.
46. Kamper, J., M. Reichmann, T. Romeis, M. Bölker, and R. Kahmann. 1995. Multiallelic recognition: nonself-dependent dimerization of the bE and bW homeodomain proteins in *Ustilago maydis*. *Cell.* 81:73-83.
47. Kawamukai, M., J. Gerst, J. Field, M. Riggs, L. Rodgers, M. Wigler, and D. Young. 1992. Genetic and biochemical analysis of the adenylyl cyclase-associated protein, cap, in *Schizosaccharomyces pombe*. *Mol. Biol. Cell.* 3:167-180.
48. Kemerait, R. 2008. Georgia plant disease loss estimate. In *Cooperative Extension Service Bulletin* 41-10, edited by A.D. Martinez. University of Georgia, Athens.
49. Kernkamp, M. F. 1939. Genetic and environmental factors affecting growth types of *Ustilago zaeae*. *Phytopathology.* 29:473-484.
50. Klose, J., M. M. de Sa, and J. W. Kronstad. 2004. Lipid-induced filamentous growth in *Ustilago maydis*. *Mol. Microbiol.* 52:823-835.

51. Klosterman, S. J., M. H. Perlin, M. Garcia-Pedrajas, S. F. Covert, and S. E. Gold. 2007. Genetics of morphogenesis and pathogenic development of *Ustilago maydis*. In *Fungal Genomics*, edited by J. C. Dunlap. St. Louis, MO: Academic Press.
52. Kritzman, G., I. Chet, and Y. Henis. 1977. Role of oxalic acid in pathogenic behavior of *Sclerotium rolfsii* Sacc. *Exp. Mycol.* 4:280-285.
53. Kronstad, J. W. 1997. Virulence and cAMP in smuts, blasts and blights. *Trends Plant Sci.* 2:193-199.
54. Krüger, J., G. Loubradou, E. Regenfelder, A. Hartmann, and R. Kahmann. 1998. Crosstalk between cAMP and pheromone signalling pathways in *Ustilago maydis*. *Mol. Gen. Genet.* 260:193-198.
55. Krüger, J., G. Loubradou, G. Wanner, E. Regenfelder, M. Feldbrugge, and R. Kahmann. 2000. Activation of the cAMP pathway in *Ustilago maydis* reduces fungal proliferation and teliospore formation in plant tumors. *Mol. Plant Microbe Interact.* 13:1034-1040.
56. Laity, C., L. Giasson, R. Campbell, and J. W. Kronstad. 1995. Heterozygosity at the *b* mating-type locus attenuates fusion in *Ustilago maydis*. *Curr. Genet.* 27:451-459.
57. Lila, T., and D. G. Drubin. 1997. Evidence for physical and functional interactions among two *Saccharomyces cerevisiae* SH3 domain proteins, an adenylyl cyclase-associated protein and the actin cytoskeleton. *Mol. Biol. Cell.* 8:367-385.
58. Martinez-Espinoza, A. D., J. Ruiz-Herrera, C. G. Leon, and S. E. Gold. 2004. MAP kinase and cAMP signaling pathways modulate the pH-induced yeast-to-mycelium dimorphic transition in the corn smut fungus *Ustilago maydis*. *Curr. Microbiol.* 49:274-281.
59. Mattila, P. K., O. Quintero-Monzon, J. Kugler, J. B. Moseley, S. C. Almo, P. Lappalainen, and B. L. Goode. 2004. A high-affinity interaction with ADP-actin monomers underlies the mechanism and in vivo function of Srv2/cyclase-associated protein. *Mol. Biol. Cell.* 15:5158-5171.
60. Moriyama, K., and I. Yahara. 2002. Human CAP1 is a key factor in the recycling of cofilin and actin for rapid actin turnover. *J. Cell Sci.* 115:1591-1601.
61. Noegel, A. A., R. Blau-Wasser, H. Sultana, R. Muller, L. Israel, M. Schleicher, H. Patel, and C. J. Weijer. 2004. The cyclase-associated protein CAP as regulator of cell polarity and cAMP signaling in *Dictyostelium*. *Mol. Biol. Cell.* 15:934-945.
62. Noegel, A. A., F. Rivero, R. Albrecht, K. P. Janssen, J. Kohler, C. A. Parent, and M. Schleicher. 1999. Assessing the role of the ASP56/CAP homologue of *Dictyostelium discoideum* and the requirements for subcellular localization. *J. Cell Sci.* 112:3195-3203.

63. Okon, Y., I. Chet, and Y. Henis. 1973. Effects of lactose, ethanol, and cyclohexamide on the translocation pattern of radioactive compounds and on sclerotium formation in *Sclerotium rolfii*. *J. Gen Microbiol.* 74:251-258.
64. Paunola, E., P. K. Mattila, and P. Lappalainen. 2002. WH2 domain: a small, versatile adapter for actin monomers. *FEBS Lett.* 513:92-97.
65. Puhalla, J. E. 1970. Genetic studies of the *b* incompatibility locus of *Ustilago maydis*. *Genet. Res.* 16:229-232.
66. Quintero-Monzon, O., E. M. Jonasson, E. Bertling, L. Talarico, Ff Chaudhry, M. Sihvo, P. Lappalainen, and B. L. Goode. 2009. Reconstitution and Dissection of the 600-kDa Srv2/CAP Complex: Roles for oligomerization and cofilin-actin binding in driving actin turnover. *J. Biol. Chem.* 284:10923-10934.
67. Rawn, C. D. 1991. Induction of sclerotia in *Sclerotium rolfii* by short low-temperature treatment. *J. Gen Microbiol.* 137:1063-1066.
68. Regenfelder, E., T. Spellig, A. Hartmann, S. Lauenstein, M. Bölker, and R. Kahmann. 1997. G proteins in *Ustilago maydis*: transmission of multiple signals? *EMBO J.* 16:1934-1942.
69. Rollins, J. A. 2003. The *Sclerotinia sclerotiorum* *pac1* gene is required for sclerotial development and virulence. *Mol. Plant Microbe Interact.* 16:785-795.
70. Romeis, T., A. Brachmann, R. Kahmann, and J. Kamper. 2000. Identification of a target gene for the bE-bW homeodomain protein complex in *Ustilago maydis*. *Mol. Microbiol.* 37:54-66.
71. Rowell, J. B. 1955. Functional rate of compatibility factors and an *in vitro* test for sexual compatibility with haploid lines of *Ustilago zaeae*. *Phytopathology.* 45:370-374.
72. Rui, O., and M. Hahn. 2007. The *Slr2*-type MAP kinase *Bmp3* of *Botrytis cinerea* is required for normal saprotrophic growth, conidiation, plant surface sensing and host tissue colonization. *Mol. Plant Path.* 8:173-184.
73. Ruiz-Herrera, J., C. G. Leon, L. Guevara-Olvera, and A. Carabez-Trejo. 1995. Yeast-mycelial dimorphism of haploid and diploid strains of *Ustilago maydis* in liquid culture. *Microbiol.* 141:695-703.
74. Scherer, M., K. Heimel, V. Starke, and J. Kamper. 2006. The Clp1 protein is required for clamp formation and pathogenic development of *Ustilago maydis*. *Plant Cell.* 18:2388-2401.
75. Segmüller, N., U. Ellendorf, B. Tudzynski, and P. Tudzynski. 2007. *BcSAK1*, a stress-activated mitogen-activated protein kinase, is involved in vegetative differentiation and pathogenicity in *Botrytis cinerea*. *Eukaryot. Cell.* 6:211-221.

76. Snetselaar, K. M., and C. W. Mims. 1992. Sporidial fusion and infection of maize seedlings by the smut fungus *Ustilago maydis*. *Mycologia*. 84:193-203.
77. Snetselaar, K. M., and C. W. Mims. 1994. Light and electron microscopy of *Ustilago maydis* hyphae in maize. *Mycological Res.* 98:347-355.
78. Toda, T., I. Uno, T. Ishikawa, S. Powers, T. Kataoka, D. Broek, S. Cameron, J. Broach, K. Matsumoto, and M. Wigler. 1985. In yeast, RAS proteins are controlling elements of adenylate cyclase. *Cell*. 40:27-36.
79. Townsend, B. B., and H. J. Willetts. 1954. The development of sclerotia of certain fungi. *Trans. Br. Mycol. Soc.* 37:213-221.
80. Uetz, P., L. Giot, G. Cagney, T. A. Mansfield, R. S. Judson, et al. 2000. A comprehensive analysis of protein-protein interactions in *Saccharomyces cerevisiae*. *Nature*. 403:623-627.
81. Urban, M., R. Kahmann, and M. Bölker. 1996. Identification of the pheromone response element in *Ustilago maydis*. *Mol. Genet. Genomics*. 251:31-37.
82. Vojtek, A. B., and J. A. Cooper. 1993. Identification and characterization of a cDNA-encoding mouse CAP - a homolog of the yeast adenylyl-cyclase associated protein. *J. Cell Sci.* 105:777-785.
83. Weber, A, V. T. Nachmias, C. R. Pennise, M. Pring, and D. Safer. 1992. Interaction of thymosin beta-4 with muscle and platelet actin: implications for actin sequestration in resting platelets. *Biochemistry*. 31:6179-6185.
84. Yu, J., C. Wang, S. J. Palmieri, B. K. Haarer, and J. Field. 1999. A cytoskeletal localizing domain in the cyclase-associated protein, CAP/Srv2p, regulates access to a distant SH3-binding site. *J. Biol. Chem.* 274:19985-19991.
85. Zarani, F., and C. Christias. 1997. Sclerotial biogenesis in the basidiomycete *Sclerotium rolfsii*. A scanning electron microscope study. *Mycologia*. 89:598-602.
86. Zarnack, K., H. Eichhorn, R. Kahmann, and M. Feldbrugge. 2008. Pheromone-regulated target genes respond differentially to MAPK phosphorylation of transcription factor Prf1. *Mol. Microbiol.* 69:1041-1053.

CHAPTER 3

IDENTIFICATION AND CHARACTERIZATION OF CAP1, THE ADENYLATE CYCLASE-ASSOCIATED PROTEIN (CAP) HOMOLOG IN *USTILAGO MAYDIS*¹

¹ J.E. Takach and S.E. Gold. 2009. Submitted to *Molecular Plant Pathology*, 09/02/09.

**Identification and Characterization of Cap1, the Adenylate Cyclase-Associated Protein
(CAP) Homolog in *Ustilago maydis***

J.E. Takach and S.E. Gold

Department of Plant Pathology, University of Georgia, Athens 30602

ABSTRACT

Ustilago maydis, the causal agent of corn smut, has emerged as a basidiomycete model system for signal transduction, dimorphism, and disease development. The well-characterized cAMP/PKA signaling pathway mediates filamentation in response to environmental cues, and in the absence of the cAMP signal, haploid cells grow filamentously. Prior to this report, the G-alpha subunit Gpa3 was the only pathway component known to function upstream of adenylate cyclase, Uac1. In other fungal systems, adenylate cyclase is also positively regulated by the adenylate cyclase-associated protein (CAP). A CAP homolog, Cap1, has been identified by sequence homology in the *U. maydis* genome. Yeast 2-hybrid analysis indicates that Cap1 can bind to itself and the C-terminus of Uac1. Deletion of *cap1* results in abnormal colony formation and filamentous cells that revert to budding in the presence of exogenous cAMP. The $\Delta cap1$ strains have a reduced ability to form mating filaments compared to wild type strains. Pathogenicity is significantly reduced in $\Delta cap1$ strains in wild type and solopathogenic genetic backgrounds. These results suggest that both Gpa3 and Cap1 coordinate production of cAMP.

INTRODUCTION

Ustilago maydis has emerged as a basidiomycete model system for the study of signaling pathways affecting dimorphism and disease development in maize (for review, see Klosterman et

al., 2007). Two interconnected signaling pathways mediate the filamentation process: the pheromone responsive MAP kinase cascade and the environment-responsive cAMP/PKA pathway. Fusion of haploid budding cells and subsequent dikaryon formation is controlled genetically by the *a* and *b* mating type loci (Holliday, 1961; Banuett, 1995; Rowell, 1995). Filamentous growth of haploid cells can also be triggered by environmental signals that include nutrient and nitrogen deprivation (Kernkamp, 1939; Banuett and Herskowitz, 1994) or exposure to air, acidic pH, or lipids (Gold et al., 1994; Ruiz-Herrera et al., 1995; Klose et al., 2004).

Proper regulation and function of the cAMP/PKA pathway are required for virulence and pathogenicity of *U. maydis*. Components of this pathway include Gpa3, a G-protein α subunit; Uac1, adenylate cyclase; Ubc1, the PKA regulatory subunit; and Adr1, the PKA catalytic subunit. Mutation of genes upstream of the cAMP signal (*gpa3* or *uac1*) results in a filamentous phenotype that can be rescued by addition of exogenous cAMP (Gold et al., 1994; Krüger et al., 1998). Disruption of the *adr1* gene encoding the catalytic subunit of PKA results in a similar filamentous phenotype but is not remedied by addition of cAMP (Dürrenberger et al., 1998). Inactivation of the PKA regulatory subunit, effectively simulating a high level of cAMP by allowing constitutive activation of the PKA catalytic subunit, results in a multiple budding yeast phenotype (Gold et al., 1994). Collectively, these results indicate that the absence of the cAMP signal results in filamentous growth and presence of cAMP promotes budding and suppresses filamentous growth in *U. maydis*.

Proper regulation and function of the cAMP/PKA pathway are also required for virulence and pathogenicity. $\Delta gpa3$, $uac1^-$, and $\Delta adr1$ mutants do not produce tumors in infected plant tissues (Kronstad, 1997). *U. maydis* strains with a constitutively active G α allele (*gpa3*_{Q206L}) can form tumors *in planta*; however, the fungal development in these plants is severely

compromised, indicating the importance of the cAMP pathway in fungal proliferation and teliospore formation within galls (Krüger et al., 2000). *Δubc1* mutants produce early symptoms of infection (chlorosis and anthocyanin production), but do not produce tumors (Gold et al., 1997).

Although much is known about the cAMP signaling cascade in *U. maydis*, there are still significant gaps in knowledge. Currently, Gpa3 is the only identified cAMP/PKA pathway component upstream of Uac1 in *U. maydis*, and no previous reports have identified additional mediators of cAMP production. In other fungal systems, multiple effectors regulate adenylate cyclase activity, including G-proteins and adenylate cyclase-associated proteins (CAPs).

The first CAP protein, Srv2, was identified in *Saccharomyces cerevisiae* as an adenylate cyclase binding protein and a mediator of RAS2 activation of adenylate cyclase (Fedor-Chaiken et al., 1990; Field et al., 1990). Subsequently, CAP/Srv2 homologs have been identified in all eukaryotic species (Hubberstey and Mottillo, 2002). All family members contain a highly conserved C-terminal region that associates with actin monomers and plays a role in cofilin-mediated actin turnover (Bertling et al., 2007; Quintero-Monzon et al., 2009). The N-terminal region, which binds Srv2 in *S. cerevisiae*, is less conserved in eukaryotes (Gerst et al., 1991; Hubberstey and Mottillo, 2002). However, CAP/Srv2 homologs have been demonstrated to bind adenylate cyclase and affect cAMP production in several fungal species, including the dimorphic human pathogens *Cryptococcus neoformans* and *Candida albicans*. The *C. neoformans* homolog Aca1 is a positive regulator of adenylate cyclase (Cac1) and required for cAMP-mediated capsule formation and virulence (Bahn et al., 2004). In *C. albicans*, Cap1 is required for the cAMP-mediated bud-hypha transition, and *cap1/cap1* mutants are avirulent (Bahn and Sundstrom, 2001).

In this study, we have identified and characterized a CAP/Srv2 homolog in *U. maydis*. Using the DelsGate method (Garcia-Pedrajas et al., 2008), we created $\Delta cap1$ strains and observed effects of the deletion on morphology, mating, and pathogenicity, particularly in light of the role of CAP/Srv2 homologs in the dimorphic transition of other fungal pathogens. Our findings from these experiments indicate that the *U. maydis* CAP/Srv2 homolog Cap1 plays an important role in haploid budding growth and the ability to cause disease in its maize host.

RESULTS

Identification of an adenylate cyclase-associated protein (CAP) homolog in *Ustilago maydis*. A BLAST search of the *U. maydis* genome (<http://mips.gsf.de/genre/proj/ustilago/>) with the *S. cerevisiae* Srv2 protein sequence identified a single gene (Altshul et al., 1997). The um10957 ORF has a predicted length of 1619 nucleotides and includes one 82-base intron confirmed here by cDNA sequencing (data not shown). The gene encodes a 511-amino-acid protein with a predicted molecular mass of 53.8 kDa that shares 34% identity with the entire *S. cerevisiae* protein. The domain structure of the *U. maydis* Cap1 is typical of the Cap1/Srv2 protein family (Figure 3.1). The predicted amino acid sequence includes the conserved N-terminal RLE/RLE motif (amino acids 15 to 24) required for adenylate cyclase binding and proper protein folding (Gerst et al., 1991; Yu et al., 1999) and two polyproline regions P1 (amino acids 261 to 269) and P2 (amino acids 351 to 359) required to bind components of the actin turnover machinery (Lila and Drubin, 1997; Bertling et al., 2007).

To confirm that the *U. maydis* Cap1 homolog binds adenylate cyclase, we demonstrated that Cap1 and Uac1 physically interact through yeast two-hybrid assays (Figure 3.2). Full length Cap1 and the C-terminal 200 amino acids of Uac1 were used as both bait and prey. Positive

interactions were determined by the growth of yeast colonies on synthetic quadruple dropout medium and production of blue pigmentation when supplemented with X- α -gal. Vigorous growth and blue coloration are characteristic of reporter gene expression and an indirect assay for interaction between bait and prey proteins. Yeast growth (Figure 3.2) and blue colorization (data not shown) resulted from cotransformation of Cap1 bait and prey plasmids. A positive interaction was also observed when plasmids containing the Cap1 protein and the C-terminal portion of Uac1 were cotransformed. These interactions were not observed when the individual plasmids were transformed into yeast (data not shown)

Deletion of the *cap1* gene in *U. maydis*. To characterize the function of Cap1 in *U. maydis*, *cap1* was replaced by the linearized deletion construct plasmid via homologous recombination (Figure 3.3a and 3.3b). The linearized plasmid was introduced into protoplasts of strains 1/2, 2/9, and the solopathogenic strain SG200 (genotypes listed in Table 3.2). The genotypes of three independent deletion strains in each mating type and two independent SG200 deletion strains were verified by diagnostic PCR (not shown) and Southern blot analysis (Figure 3.3c).

Effects of *cap1* deletion on morphology, mating, and pathogenesis. Colony morphology of $\Delta cap1$ strains was pleiotrophic. Initial transformant colonies were dark and filamentous, but subsequent transfer to fresh PDA plates resulted in a mixed population of dark/filamentous colonies, white/filamentous colonies, and white/smooth colonies (Figure 3.4). Upon repeated transfers, the white/filamentous colonies gave rise to white/filamentous colonies and white/smooth colonies, but never dark/filamentous colonies, and yeast colonies failed to give rise to filamentous colonies. These results were observed in several independent mutant strains in all genetic backgrounds. Often, white/filamentous colonies would have a darkened basal

layer, making the colonies appear gray. Similar colony morphology was reported for $\Delta gpa3$ colonies (Regenfelder et al., 1997). For the sake of consistency, we routinely started fresh cultures from storage and chose dark or gray filamentous colonies. All colony types, however, resulted in a similar short filamentous phenotype when grown in liquid medium.

The $\Delta cap1$ strains of *U. maydis* are defective in polar budding (Figure 3.5). Deletion strains grown in PDB produce short filamentous cells with one or more branches. A similar phenotype is observed in $\Delta gpa3$ strains. However, neither deletion strain fully mimics the *uac1*⁻ mutant, which produces thinner and longer filaments (Figure 3.5). The phenotype of $\Delta cap1$ cells reverts to wild type budding in the presence of cAMP, as do $\Delta gpa3$ and *uac1*⁻ cells (Figure 3.5).

The mating ability of $\Delta cap1$ strains appears to be partially, but not completely, abolished (Figure 3.6). Co-spotted compatible wild-type cells produce white filamentous growth, indicating a successful mating reaction. The combination of compatible $\Delta cap1$ strains results in some filamentation but not to the extent observed in the wild-type mating reaction, which indicates a decreased ability of the $\Delta cap1$ strains to produce the filamentous dikaryon.

Pathogenicity is significantly decreased in the absence of *cap1* (Table 3.1). Inoculation of compatible $\Delta cap1$ strains into week-old corn seedlings results in decreased gall formation (35% of infections vs 85% of infections with compatible wild-type strains) and primarily results in chlorotic spots or anthocyanin production in leaves (data not shown). To ascertain if this pathogenicity defect was a result of decreased mating, pathogenicity assays were performed with a SG200 $\Delta cap1$ solopathogenic strain. The SG200 $\Delta cap1$ strain was also significantly reduced in pathogenicity (Table 3.1).

DISCUSSION

The cAMP signaling cascade in *U. maydis* is well characterized and required for normal haploid budding growth. In this study, we identified *cap1*, the CAP/Srv2 homolog in *U. maydis*, through a BLAST search of the *U. maydis* genome. Cap1 shares 34%, 39%, and 43% identity with the CAP/Srv2 proteins in *S. cerevisiae*, *C. albicans*, and *C. neoformans*, respectively (Figure 3.1). Yeast two-hybrid experiments demonstrate that the *U. maydis* Cap1 binds itself and the C-terminus of the adenylate cyclase protein, Uac1 (Figure 3.2). This activity is not conserved in all CAP/Srv2 homologs, but does occur in other fungal species such as *S. cerevisiae*, *C. neoformans*, *C. albicans*, and *Schizosaccharomyces pombe* (Bahn and Sundstrom, 2001; Bahn et al., 2004; Gerst et al., 1991; Kawamukai et al., 1992).

Deletion of the *cap1* gene results in a pleiotrophic colony morphology (Figure 3.4). Wild type *U. maydis* colonies are typically smooth and rounded on PDA, but $\Delta cap1$ colonies range from pigmented and filamentous to pale and smooth. Repeated transfers of colonies onto PDA and PDA-carboxin results in a loss of the pigmented and filamentous phenotype and an accumulation of smooth, pale colonies. This directional shift in phenotype suggests that the colony morphology of $\Delta cap1$ strains is pigmented and filamentous, and that secondary suppressor mutations are developing in these strains that results in a more stable yeast-like phenotype. The development of secondary suppressors is not an uncommon occurrence in *U. maydis*, and these $\Delta cap1$ yeast strains may yield valuable information regarding additional roles of Cap1.

Despite the variation in colony morphology, all $\Delta cap1$ colony phenotypes produce short, branched filaments when grown in liquid medium (Figure 3.5). The addition of cAMP to the medium causes a reversion to a wild type budding phenotype, suggesting that Cap1 functions

upstream of cAMP signal production. Prior to this report, the only pathway component demonstrated to function upstream of adenylate cyclase was Gpa3, the G-protein α subunit (Krüger et al., 1998).

The *uac1⁻* strains of *U. maydis* are filamentous and grow by hyphal extension (Gold et al., 1994). By contrast, Δ *cap1* and Δ *gpa3* strains branch and grow as relatively short filaments (Figure 3.5). Neither deletion strain fully mimics the phenotype of the *uac1⁻* strain, suggesting that the presence of either Cap1 or Gpa3 allows some cAMP production by Uac1 but not enough to compensate for the loss of the other component. Similar results were observed with the analogous deletion mutants Δ *aca1* and Δ *gpa1* in *C. neoformans* (Bahn et al., 2004).

In *S. cerevisiae*, the Srv2 dimer binds Cyr1 (adenylate cyclase) to mediate cAMP production and in the process opens up a second ras-binding domain in Cyr1 required for ras-mediated effects on cAMP signaling (Masumoto et al., 1982; Shima et al., 2000). Two ras genes have been identified in *U. maydis* (Müller et al., 2003; Lee and Kronstad 2002). Ras1 does not play a direct role in cellular morphology, but does promote the transcription of cAMP-regulated genes (Müller et al., 2003). Ras2 promotes filamentous growth via the MAP kinase cascade but is not involved with cAMP signaling (Lee and Kronstad, 2002; Müller et al., 2003). Despite its putative role in the cAMP pathway, Ras1 has not yet been demonstrated to interact directly with the Uac1 Ras association (RA) domain (amino acids 970-1050). Based on the *S. cerevisiae* Srv2/Cyr1/Ras2 model, we speculate that Cap1 may be required to mediate Ras1 binding to Uac1. Interestingly, the *C. neoformans* adenylate cyclase Aca1 does not include an RA domain, and neither Ras homolog has been demonstrated to be involved in cAMP signaling in this species (Bahn et al., 2004).

Not surprisingly, the perturbation in the cAMP signaling pathway caused by deletion of *cap1* resulted in a significantly decreased ability to cause disease (Table 3.1). However, unlike $\Delta gpa3$ strains, which resulted in an inability to form mating filaments and a complete lack of tumor formation, $\Delta cap1$ strains are only reduced in mating and pathogenicity (Regenfelder et al., 1997; Krüger et al., 1998). One possible interpretation of these results is that the environmental or plant signals that stimulate mating filament/dikaryon formation are mediated by Gpa3, not Cap1, thus resulting in a less severe mating/pathogenicity phenotypes in $\Delta cap1$ than in $\Delta gpa3$ strains. Future studies will be necessary to understand the extent of influence that Cap1 and Gpa3 have on cAMP production and morphology in *U. maydis*.

EXPERIMENTAL PROCEDURES

Fungal strains and growth conditions. The *U. maydis* strains used in this study are presented in Table 3.2. Fungal cultures were routinely grown at 30°C on potato dextrose agar (PDA, Sigma, St. Louis, MO) plates supplemented to 2% agar (2PDA) or in potato dextrose broth (PDB) with shaking at 200 rpm. Transformants were grown on YEPS-2% agar medium supplemented with 1 M sorbitol and appropriate selective agent (3 µg/ml carboxin). Mating assays were performed on complete medium containing 1% activated charcoal (Holliday, 1974). cAMP response growth assays were performed in PDB amended with 10 or 25 mM cAMP (Sigma).

Plasmid construction and sequencing. The *cap1* deletion construct was prepared using the DelsGate method (Garcia-Pedrajas *et al.*, 2008) with primers CapP1-CapP4 (described in Table 3.3). The *cap1* ORF was amplified from genomic DNA and cDNA using primers JT070/JT071 (Table 3.3) using Expand high fidelity *Taq* polymerase (Roche, Indianapolis, IN)

according to manufacturer's instructions and cloned into pCR2.1 (Invitrogen Carlsbad, CA). Plasmids were subsequently sequenced using the M13F and M13R primers, and the sequences were compared to confirm the presence of the *cap1* intron.

For yeast two-hybrid assay constructs, the *cap1* ORF and the 3' portion of the *uac1* gene were amplified from *U. maydis* cDNA using restriction enzyme linker primers (JT070/JT071 and JT072/JT073, respectively, described in Table 3.3) and Expand high fidelity *Taq* polymerase according to the manufacturer's instructions and cloned into pCR2.1 (Invitrogen, Carlsbad, CA). Inserts were subsequently cut from pCR2.1 with the appropriate restriction enzyme and ligated in frame with the GAL4 activation domain of the prey plasmid pGADT7 and the DNA binding domain of the bait plasmid pGBDT7 (BD Biosciences, San Jose, CA). All constructs were sequenced across the polylinker-start codon junction to verify the sequence insertion occurred in the correct reading frame.

Sequencing reactions were carried out in our laboratory using the Big Dye (v3.1) Terminator Cycle Sequencing Kit (Applied Biosystems, Foster City, CA) following the manufacturer's instructions run on an ABI Prism 310 Capillary Automated Genetic Analyzer (Applied Biosystems) at the Genome Analysis Facility on site. DNA sequences were analyzed with the Lasergene sequence analysis suite (DNASTAR, Madison, WI).

Yeast two-hybrid assays. The Matchmaker GAL4 Two-Hybrid System 3 (BD Biosciences) was used to perform all two-hybrid assays. Bait and prey plasmid constructs were introduced into *S. cerevisiae* strain AH109 (BD Biosciences) by cotransformation according to the manufacturer's directions. All suggested positive and negative control experiments were performed. Growth was assessed after 5 days on -Ade/-His/-Leu/-Trp SD medium, then transferred to similar medium overlaid with X- α -Gal (BD Biosciences).

***Ustilago maydis* transformation.** *U. maydis* transformations were performed using a protocol modified from Tsukuda et al. (1988). Briefly, strains were grown overnight in 100 ml YEPS medium (1% yeast extract, 2% peptone, 2% sucrose) to an OD₆₀₀ of 1.0. Cells were washed, concentrated, and treated with 77 mg/ml vinoflow enzyme (Novozymes, Denmark) for 10 m. Protoplasts were washed and resuspended in cold STC (10 mM Tris-HCL pH 7.5, 100 mM CaCl₂, 1 M sorbitol). Protoplasts were transformed immediately or amended with 7% DMSO and stored at -80°C. When transformant colonies became visible (4-10 days post-inoculation), individual colonies were transferred to 2PDA plates amended with 3 µg/ml carboxin.

Genomic DNA was isolated from transformant strains and screened for the absence of the ORF of the gene of interest using PCR primers JT042 and JT043 designed to amplify within the ORF (Table 3.3). Transformants with no amplification product were subsequently screened for homologous integration of the deletion construct via PCR using primers JT021 and DonrR (Table 3.3).

To confirm gene deletion, 10 µg of genomic DNA from transformant and wild-type strains were digested with the appropriate restriction enzymes and run on a 0.8% agarose gel at 50 V until the bromophenol blue dye migrated to within 1 cm of the end of the gel. The gel was washed in 0.4 M NaOH and blotted onto a Hybond nylon membrane (Ambion, Foster City, CA) overnight. Blots were probed with DIG-labeled PCR product corresponding to the 5' flank of the deletion construct to determine the presence or absence of the wild-type locus.

Mating, pathogenicity, and morphogenesis assays. The mating response of deletion mutant strains was assayed as described in Holliday (1974). A modified mating assay was also performed in which cells were grown 24 hr in 1 ml PDB containing 10 mM cAMP (Sigma),

transferred to 5 ml of fresh PDB/10 mM cAMP medium and grown 48 hr. Cultures were diluted to 1×10^7 cells/ml and co-spotted on mating plates as described in Holliday (1974).

Pathogenicity assays were carried out on the susceptible maize variety 'Golden Bantam' (Rich Farm Garden Supply, Winchester, IN). Seedlings were inoculated just above the soil line seven days after planting with a 1×10^6 cells/ml suspension of compatible deletion strains. Disease symptom data were collected at 7, 10 and 14 days after inoculation. Disease ratings were as described previously by Gold et al. (1997). In summary, symptoms were rated 0–5 as follows: 0, no disease; 1, anthocyanin or chlorosis; 2, leaf galls; 3, small stem galls; 4, large stem galls; 5, plant death due to disease. Statistical significance of experimental results was determined using nonparametric analysis as described by Shah and Madden (2003).

Morphological response to exogenous cAMP was assayed as described by Gold et al., (1994). Cell density, number of cell clusters, and lateral buds were tallied using an Improved Neubauer hemocytometer (Hausser Scientific, Horsham, PA), with $n = 100$ as the minimum number of cells observed per sample.

REFERENCES

- Altschul, S. F., T.L. Madden, A.A. Schaffer, J. Zhang, Z. Zhang, W. Miller, and D.J. Lipman.** (1997) Gapped BLAST and PSI-BLAST: a new generation of protein database search programs. *Nuc Acids Res.* **25**, 3389-3402.
- Bahn, Y. S. and Sundstrom, P.** (2001) CAP1, an adenylate cyclase-associated protein gene, regulates bud-hypha transitions, filamentous growth, and cyclic AMP levels and is required for virulence of *Candida albicans*. *J Bacteriol.* **183**, 3211-3223.
- Bahn, Y. S., Hicks, J. K., Giles, S. S., Cox, G. M. and Heitman, J.** (2004) Adenylyl cyclase-associated protein Aca1 regulates virulence and differentiation of *Cryptococcus neoformans* via the cyclic AMP-protein kinase A cascade. *Eukaryot Cell*, **3**, 1476-1491.
- Banuett, F.** (1995) Genetics of *Ustilago maydis*, a fungal pathogen that induces tumors in maize. *Annu. Rev. Genet.* **29**, 179-208.

- Banuett, F. and Herskowitz, I.** (1994) Morphological transitions in the life cycle of *Ustilago maydis* and their genetic control by the *a* and *b* loci. *Exp. Mycol.* **18**, 247-266.
- Bertling, E., Quintero-Monzon, O., Mattila, P. K., Goode, B. L. and Lappalainen, P.** (2007) Mechanism and biological role of profilin-Srv2/CAP interaction. *J Cell Sci.* **120**, 1225-1234.
- Bölker, M., Genin, S., Lehmler, C. and Kahmann, R.** (1995) Genetic regulation of mating and dimorphism in *Ustilago maydis*. *Can. J Bot.* **73**, 320-325.
- Dürrenberger, F., Wong, K. and Kronstad, J. W.** (1998) Identification of a cAMP-dependent protein kinase catalytic subunit required for virulence and morphogenesis in *Ustilago maydis*. *Proc. Natl Acad. Sci. USA*, **95**, 5684-5689.
- Fedor-Chaiken, M., Deschenes, R. J. and Broach, J. R.** (1990) SRV2, a gene required for RAS activation of adenylate cyclase in yeast. *Cell*, **61**, 329-340.
- Field, J., Vojtek, A., Ballester, R., Bolger, G., Colicelli, J., Ferguson, K., Gerst, J., Kataoka, T., Michaeli, T. and Powers, S.** (1990) Cloning and characterization of CAP, the *Saccharomyces cerevisiae* gene encoding the 70 kd adenylyl cyclase-associated protein. *Cell*, **61**, 319-327.
- García-Pedrajas, M. D., Nadal, M., Kapa, L. B., Perlin, M. H., Andrews, D. L. and Gold, S. E.** (2008) DelsGate, a robust and rapid gene deletion construction method. *Fungal Genet. Biol.* **45**, 379-388.
- Gerst, J. E., Ferguson, K., Vojtek, A., Wigler, M. and Field, J.** (1991) Cap Is a bifunctional component of the *Saccharomyces cerevisiae* adenylyl cyclase complex. *Mol. Cell. Biol.* **11**, 1248-1257.
- Gold, S. E., Brogdon, S. M., Mayorga, M. E. and Kronstad, J. W.** (1997) The *Ustilago maydis* regulatory subunit of a cAMP-dependent protein kinase is required for gall formation in maize. *Plant Cell*, **9**, 1585-1594.
- Gold, S., Duncan, G., Barrett, K. and Kronstad, J.** (1994) cAMP regulates morphogenesis in the fungal pathogen *Ustilago maydis*. *Genes Dev.* **8**, 2805-2816.
- Holliday, R.** (1961) Induced mitotic crossing-over in *Ustilago maydis*. *Genet. Res.* **2**, 231-248.
- Holliday, R.** (1974) *Ustilago maydis*. In: *Handbook of Genetics*. (King, R. C., ed.). New York: Plenum Press, pp. 575-595.
- Hubberstey, A., Yu, G., Loewith, R., Lakusta, C. and Young, D.** (1996) Mammalian CAP interacts with CAP, CAP2, and actin. *J Cell. Biochem.* **61**, 459-466.
- Kawamukai, M., Gerst, J., Field, J., Riggs, M., Rodgers, L., Wigler, M. and Young, D.** (1992) Genetic and biochemical analysis of the adenylyl cyclase-associated protein, cap, in *Schizosaccharomyces pombe*. *Mol. Biol. Cell*, **3**, 167-180.

- Kernkamp, M. F.** (1939) Genetic and environmental factors affecting growth types of *Ustilago zea*. *Phytopathology*, **29**, 473-484.
- Klose, J., de Sa, M. M. and Kronstad, J. W.** (2004) Lipid-induced filamentous growth in *Ustilago maydis*. *Mol. Microbiol.* **52**, 823-835.
- Klosterman, S., Perlin, M., Garcia-Pedrajas, M., Covert, S. and Gold, S.** (2007) Genetics of morphogenesis and pathogenic development of *Ustilago maydis*. In: *Fungal Genomics*. (Dunlap, J. C., ed.). St. Louis, MO: Academic Press, pp. 1-47.
- Kronstad, J. W.** (1997) Virulence and cAMP in smuts, blasts and blights. *Trends Plant Sci.* **2**, 193-199.
- Krüger, J., Loubradou, G., Regenfelder, E., Hartmann, A. and Kahmann, R.** (1998) Crosstalk between cAMP and pheromone signalling pathways in *Ustilago maydis*. *Mol. Gen. Genet.* **260**, 193-198.
- Krüger, J., Loubradou, G., Wanner, G., Regenfelder, E., Feldbrugge, M. and Kahmann, R.** (2000) Activation of the cAMP pathway in *Ustilago maydis* reduces fungal proliferation and teliospore formation in plant tumors. *Mol. Plant-Microbe Interact.* **13**, 1034-1040.
- Lee, N. and Kronstad, J. W.** (2002) Ras2 controls morphogenesis, pheromone response, and pathogenicity in the fungal pathogen *Ustilago maydis*. *Eukaryot Cell*, **1**, 954-966.
- Lila, T. and Drubin, D. G.** (1997) Evidence for physical and functional interactions among two SH3 domain proteins, an adenylyl cyclase-associated protein and the actin cytoskeleton. *Mol. Biol. Cell*, **8**, 367-385.
- Matsumoto, K., Uno, I., Oshima, Y. and Ishikawa, T.** (1982) Isolation and characterization of yeast mutants deficient in adenylate cyclase and cAMP-dependent protein kinase. *Proc. Natl Acad. Sci. USA*, **79**, 2355-2359.
- Muller, P., Katzenberger, J. D., Loubradou, G. and Kahmann, R.** (2003) Guanyl nucleotide exchange factor Ssl2 and Ras2 regulate filamentous growth in *Ustilago maydis*. *Eukaryot Cell*, **2**, 609-617.
- Quintero-Monzon, O., Jonasson, E. M., Bertling, E., Talarico, L., Chaudhry, F., Sihvo, M., Lappalainen, P. and Goode, B.L.** (2009) Reconstitution and dissection of the 600-kDa Srv2/CAP complex: Roles for oligomerization and cofilin-actin binding in driving actin turnover. *J Biol. Chem.* **284**, 10923-10934.
- Regenfelder, E., Spellig, T., Hartmann, A., Lauenstein, S., Bölker, M. and Kahmann, R.** (1997) G proteins in *Ustilago maydis*: transmission of multiple signals? *EMBO J.* **16**, 1934-1942.
- Rowell, J. B.** (1955) Functional rate of compatibility factors and an *in vitro* test for sexual compatibility with haploid lines of *Ustilago zea*. *Phytopathology*, **45**, 370-374.

- Ruiz-Herrera, J., Leon, C. G., Carabez-Trejo, A. and Reyes-Salinas, E.** (1996) Structure and chemical composition of the cell walls from the haploid yeast and mycelial forms of *Ustilago maydis*. *Fungal Genet. Biol.* **20**, 133-142.
- Shah, D. and Madden, L.** (2004) Nonparametric analysis of ordinal data in designed factorial experiments. *Phytopathology*, **94**, 33-43.
- Shima, F., Okada, T., Kido, M., Sen, H., Tanaka, Y., Tamada, M., Hu, C., Yamawaki-Kataoka, Y., Kariya, K. and Kataoka, T.** (2000) Association of yeast adenylyl cyclase with cyclase-associated protein CAP forms a second Ras-binding site which mediates its Ras-dependent activation. *Mol. Cell. Biol.* **20**, 26-33.
- Tsukuda, T., Carleton, S., Fotheringham, S. and Holloman, W.** (1988) Isolation and characterization of an autonomously replicating sequence from *Ustilago maydis*. *Mol. Cell. Biol.* **8**, 3703-3709.
- Yu, J., Wang, C., Palmieri, S. J., Haarer, B. K. and Field, J.** (1999) A cytoskeletal localizing domain in the cyclase-associated protein, CAP/Srv2p, regulates access to a distant SH3-binding site. *J Biol. Chem.* **274**, 19985-19991.

Table 3.1. Pathogenicity and gall formation in $\Delta cap1$ strains

Genotype	No. infected plants	Average disease index ^a	No. plants with tumors	Percentage plants with tumors
<i>alb1</i> x <i>a2b2</i>	60	3.6a	51	85%
<i>alb1</i> x <i>a2b2</i> $\Delta cap1$	60	2.9b	47	78%
<i>alb1</i> $\Delta cap1$ x <i>a2b2</i>	60	2.9b	48	80%
<i>alb1</i> $\Delta cap1$ x <i>a2b2</i> $\Delta cap1$	60	1.2c	21	35%
SG200	60	3.2a	59	98%
<i>mfa1 pra1 mfa2 bW2 bE1</i>				
SG200 + ectopic construct integration	60	3.5a	59	98%
SG200 $\Delta cap1$	60	1.1b	28	47%

^a Average disease index of three trials on day 14. The disease index ranges from 0 to 5, with 0 = no disease symptoms, 1 = chlorosis or anthocyanin production, 2 = leaf gall, 3 = small stem gall, 4 = large stem gall, and 5 = plant death. The letter given to the right of the average disease index indicates statistical significance as determined by non-parametric analysis.

Table 3.2. Strains of *Ustilago maydis* used in this study

Strain	Genotype	Reference
1/2	<i>a1b1</i> (521)	Gold et al., 1997
2/9	<i>a2b2</i>	Gold et al., 1997
1/9	<i>a1b1uac1::ble</i>	Gold et al., 1997
7/14	<i>a1b1gpa3::ble</i>	Regenfelder et al., 1997
17/13	<i>a1b1Δcap1::cbx</i>	This study
17/16	<i>a1b1Δcap1::cbx</i>	This study
17/28	<i>a2b2Δcap1::cbx</i>	This study
17/29	<i>a2b2Δcap1::cbx</i>	This study
SG200	<i>mfa1 pra1 mfa2 bW2 bE1</i>	Bölker et al., 1995
17/32	SG200 background, <i>cbx</i>	This study
17/30	SG200 background, <i>Δcap1::cbx</i>	This study
17/31	SG200 background, <i>Δcap1::cbx</i>	This study

Table 3.3. Primer sequences used in this study

Primer ID	Primer Sequence
CapP1	5'-TAGGGATAACAGGGTAATCGCGATGCAGGAAG AGTATGAAAA-3'
CapP2	5'-GGGGACAAGTTTGTACAAAAAAGCAGGCTAATG TTGCTGATAAACGGGGGATG-3'
CapP3	5'-GGGGACCACTTTGTACAAGAAAGCTGGGTAGGGG CAGGCGATCCTTCTGACT-3'
CapP4	5'-ATTACCCTGTTATCCCTACAAAGCTGTTCGTAGTTG AGACCAT-3'
DonrR	5'-GTGGCGAAACCCGACAGGACT-3'
JT021	5'-AACACGAACGGACGCAACACAAAC-3'
JT042	5'-CCAGGCATCGGAACTTGAG-3'
JT043	5'-GCCTCGCAGCTCGGGATTC-3'
JT060	5'-AAAAAGGATCCATGTCGGCTCCAGGCATC-3'
JT061	5'-AAAAAAGCATGCCATGGTGGCGCTGATTTGA-3'
JT070	5'-CATATGGGAGAGCGCAGACTCAAGGG-3'
JT071	5'-CATATGGGGAACCAGCTCCAACAG-3'
JT072	5'-CATATGATGTCGGCTCCAGGCATC-3'
JT073	5'-CATATGAGCAGTGTGAGCAACAACCTTC-3'

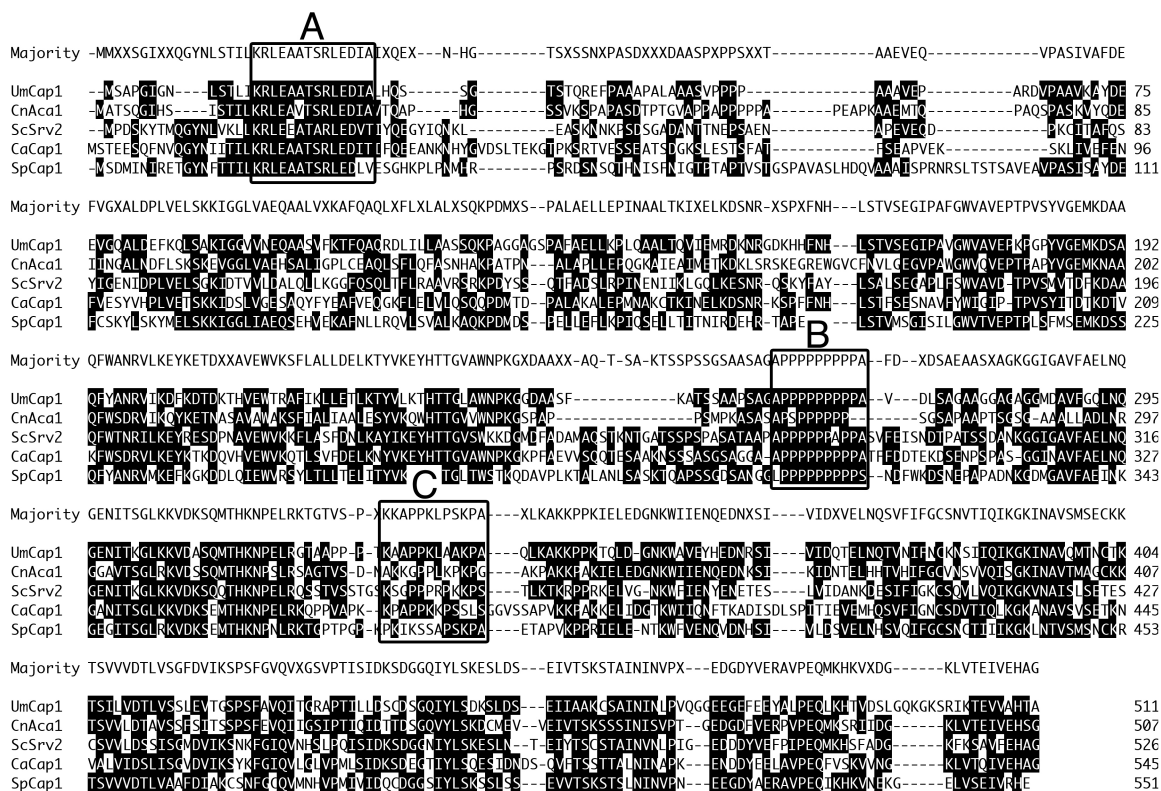


Figure 3.1. Protein alignment of the putative *U. maydis* Cap1 sequence with fungal CAP/Srv2 homologs. The protein sequences of CAP/Srv2 homologs from *U. maydis* (Um), *Cryptococcus neoformans* (Cn), *Saccharomyces cerevisiae* (Sc), *Candida albicans* (Ca), and *Schizosaccharomyces pombe* (Sp) were aligned using the Clustal W method. Residues that match or are highly similar to the consensus (majority) are highlighted in black. Boxes denote conserved protein domains. A: RLE/RLE motif B: polyproline region 1 (P1) C: polyproline region 2 (P2).

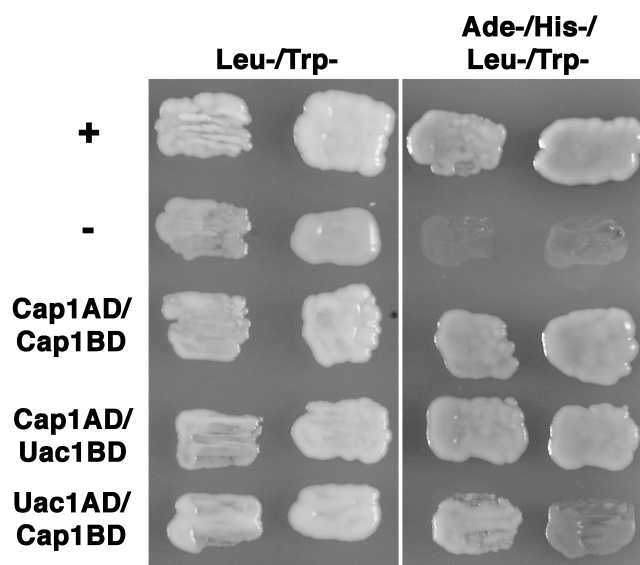


Figure 3.2. Cap1 protein-protein interactions. The *cap1* ORF and the 222 amino acid C-terminus of the *uac1* gene were cloned into yeast 2-hybrid expression vectors to produce Cap1AD (*cap1* ligated in frame to the GAL4 activation domain), Cap1BD (*cap1* ligated in frame to the GAL4 DNA binding domain), Uac1AD (the *uac1* gene fragment ligated in frame to the GAL4 activation domain), and Uac1BD (the *uac1* gene fragment ligated in frame to the GAL4 DNA binding domain). Vectors were cotransformed into yeast. Protein-protein interaction was indirectly assayed by the ability of transformed yeast colonies to grow on Ade-/His-/Leu-/Trp-SD medium as demonstrated by the positive and negative control transformations, labeled as + and -, respectively. Cap1AD/Cap1BD: yeast strains cotransformed with the Cap1AD and Cap1BD vectors. Cap1AD/Uac1BD: yeast strains cotransformed with Cap1AD and Uac1BD vectors. Uac1AD/Cap1BD: yeast strains cotransformed with Uac1AD and Cap1BD vectors.

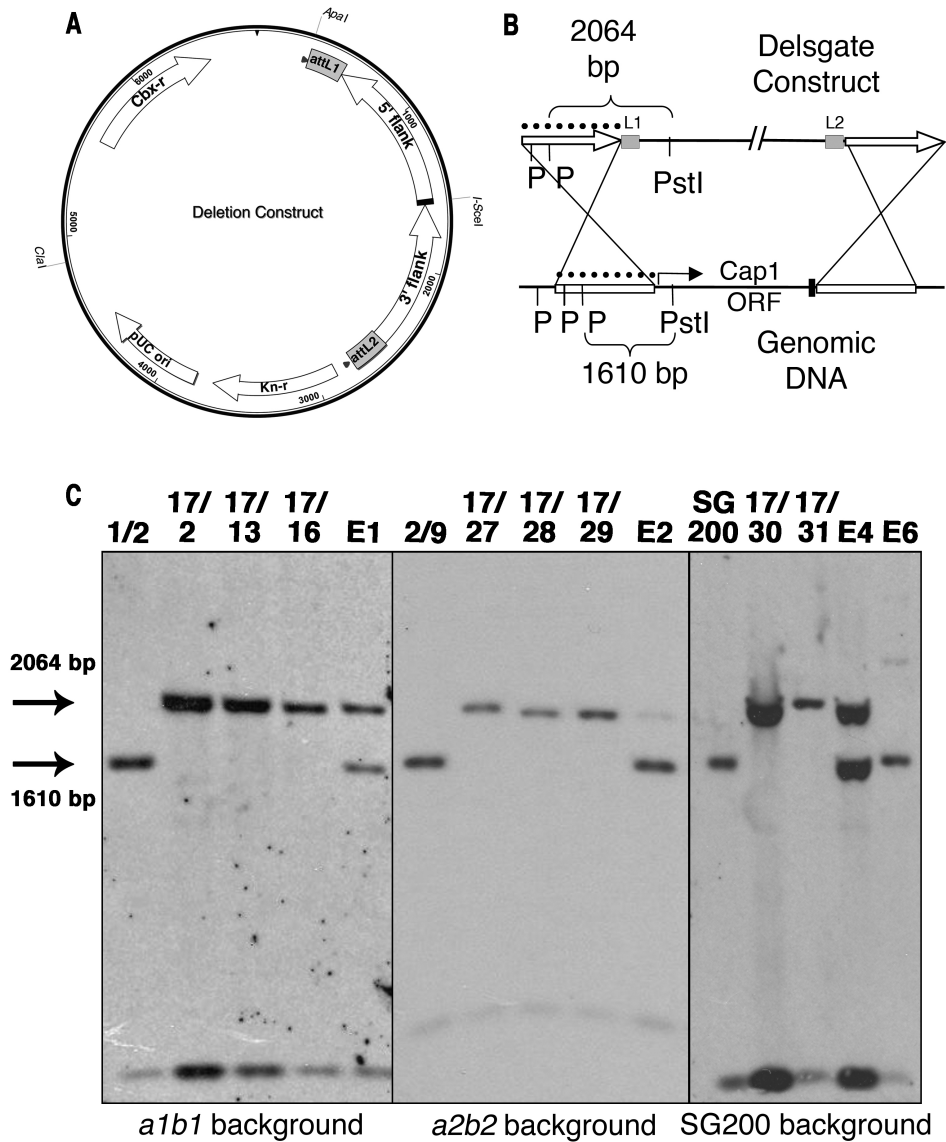


Figure 3.3. Deletion of the *cap1* gene in *U. maydis*. **A:** Diagram of the DelsGate *cap1* deletion construct. The plasmid contains a carboxin resistance gene (Cbx-r) and 1.0 kb fragments corresponding to the 5' and 3' flanks of the *cap1* gene. **B:** Diagram of the homologous recombination of the I-Sce-I linearized deletion construct. The dotted line represents the 1.0 kb fragment of the 5' flank utilized as a probe for Southern blot analysis. **C:** Southern blot analyses of *cap1* transformants. Each lane contains approximately 10 μ g of *Pst*I digested genomic DNA per strain. Arrows mark the positions of the expected hybridization pattern for wild type and deletion strains (1.6 and 2.1 kb, respectively). E1, E2, E4, and E6 are strains with ectopic integration of the deletion construct.

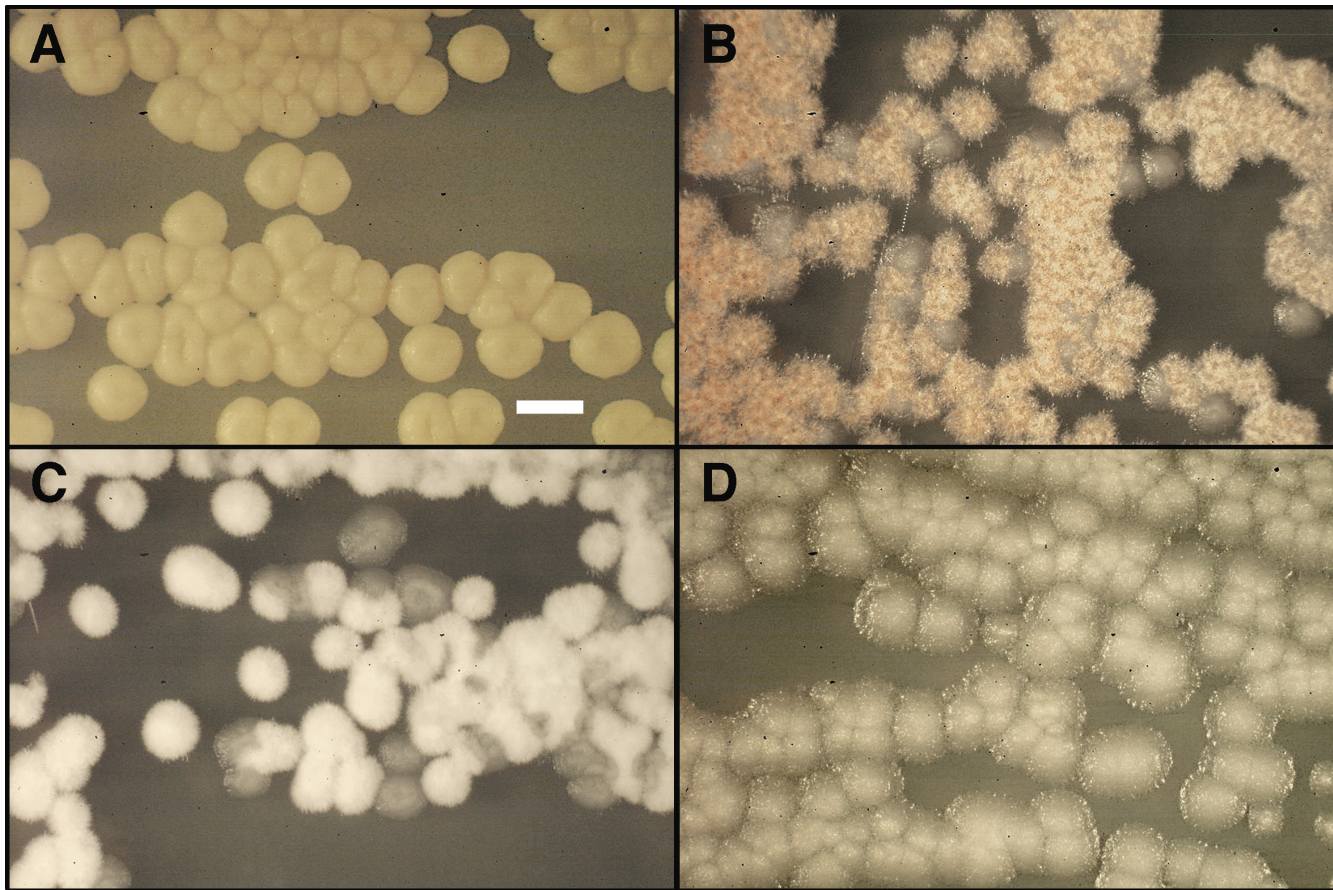


Figure 3.4. Effect of *cap1* deletion on colony morphology. Initial $\Delta cap1$ transformant colonies were dark and filamentous, but subsequent transfer to fresh PDA plates resulted in mixed populations of dark/filamentous colonies, white/filamentous colonies, and smooth yeast colonies. Individual colonies isolated from $\Delta cap1$ strain 17/16 that corresponded to each phenotype were selected and streaked onto fresh PDA plates, incubated at 30°C for 4 days, and observed for resultant colony morphologies. A: Wild type strain 1/2. B: Streak of a dark/filamentous colony derived from $\Delta cap1$ strain 17/16. C: Streak of a white/filamentous colony derived from $\Delta cap1$ strain 17/16. D: Streak of a smooth yeast colony derived from $\Delta cap1$ strain 17/16. Bar = 2 mm.

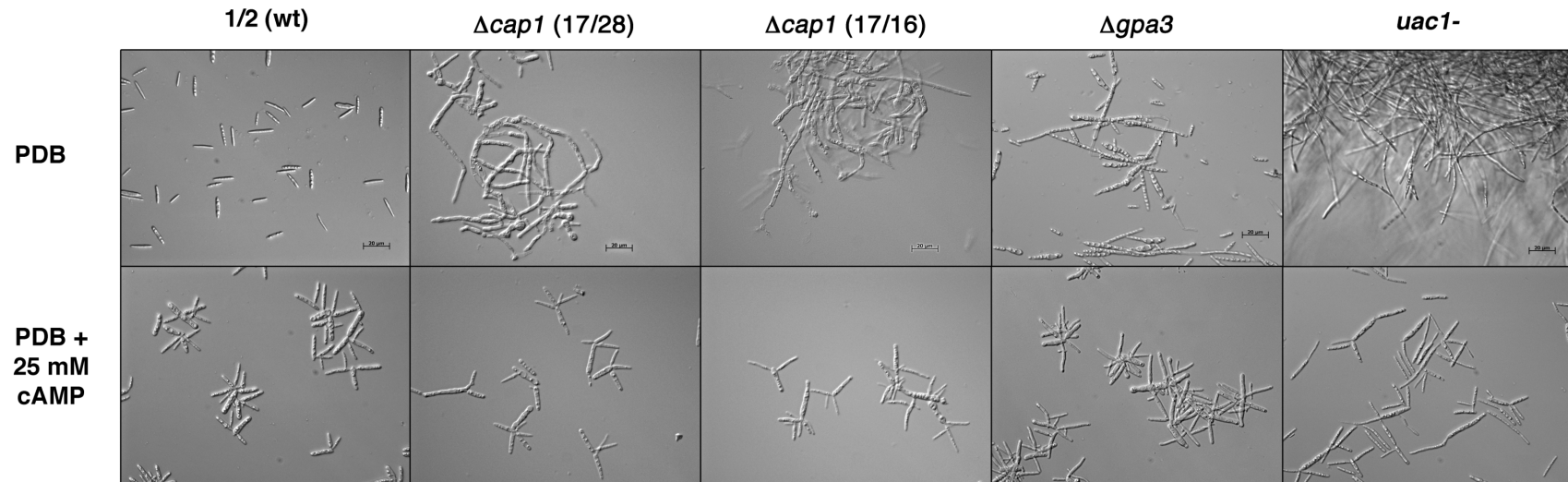


Figure 3.5. Morphology of *U. maydis* strains defective in cAMP production. The designated *U. maydis* strains were grown in PDB and PDB amended with 25 mM cAMP and observed for differences in morphology. Bar = 20 μ m.

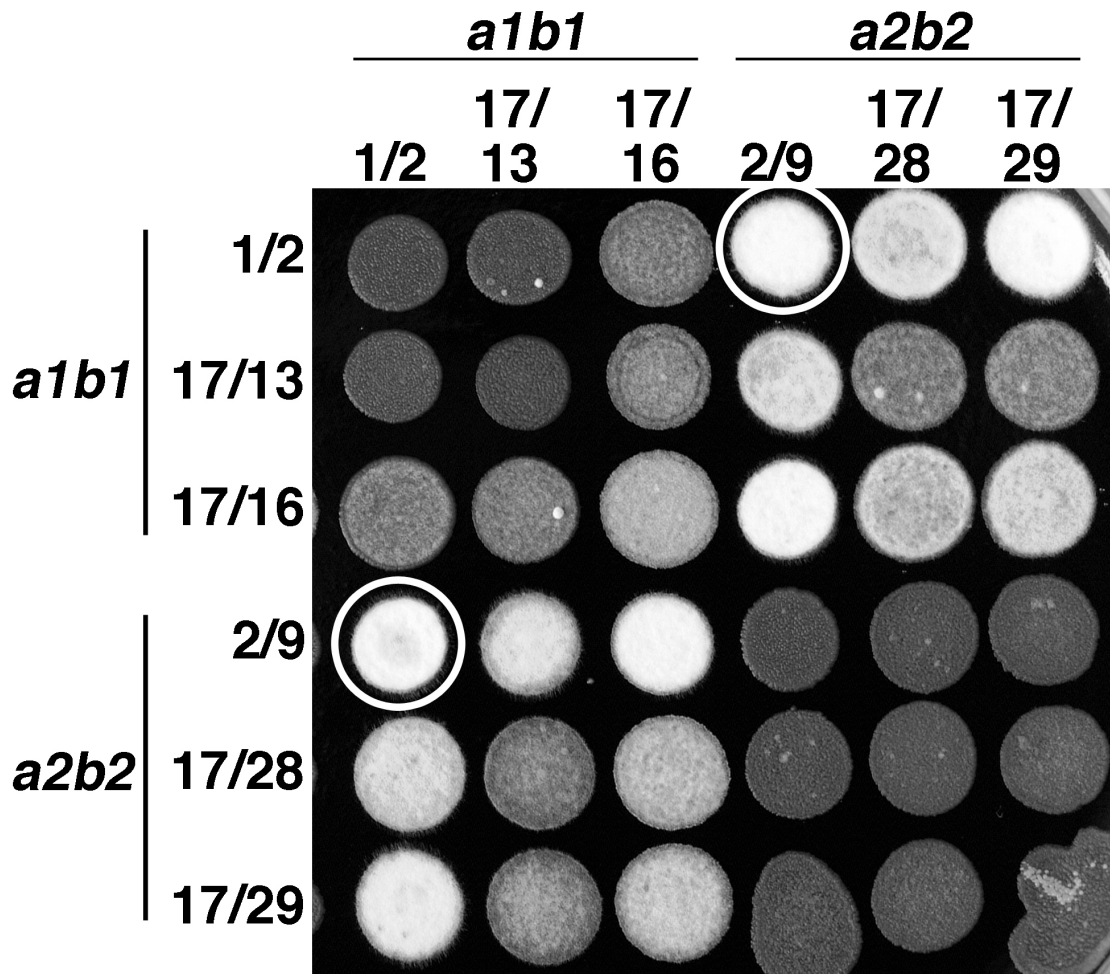


Figure 3.6. Mating response of $\Delta cap1$ strains. Strains were co-spotted onto mating plates containing charcoal and observed for the production of mating filaments signifying a successful mating interaction. White circles indicate a positive mating response between two compatible wild type strains.

CHAPTER 4

IDENTIFICATION AND CHARACTERIZATION OF CAB1, A POTENTIAL cAMP BINDING PROTEIN AND NEUROPATHY TARGET ESTERASE (NTE) HOMOLOG IN *USTILAGO MAYDIS*

INTRODUCTION

Ustilago maydis, the causal agent of corn smut, has emerged as a basidiomycete model system for the study of signaling pathways affecting dimorphism and disease development (for review, see Klosterman et al, 2007). Two interconnected signaling pathways mediate the filamentation process: the pheromone responsive MAP kinase cascade and the environment-responsive cAMP/PKA pathway. Fusion of haploid budding cells and subsequent dikaryon formation is controlled genetically by the *a* and *b* mating type loci (Holliday, 1961; Banuett, 1995; Rowell, 1995). Filamentous growth of haploid cells can also be triggered by environmental signals that include nutrient and nitrogen deprivation (Kernkamp, 1939; Banuett and Herskowitz, 1994) or exposure to air, acidic pH, or lipids (Gold et al 1994; Ruiz-Herrera et al, 1995; Klose et al, 2004).

Proper regulation and function of the cAMP/PKA pathway are required for virulence and pathogenicity of *U. maydis*. Components of this pathway include Gpa3, a G-protein α subunit;

Uac1, adenylate cyclase; Ubc1, the PKA regulatory subunit; and Adr1, the PKA catalytic subunit. Disruption of genes upstream of the cAMP signal (caused by deletion or disruption of *gpa3* or *uac1*) results in a filamentous phenotype that can be rescued by addition of exogenous cAMP (Gold et al, 1994, Krüger et al, 1998). Disruption of the *adr1* gene encoding the catalytic subunit of PKA results in a similar filamentous phenotype but is not remedied by addition of cAMP (Dürrenberger *et al.*, 1998). Inactivation of the PKA regulatory subunit, effectively simulating a high level of cAMP by allowing constitutive activation of the PKA catalytic subunit, results in a multiple budding phenotype (Gold et al, 1994). Collectively, these results indicate that the absence of the cAMP signal results in filamentous growth and presence of cAMP promotes budding growth and suppresses filamentous growth in *U. maydis*.

Two lines of evidence suggest that an additional cAMP pathway in *U. maydis* influences cellular morphology. Krüger and colleagues reported that wild-type strains of *U. maydis* showed an induction of the pheromone gene *mfa* in the presence of 6 mM cAMP and a reduction of pheromone gene expression in the presence of 15 mM cAMP (1998). This dose-dependent effect of cAMP on *mfa* transcription was also observed in a strain of *U. maydis* lacking Ubc1, the only protein known to interact directly with cAMP (Hartmann et al, 1999). These results suggest that a second cAMP pathway, independent of Ubc1, mediates this transcriptional repression. A second line of evidence involves the pH-mediated filamentation pathway. Wildtype haploid cells grow as filaments when introduced to acidic medium (Ruiz-Herrera et al, 1995). Addition of 25 mM exogenous cAMP results in a reversion to the budding phenotype (Martinez-Espinoza et al, 2004). $\Delta ubc1$ mutants also filament when grown in acidic conditions and, although lacking the only known protein to interact with cAMP, are restored to budding growth with the addition

of 25 mM cAMP. These results suggest the existence of an alternate rPKA subunit or the presence of another factor that interacts with cAMP.

In this study, we have identified a putative protein in *U. maydis* that contains sequence similar to the cAMP binding domain of Ubc1. This protein has sequence similarity to neuropathy target esterase (NTE), a conserved eukaryotic protein that mediates phospholipid homeostasis (Glynn, 2005).

RESULTS

Identification of *U. maydis* proteins with putative cAMP binding domains. The Ubc1 protein sequence contains two adjacent cAMP binding domains (Figure 4.1a). The Ubc1 protein sequence spanning both domains (amino acids 213 to 463) was used to BLASTp search the *U. maydis* predicted protein set. A 159 amino acid segment (amino acids 1,151 to 1,309) of a hypothetical protein encoded by um01230 was similar to the second Ubc1 binding domain (amino acids 347 to 463) (Figure 4.1b). The um01230 ORF has a predicted length of 5,552 nucleotides and encodes a 1,883 amino-acid protein. Due to the presence of the putative cAMP binding domain, um01230 was dubbed *cab1* for cAMP binding protein. A BLASTp search of the *cab1* predicted protein sequence in the NCBI non-redundant protein database revealed that it is highly similar to fungal members of the NTE family, including sequences in *Saccharomyces cerevisiae* (YML059C), *Schizosaccharomyces pombe* (SPCC4B3.04c), and *Cryptococcus neoformans* (CNBD2140) (Figure 4.2). In addition to the predicted cAMP binding domain, sequence analysis using the Conserved Domain Database (CDD) predicts a fungal patatin-like

phospholipase domain in the C-terminus of Cab1 that is present in all NTE family members (Marchler-Bauer et al, 2005) (Figure 4.2a).

Deletion of the *U. maydis* NTE homolog *cab1*. To characterize the function of Cab1 in *U. maydis*, the entire *cab1* ORF was replaced by a carboxin resistance gene via homologous recombination (Figure 4.3). The *EcoRI* fragment of the pCR2.1-cabko deletion construct was introduced into the *alb1* wild type strain 1/2 (Table 4.1). Three independent $\Delta cab1$ strains were isolated and verified by diagnostic PCR (data not shown). To isolate $\Delta cab1$ strains in additional mating backgrounds, the $\Delta cab1$ strain 6/35 and the compatible wild type strain 2/9 were co-inoculated into 7 day-old Golden Bantam maize seedlings. Individual progeny strains were screened for carboxin resistance and verified by diagnostic PCR (data not shown). The genotypes of progeny strains were confirmed with mating assays (data not shown). Deletion of *cab1* in all strains was confirmed by Southern blot analysis (Figure 4.3).

Effects of *cab1* deletion on morphology, mating, and pathogenesis. Deletion of *cab1* had no discernible effect on cellular morphology. The $\Delta cab1$ strains grew in PDB at a rate similar to wild type (data not shown) and produced polar buds in a manner similar to wild type (Figure 4.4). To observe if the absence of Cab1 would affect cellular response to cAMP, $\Delta cab1$ strains were treated with exogenous cAMP. Both wild type and $\Delta cab1$ cells responded by forming multiple buds with an increased incidence of lateral budding, with no statistical differences observed between wild type and $\Delta cab1$ strains (Table 4.2).

Deletion of *cab1* had no effect on mating ability (data not shown) or pathogenicity (Table 4.3). Both wild type and mutant crosses formed an abundance of white filamentous growth on charcoal mating plates, indicating a successful mating reaction. Inoculation of compatible $\Delta cab1$

strains into week-old corn seedlings resulted in symptom development and gall formation similar to inoculation with wild type strains (Table 4.3).

Effects of *cab1* deletion on growth rate. The growth rate of wild type and $\Delta cab1$ strains in PDB, minimal, and complete medium was observed. In preliminary experiments, all strains grew well in PDB and minimal medium, but growth of $\Delta cab1$ strains in complete medium appeared to be reduced (data not shown). Complete medium contains all the components of minimal medium, but is enriched with yeast extract and casamino acids (Holliday, 1974). In complete medium prepared without yeast extract, both wild type and $\Delta cab1$ strains grew at a similar rate, reaching an O.D. near 1.0 by 12 hours post-inoculation (Figure 4.5A). In complete medium, however, wild type cells grew exponentially by 12 hours post-inoculation, but $\Delta cab1$ strains grow at a significantly slower rate (Figure 4.5B). Growth of strains in complete medium prepared without casamino acids was similar to complete medium (data not shown). The reduced growth rate of $\Delta cab1$ strains was observed up to 48 hours post-inoculation (data not shown).

DISCUSSION

In this study, we identified um01230 as a potential cAMP binding protein based on sequence homology to Ubc1, the PKA regulatory subunit. Furthermore, based on sequence homology, we determined that um01230 encodes the NTE homolog in *U. maydis*. NTE is a conserved eukaryotic protein originally identified in humans as a target for organophosphates that cause a delayed-onset paralyzing neuropathy (Johnson, 1969). Homologs of the Nte gene were subsequently identified in all sequenced eukaryotic genomes and have been characterized

in mice, flies, and yeast (Kretzschmar et al, 1997; Lush et al, 1998; Moser et al, 2000; Quistad et al, 2003; Murray and McMaster, 2005). Although NTE homologs have not been found in plants, the catalytic domain of the NTE protein does share some sequence similarity with a family of plant proteins with phospholipase activity, suggesting the protein function is conserved in all eukaryotes even if the regulatory domains have diverged (Glynn, 2005).

Members of the NTE protein family catalyze the hydrolysis of membrane lipids, specifically phosphatidylcholine (PtdCho) (van Tienhoven et al, 2002; Zaccheo et al, 2004). In yeast, NTE has been demonstrated to interact with Sec14p, a cytoplasmic phosphatidylinositol/phosphatidylcholine transferase (Murray and McMaster, 2005). This interaction facilitates the degradation of PtdCho in yeast cells, which is countered by an increase in the uptake of choline for PtdCho synthesis, suggesting a key role for NTE in turnover and lipid composition of membranes. However, the *Nte1* gene in *Saccharomyces cerevisiae* is not essential for viability and gene knockout strains yield no observable phenotypes (Giaever et al, 2002; Zaccheo et al, 2004). The NTE homolog in *U. maydis*, *cab1*, is also not essential for viability. $\Delta cab1$ cells grow vigorously in PDB and are indistinguishable from wild type under microscopic examination (Figure 4.4). Wild type and the $\Delta cab1$ strains respond similarly to treatment with exogenous cAMP (Table 4.2). This result is unsurprising, since both wild type and $\Delta cab1$ strains contain a copy of *ubc1*, which encodes a known mediator of the cAMP response. Additionally, mating and pathogenicity appear to be unaffected by deletion of *cab1* (Table 4.3).

However, $\Delta cab1$ strains do show a distinctive growth defect in media enriched with yeast extract (complete medium) (Figure 4.5). It is interesting to note that the wild type also grows more slowly in media containing yeast extract, but does reach exponential growth after

incubation for several hours, unlike $\Delta cab1$ mutants. The growth rate of $\Delta cab1$ strains in complete medium remains significantly reduced up to 24 hours, indicating that deletion of *cab1* does affect the ability of *U. maydis* cells to grow in enriched medium. The exact mechanism of the $\Delta cab1$ growth defect cannot be ascertained without further investigation of Cab1 function in *U. maydis*.

The evidence provided by this study indicates that Cab1 does not play a significant role in cAMP signaling and morphology in *U. maydis*. Future investigations are necessary to identify other possible downstream targets of cAMP signaling and fill the remaining gaps in knowledge of this important signaling pathway.

MATERIALS AND METHODS

Bioinformatic analyses. The amino acid sequence spanning both cAMP binding domain of Ubc1 (amino acids 213 to 463, indicated in Figure 4.1) was used to BLASTp search the *U. maydis* genome (<http://mips.gsf.de/genre/proj/ustilago>). Proteins identified in the cAMP domain genome search were subsequently used to BLAST search the NCBI non-redundant protein database (Altschul et al, 1997).

Plasmid construction. The *cab1* deletion construct was created using overlap PCR as described by Davidson and colleagues (2002). In brief, the first amplifications utilized three sets of primers (Table 4.4) designed to amplify 1 kb regions upstream and downstream of the *cab1* ORF and the *Ustilago* carboxin resistance gene (Keon et al, 1991). Amplifications were performed using Expand High Fidelity *Taq* polymerase (Roche, Indianapolis, IN). The three products were gel purified using a Qiagen gel extraction kit, quantified by measuring absorbance

at 260 nm, and 25 ng of each product were used as template for the overlap PCR. Primers JTCAB1 and JTCAB6 were utilized to amplify the overlapping templates, and the resultant product was then amplified using nested primers JET001 and JET002 (Table 4.1) to produce a 3.8 kb product. The final PCR product was cloned into vector pCR2.1 using a TOPO Cloning Kit as directed by the manufacturer's directions (Invitrogen, Carlsbad, CA). Clones were screened by blue/white selection on LB plates amended with 50 µg/ml ampicillin and 40 µg/ml X-gal. Plasmid DNA was extracted from a subset of clones and digested with *EcoRI* and *EcoRV* restriction enzymes (New England Biolabs, Ipswich, MA) to identify clones containing the entire deletion construct. The final construct, pCR2.1-cab1ko, was verified by sequencing the 5' and 3' *cab1* flanking regions.

Fungal strains and growth conditions. The *U. maydis* strains used in this study are presented in (Table 4.1). Fungal cultures were routinely grown at 30°C on potato dextrose agar (PDA, Sigma, St. Louis, MO) plates supplemented to 2% agar (2PDA) or in potato dextrose broth (PDB) with shaking at 200 rpm. For protoplast production, strains were grown in YEPS medium (1% yeast extract, 2% peptone, 2% sucrose). Transformants were grown on double complete medium (DCM)-2% agar medium supplemented with 1 M sorbitol and 3 µg/ml carboxin. Mating assays were performed on complete medium containing 1% activated charcoal (Holliday, 1974). cAMP response growth assays were performed in PDB amended with 10 or 25 mM cAMP (Sigma). Growth assays were conducted using minimal and complete medium as described by Holiday (1974), as well as with preparations of complete medium without the addition of yeast extract or casamino acids as described.

***U. maydis* transformation.** Protoplasts of wildtype strain 1/2 and 2/9 were created using a protocol modified from Tsukuda et al, (1988) as described previously (Gold et al, 1994;

Mayorga and Gold, 1998). Briefly, strains were grown overnight in 100 ml YEPS to an OD₆₀₀ of 1.0. Cells were washed, concentrated, and treated with 20 mg/ml Novozyme (Novozymes, Denmark) for 10 m. Protoplasts were washed and resuspended in cold STC (10 mM Tris-HCL pH 7.5, 100 mM CaCl₂, 1 M sorbitol). Protoplasts were transformed immediately or amended with 7% DMSO and stored at -80°C. When transformant colonies became visible (4-10 days post-inoculation), individual colonies were transferred to 2PDA plates amended with 3 µg/ml carboxin (2PDA-cbx). Genomic DNA was isolated from carboxin-resistant strains and screened for homologous recombination of the deletion construct with PCR primers JT011 and JT012 (Table 4.1).

Isolation of progeny from teliospores. Week-old ‘Golden Bantam’ (Rich Farm Garden Supply, Winchester, IN) maize seedlings were inoculated with a suspension containing 5×10^7 cells/ml of the $\Delta cab1$ strain 6/35 and wild type strain 2/9 (Table 4.2). Mature leaf and stem galls were isolated 28 days post-inoculation and air dried. Gall tissue was ground in a 1.5% copper sulfate solution and filtered through cheesecloth. Teliospores were washed in sterile water and germinated on 2PDA plates. Resultant colony cells were suspended in PDB, spread on 2PDA-cbx plates, and grown 24-48 hours at 30°C. Individual colonies were isolated and further characterized to confirm gene deletion and mating background.

Confirmation of gene deletion. Gene deletion for all strains was confirmed by Southern analysis. Approximately 10 µg of genomic DNA from transformant, progeny, and wild type strains were digested with *EcoRI* and run on a 0.8% agarose gel at 50 V until the bromophenol blue dye migrated to within 1 cm of the end of the gel. The gel was washed in 0.4 M NaOH and blotted onto a Hybond nylon membrane (Ambion, Foster City, CA) overnight. Blots were

probed with DIG-labeled PCR product corresponding to a 900-bp fragment downstream of the 3' flank to determine the presence or absence of the wild-type locus (Figure 4.3).

Mating, pathogenicity, and morphology assays. To ascertain the mating background of progeny strains isolated from the $\Delta cab1$ /wild type cross, individual strains were co-spotted with wild type strains 1/2, 2/9, 2/11, and 2/14 (Table 4.1) on charcoal mating plates. Plates were incubated at room temperature in the dark for 24 hours and observed for the formation of white filaments that indicate a successful mating reaction had taken place (Holliday, 1974). Compatible $\Delta cab1$ strains were cospotted and observed using the same protocol.

Pathogenicity assays were carried out on the susceptible maize variety 'Golden Bantam'. Seedlings were inoculated just above the soil line seven days after planting with a 1×10^6 cells/ml suspension of compatible deletion strains. Disease symptom data were collected at 7, 10 and 14 days after inoculation. Disease ratings were as described previously by Gold et al., (1997). In summary, symptoms were rated 0–5 as follows: 0, no disease; 1, anthocyanin or chlorosis; 2, leaf galls; 3, small stem galls; 4, large stem galls; 5, plant death due to disease.

Cellular morphology was assayed in PDB and in PDB amended with 25 mM cAMP as described by Gold and colleagues (1994). Cell density, number of cell clusters, and lateral buds were tallied using an Improved Neubauer hemocytometer (Hausser Scientific, Horsham, PA), with $n = 100$ as the minimum number for cells observed per sample. Data from three independent trials was compared and analyzed for statistical significance with a Tukey's HSD test.

LITERATURE CITED

1. Altschul, S. F., T.L. Madden, A.A. Schaffer, J. Zhang, Z. Zhang, W. Miller, and D.J. Lipman. 1997. Gapped BLAST and PSI-BLAST: a new generation of protein database search programs. *Nuc. Acids Res.* 25:3389-3402.
2. Banuett, F. 1995. Genetics of *Ustilago maydis*, a fungal pathogen that induces tumors in maize. *Annu. Rev. Genet.* 29:179-208.
3. Banuett, F., and I. Herskowitz. 1994. Morphological transitions in the life cycle of *Ustilago maydis* and their genetic control by the *a* and *b* loci. *Exp. Mycol.* 18:247-266.
4. Davidson, Robert C., Jill R. Blankenship, Peter R. Kraus, Marisol de Jesus Berrios, Christina M. Hull, Cletus D'Souza, Ping Wang, and Joseph Heitman. 2002. A PCR-based strategy to generate integrative targeting alleles with large regions of homology. *Microbiology.* 148:2607-2615.
5. Dürrenberger, F., and J. Kronstad. 1999. The *ukc1* gene encodes a protein kinase involved in morphogenesis, pathogenicity and pigment formation in *Ustilago maydis*. *Mol. Gen Genet.* 261:281-289.
6. Giaever, G., A. M. Chu, L. Ni, C. Connelly, L. Riles, et al. 2002. Functional profiling of the *Saccharomyces cerevisiae* genome. *Nature.* 418:387-391.
7. Glynn, P. 2005a. A mechanism for organophosphate-induced delayed neuropathy. *Toxicol. Lett.*
8. Glynn, P. 2005b. Neuropathy target esterase and phospholipid deacylation. *Biochim. Biophys. Acta.* 1736:87-93.
9. Gold, S., G. Duncan, K. Barrett, and J. Kronstad. 1994. cAMP regulates morphogenesis in the fungal pathogen *Ustilago maydis*. *Genes Dev.* 8:2805-2816.
10. Gold, S. E., S. M. Brogdon, M. E. Mayorga, and J. W. Kronstad. 1997. The *Ustilago maydis* regulatory subunit of a cAMP-dependent protein kinase is required for gall formation in maize. *Plant Cell* 9:1585-1594.
11. Hartmann, H. A., J. Krüger, F. Lottspeich, and R. Kahmann. 1999. Environmental signals controlling sexual development of the corn smut fungus *Ustilago maydis* through the transcriptional regulator *prf1*. *Plant Cell* 11:1293-1305.
12. Holliday, R. 1961. Induced mitotic crossing-over in *Ustilago maydis*. *Genet. Res.* 2:231-248.
13. Holliday, R. 1974. *Ustilago maydis*. In *Handbook of Genetics*, edited by R. C. King. New York: Plenum Press.

14. Johnson, M. K. 1969. Delayed neurotoxic effect of some organophosphorus compounds - identification of phosphorylation site as an esterase. *Biochem. J.* 114:711-7.
15. Keon, J. P., G. A. White, and J. A. Hargreaves. 1991. Isolation, characterization and sequence of a gene conferring resistance to the systemic fungicide carboxin from the maize smut pathogen, *Ustilago maydis*. *Curr. Genet.* 19:475-481.
16. Kernkamp, M. F. 1939. Genetic and environmental factors affecting growth types of *Ustilago zaeae*. *Phytopathology* 29:473-484.
17. Klosterman, SJ, MH Perlin, M Garcia-Pedrajas, SF Covert, and SE Gold. 2007. Genetics of morphogenesis and pathogenic development of *Ustilago maydis*. In *Fungal Genomics*, edited by J. C. Dunlap. St. Louis, MO: Academic Press.
18. Klose, J., M. M. de Sa, and J. W. Kronstad. 2004. Lipid-induced filamentous growth in *Ustilago maydis*. *Mol. Microbiol.* 52:823-835.
19. Kretzschmar, D., G. Hasan, S. Sharma, M. Heisenberg, and S. Benzer. 1997. The Swiss cheese mutant causes glial hyperwrapping and brain degeneration in *Drosophila*. *J. Neurosci.* 17:7425-7432.
20. Krüger, J., G. Loubradou, E. Regenfelder, A. Hartmann, and R. Kahmann. 1998. Crosstalk between cAMP and pheromone signalling pathways in *Ustilago maydis*. *Mol. Gen Genet.* 260:193-198.
21. Lush, M. J., Y. Li, D. J. Read, A. C. Willis, and P. Glynn. 1998. Neuropathy target esterase and a homologous *Drosophila* neurodegeneration-associated mutant protein contain a novel domain conserved from bacteria to man. *Biochem. J.* 332:1-4.
22. Marchler-Bauer, A., J. B. Anderson, P. F. Cherukuri, C. DeWeese-Scott, L. Y. Geer, et al. 2005. CDD: a Conserved Domain Database for protein classification. *Nucl. Acids Res.* 33:D192-196.
23. Mayorga, M. E., and S. E. Gold. 1998. Characterization and molecular genetic complementation of mutants affecting dimorphism in the fungus *Ustilago maydis*. *Fung. Genet. Biol.* 24:364-376.
24. Moser, M., Y. Li, K. Vaupel, D. Kretzschmar, R. Kluge, P. Glynn, and R. Buettner. 2004. Placental failure and impaired vasculogenesis result in embryonic lethality for neuropathy target esterase-deficient mice. *Mol. Cell. Biol.* 24:1667-1679.
25. Murray, J. P. F., and C. R. McMaster. 2005. Deacylation of phosphatidylcholine by Nte1p functionally interacts with Sec14p. *FASEB J.* 19:A845-A845.
26. Quistad, G. B., C. Barlow, C. J. Winrow, S. E. Sparks, and J. E. Casida. 2003. Evidence that mouse brain neuropathy target esterase is a lysophospholipase. *Proc. Natl. Acad. Sci. USA.* 100:7983-7987.

27. Rowell, J. B. 1955. Functional rate of compatibility factors and an *in vitro* test for sexual compatibility with haploid lines of *Ustilago zaeae*. *Phytopathology* 45:370-374.
28. Ruiz-Herrera, J., C. G. Leon, L. Guevara-Olvera, and A. Carabez-Trejo. 1995. Yeast-mycelial dimorphism of haploid and diploid strains of *Ustilago maydis* in liquid culture. *Microbiology*. 141:695-703.
29. Tsukuda, T., S. Carleton, S. Fotheringham, and W. K. Holloman. 1988. Isolation and characterization of an autonomously replicating sequence from *Ustilago maydis*. *Mol. Cell. Biol.* 8:3703-3709.
30. van Tienhoven, M., J. Atkins, Y. Li, and P. Glynn. 2002. Human neuropathy target esterase catalyzes hydrolysis of membrane lipids. *J. Biol. Chem.* 277:20942-20948.
31. Zaccheo, O., D. Dinsdale, P. A. Meacock, and P. Glynn. 2004. Neuropathy target esterase and its yeast homologue degrade phosphatidylcholine to glycerophosphocholine in living cells. *J. Biol. Chem.* 279:24024-24033.

Table 4.1. Strains of *Ustilago maydis* used in this study.

Strain	Genotype	Reference
1/2	<i>alb1</i> (521)	Gold et al., 1997
2/9	<i>a2b2</i>	Gold et al., 1997
2/11	<i>a2b1</i>	Gold et al., 1997
2/14	<i>alb2</i>	Gold et al., 1997
6/34	<i>alb1Δcab1::cbx</i>	This study
6/35	<i>alb1Δcab1::cbx</i>	This study
6/38	<i>alb1Δcab1::cbx</i>	This study
6/39	<i>alb1Δcab1::cbx</i>	This study
6/40	<i>a2b2Δcab1::cbx</i>	This study
6/41	<i>a2b2Δcab1::cbx</i>	This study
6/42	<i>alb2Δcab1::cbx</i>	This study
6/43	<i>alb2Δcab1::cbx</i>	This study
6/44	<i>a2b1Δcab1::cbx</i>	This study
6/45	<i>a2b1Δcab1::cbx</i>	This study

Table 4.2. Response of $\Delta cab1$ to 25 mM cAMP

Strain	Time (h)	Cells incubated in PDB						Cells incubated in PDB + 25 mM cAMP					
		Cell density (10^6 /ml)	Total cells	Total units ^a	Avg cells/unit ^b	Max cells/unit	Total lateral buds	Cell density (10^6 /ml)	Total cells	Total units ^a	Avg cells/unit ^b	Max cells/unit	Total lateral buds
<i>(a1b1)</i>	8	15.1	303	207	1.46	3	6	37.9	757	421	1.80	15	21
	24	239.5	479	474	1.01	2	1	242	484	134	3.61	13	138
	48	357.5	715	706	1.01	3	5	434.5	869	344	2.53	17	281
<i>(a2b2)</i>	8	21.7	217	157	1.38	3	2	33.7	674	332	2.03	17	55
	24	207	414	411	1.01	2	0	239.5	479	91	5.26	23	145
	48	399	798	792	1.01	2	2	354.5	709	152	4.66	30	236
<i>(a1b1)</i>	8	10.4	207	131	1.58	6	4	28.1	562	323	1.74	10	24
	24	216.5	433	429	1.01	2	1	275	550	225	2.44	21	134
	48	281.5	563	550	1.02	2	7	401	802	333	2.41	15	241
<i>(a2b2)</i>	8	8.7	173	118	1.47	4	1	37.5	750	434	1.73	9	41
	24	194.5	389	385	1.01	2	0	238.5	477	177	2.69	15	144
	48	297.5	595	590	1.01	2	2	472.5	945	312	3.03	13	337

Results from one morphological assay of $\Delta cab1$ strains. ^a A unit was defined as a single cell or a multiple cells in which the cells have failed to completely detach from the mother cell during budding. ^b Average cells/unit was calculated by dividing the total cells by the total number of units observed. Statistical analysis did not find any significant differences between the three experimental replications. No significant difference was found between wild type strains and $\Delta cab1$ strains or between strains with different mating backgrounds.

Table 4.3. Pathogenicity and gall formation in $\Delta cab1$ strains

Strain	No. infected plants	Average disease index ^a	No. plants with tumors	Percentage plants with tumors
<i>alb1</i> x <i>a2b2</i>	60	2.02	34	56.7%
<i>alb1</i> x <i>a2b2</i> $\Delta cab1$	60	1.78	31	51.7%
<i>alb1</i> $\Delta cab1$ x <i>a2b2</i>	57	2.26	39	68%
<i>alb1</i> $\Delta cab1$ x <i>a2b2</i> $\Delta cab1$	60	1.88	36	60%

^aAverage disease index of three trials on day 10. The disease index ranges from 0 to 5, with 0 = no disease symptoms, 1 = chlorosis or anthocyanin production, 2 = leaf gall, 3 = small stem gall, 4 = large stem gall, and 5 = plant death.

Table 4.4 Primer sequences used in this study.

Primer ID	Primer Sequence
JTCab1	5'-ATGGCAGGTAGTGATAAG-3'
JTCab2	5'-TCCTGTGTTCTCCTGCTATGTGGTCGACGCCTCTTG-3'
JTCab3	5'-CAAGAGGCGTCGACCACATAGCAGGAGAACACAGGA-3'
JTCab4	5'-AAGTGTCTGGCCTGCGTCCGACTTGTCAGTTGTCAGC-3'
JTCab5	5'-GCTGACAACTGCAAGTCGGACGCAGGCCAGACACTT-3'
JTCab6	5'-ATGAGAGGCGAGACACGT-3'
JT001	5'-AGCTTTTGGCCTTCTCGGCGTCACC-3'
JT002	5'-AGCGCGATCCGACGAAGTAAATACC-3'
JT011	5'-GCGAAACTATGCACAGCGACGACA-3'
JT012	5'-AGATGACGGTAGCGAAGCCAGATG-3'

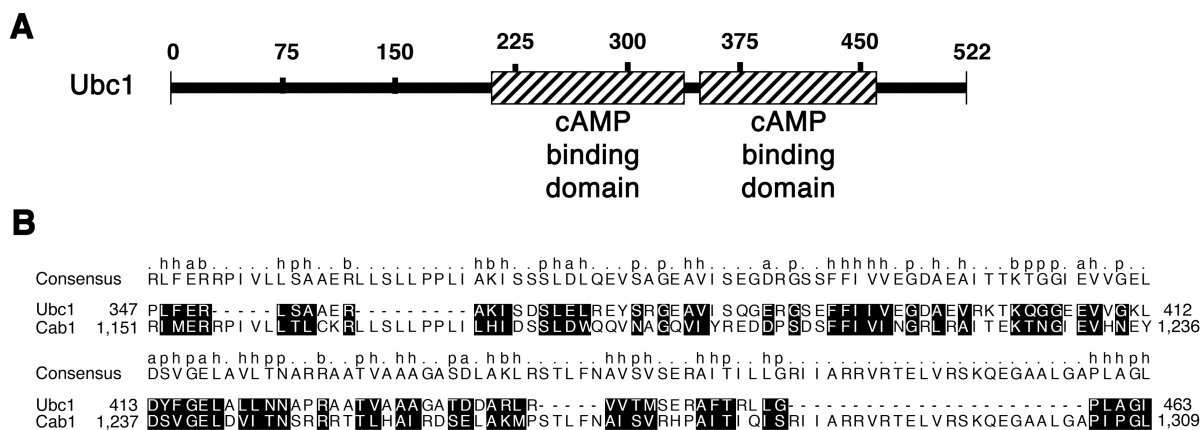


Figure 4.1. Alignment of the Ubc1 cAMP binding domain with the predicted um01230/Cab1 protein sequence. A: Diagrammatic representation of the Ubc1 protein and location of the cAMP binding domains. B: Alignment of the second cAMP binding domain of Ubc1 to a 159 amino acid region of the um01230/Cab1 protein. Residues that have the same functional classification (i.e. acidic or basic) are shaded and labeled above the consensus sequence. a: acidic; b: basic; h: hydrophobic; p: polar. Sequences were aligned using the ClustalW method.

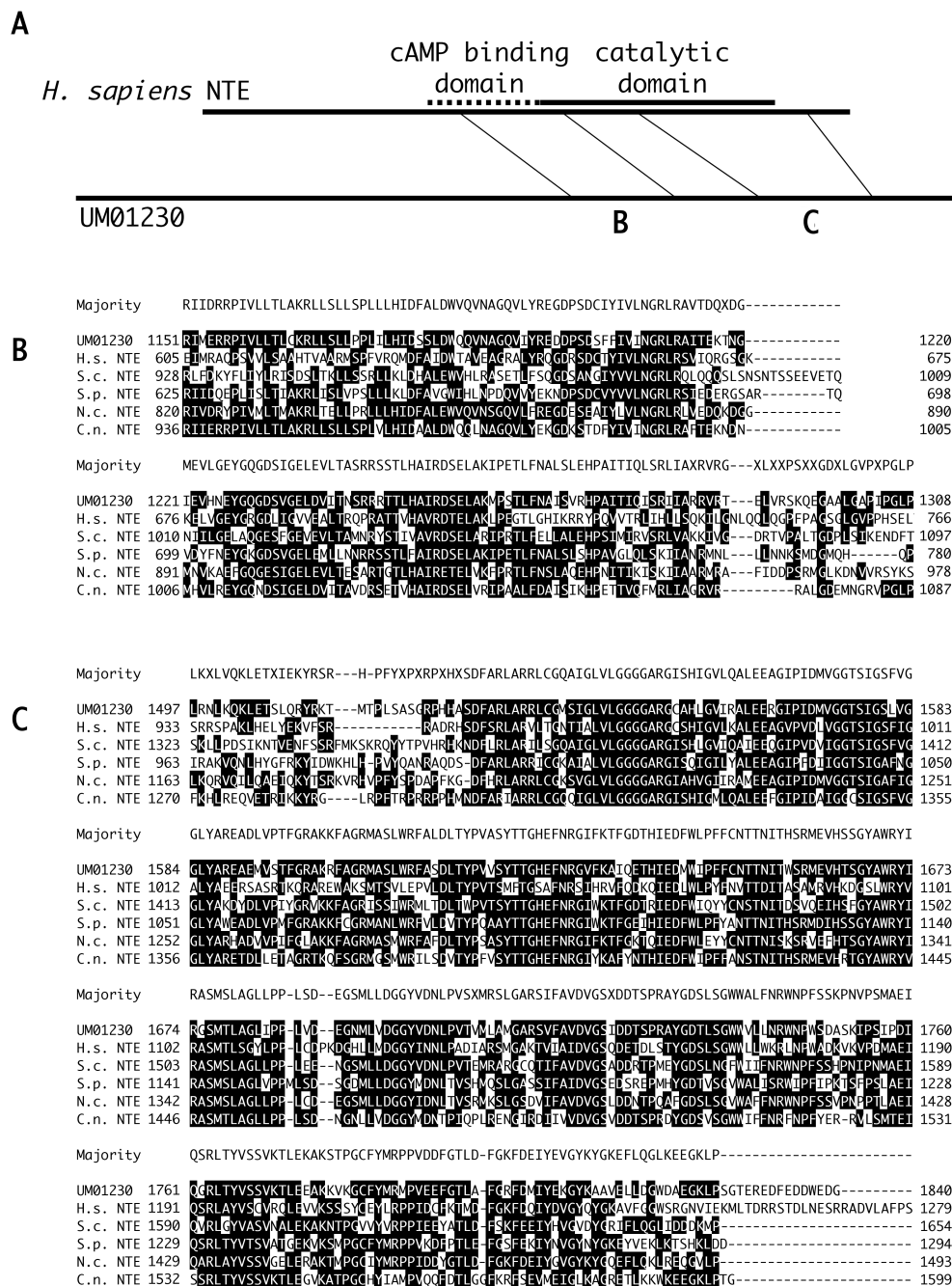


Figure 4.2. Alignment of the predicted Cab1 protein sequence and members of the neuropathy target esterase (NTE) protein family. **A:** Diagram of the protein alignment of Cab1 and the *H. sapiens* NTE protein sequence. The dotted line indicates the location of the conserved cAMP binding domain, and the solid region indicates a highly homologous esterase domain. Regions of extensive homology are designated by B and C. **B:** Alignment of the cAMP binding region of human and fungal NTE homologs. **C:** Alignment of the esterase catalytic domain of human and fungal NTE homologs. H.s.: *Homo sapiens*; S.c.: *S. cerevisiae*; S.p.: *S. pombe*; N.c.: *N. crassa*; C.n.: *C. neoformans*.

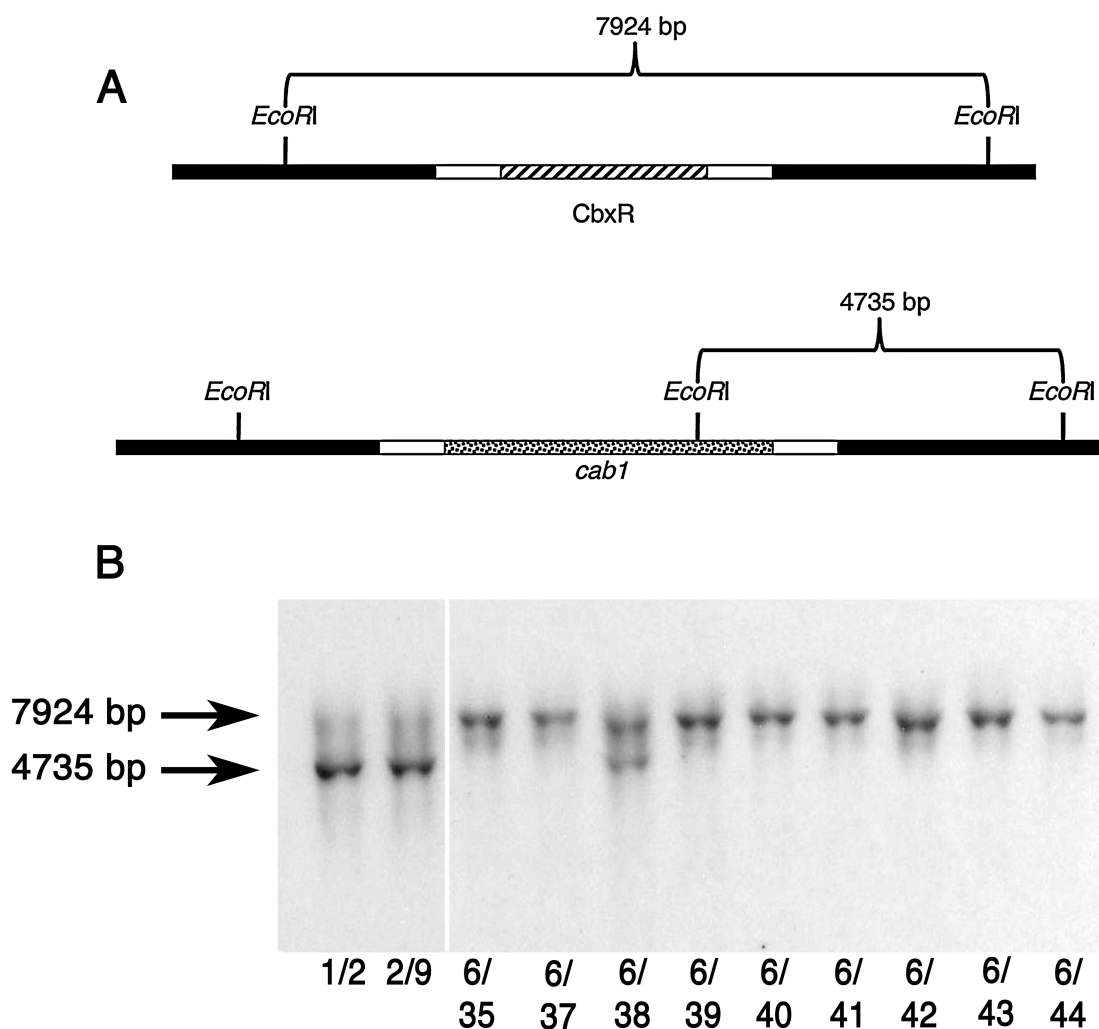


Figure 4.3. Southern blot analysis of putative $\Delta cab1$ strains. A: Diagrammatic representation of the expected *EcoRI* restriction digest pattern for strains with an intact *cab1* ORF or a homologous integration of the deletion construct. The white sections represent the 1.0 kb regions up- and downstream of the *cab1* ORF that are included in the deletion construct to target homologous recombination into the *cab1* locus. The black line labeled P represents the 900-kb probe utilized in the Southern blot analysis. B: Southern blot analyses of suspected $\Delta cab1$ strains. Each lane contains approximately 10 μ g of *EcoRI*-digested genomic DNA. Arrows mark the positions of the expected hybridization pattern for wild type and deletion strains (4.7 and 7.9 kb, respectively).

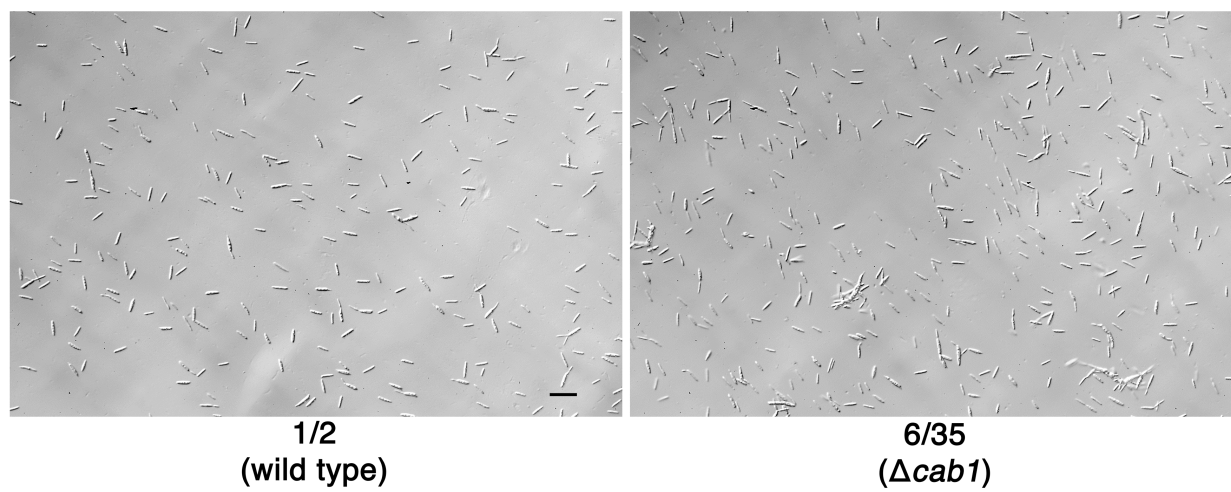


Figure 4.4. Morphology of wild type and $\Delta cab1$ strain 6/35 grown in PDB. Bar = 50 μm

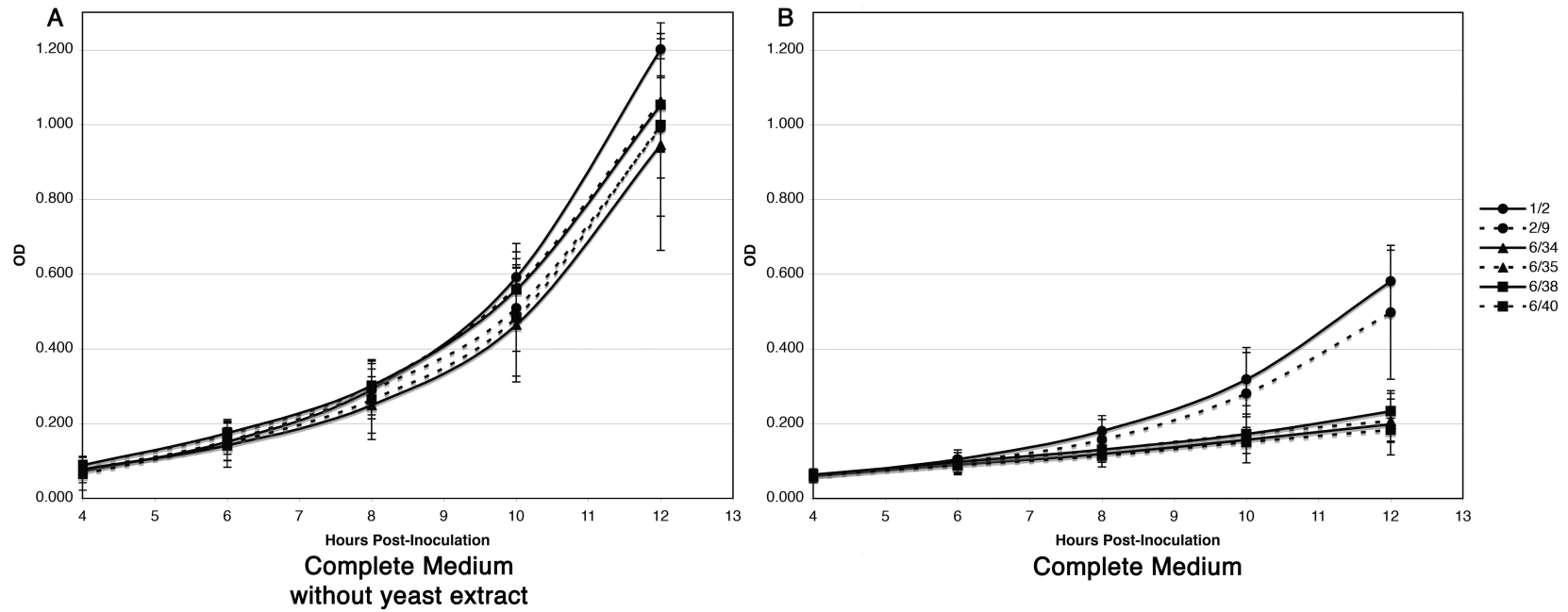


Figure 4.5. Growth rate of *U. maydis* strains in the presence of yeast extract. A: Growth of wild type and $\Delta cab1$ strains in complete medium prepared without yeast extract. B: Growth of wild type and $\Delta cab1$ strains in complete medium. OD: optical density. Bars represent standard deviation of three replicated experiments.

CHAPTER 5

IDENTIFICATION AND CHARACTERIZATION OF GENES DIFFERENTIALLY EXPRESSED DURING SCLEROTIUM FORMATION IN *SCLEROTIUM ROLFSII*¹

¹ J.E. Takach and S.E. Gold. 2009. Submitted to *Phytopathology*, 09/02/09.

**Identification and Characterization of Genes Differentially Expressed During Sclerotium
Formation and Development in *Sclerotium rolfsii***

J.E. Takach and S.E. Gold

Department of Plant Pathology, University of Georgia, Athens 30602

ABSTRACT

Sclerotium rolfsii is a soil-borne basidiomycete that causes stem rot in a wide range of plant hosts. Although the pathogen overwinters and spreads by means of small melanized sclerotia, little is known about the molecular processes required for sclerotium production. To better understand the cellular events that occur during sclerotium formation and development, genes differentially expressed during this process were identified. Two Suppressive Subtractive Hybridization PCR (SSH) libraries were created and screened to confirm differential expression of clone sequences. Sequence analysis of selected clones identified 53 unique sequences, 31 of which had homology to expressed sequences in other fungal systems, including a lectin, cytochrome P450, and two ribosomal proteins. Relative gene expression was estimated using quantitative real-time PCR (qRT-PCR) and a subset of genes were verified by northern blot analysis. Genes, such as a previously characterized *S. rolfsii* lectin and a potassium channel subunit, were highly and consistently up- or downregulated during sclerotium development. Several protein synthesis and processing genes were observed to be upregulated in the earliest stage of sclerotium development but downregulated in mature sclerotia, indicating that differential gene expression occurs between sclerotium stages of development. These findings provide a foundation for future genetic studies in *S. rolfsii*.

INTRODUCTION

Sclerotium rolfsii is a soil-borne basidiomycete fungus with an extremely wide host range of over 500 plant species in 100 families. The pathogen causes white mold, or stem rot, of peanut, resulting in major losses in Georgia peanut production; in 2007 *S. rolfsii* alone caused a 10% reduction in crop value and cost farmers \$44.4 million (Martinez, 2008). Current management strategies include crop rotation with grasses and cotton, planting resistant peanut varieties, and chemical control. These strategies have limited effectiveness due to the wide host range of the pathogen and the costs associated with fungicide applications.

S. rolfsii is transmitted primarily in the form of small melanized sclerotia. These resistant structures germinate midseason under wet or humid conditions, producing fluffy white mycelia on aboveground portions of plant hosts. The mycelium grows until it exhausts the nutrient supply and then produces copious sclerotia, which serve as both primary and secondary inoculum. The sclerotia allow the pathogen to overwinter in the soil, thus playing a crucial role in the persistence of disease potential.

Because sclerotia are the primary means of disease spread, several studies have investigated factors that stimulate or suppress their production by *S. rolfsii*. Sclerotium formation can be stimulated by the restriction of hyphal growth through physical manipulation, cold treatment, or exposure to light and oxygen (Chet and Henis, 1968; Miller and Limberta, 1976; Griffin and Nair, 1968; Rawn, 1991). Glucose depletion triggers the formation of sclerotia, while addition of glucose to starved tissue results in suppression of sclerotial initiation (Hadar et al, 1983). Fungal growth medium containing EDTA, iron, or L-threonine also promotes sclerotium production (Chet and Henis, 1968; Griffin and Nair, 1968; Henis et al, 1973; Kritzman et al 1977). Sclerotium production can be suppressed by disruption of protein

synthesis or metabolite translocation (Okon et al, 1973). Exogenous application of antioxidant compounds beta-carotene and ascorbate cause a concentration-dependent reduction in both sclerotium formation and development in culture (Georgiou et al, 2001; Georgiou et al, 2003).

Although many studies have identified physical factors that trigger or inhibit sclerotium formation and development in *S. rolfsii*, little attention has been paid to the genetic basis of these processes. Studies in other sclerogenic fungi have begun to identify genetic factors involved in the induction or suppression of sclerotium formation. In *Aspergillus flavus* and *A. parasiticus*, sclerotium formation is linked to secondary metabolite formation (Calvo et al, 2002), with the *veA* and *laeA* genes required for both sclerotium formation and mycotoxin production in *A. flavus* (Calvo et al, 2004; Duran et al, 2007). Sclerotium production in *Botrytis cinerea* is regulated by *bcSAK1* and *bmp3* MAP kinases (Segmüller et al, 2007; Rui and Hahn, 2007) and requires the NADPH oxidase genes *bcnoxA* and *bcnoxB* (Segmüller et al, 2008). Genes in both the cAMP and MAPK signaling pathways in *Sclerotinia sclerotiorum* mediate sclerotium formation (reviewed in Erental et al, 2008). Molecular studies in *S. rolfsii* will allow a comparison of proteins and pathways necessary to regulate sclerotium formation and development in these evolutionarily divergent fungi.

The goal of this study was to begin to identify genes differentially regulated during sclerotium formation and development in *S. rolfsii* to gain a better understanding of the cellular events leading to and occurring during sclerotium formation.

MATERIALS AND METHODS

***S. rolfsii* isolate information and growth conditions.** The *S. rolfsii* strain Wm 98-01 was isolated from peanut in Georgia (kindly provided by T. Brenneman). The culture was stored

as 3-mm agar plugs in sterile water and plugs were routinely used to start fresh cultures on potato dextrose agar plates amended to contain 2% agar (2PDA) (Difco, Franklin Lakes, NJ). For tissue extractions, the fungus was grown on 2PDA at 30°C in disposable Petri dishes sealed with parafilm.

Agar plugs (3 mm diameter) from fresh 2-3 day-old 2PDA plates were used to inoculate 2PDA plates covered with a cellophane filter. The cellophane filters were boiled in a 10 mM EDTA solution for 5-10 min, rinsed 2x in deionized water, autoclaved, and placed on the surface of 2PDA plates with sterilized forceps. The PDA-cellophane cultures were grown for 2-21 days and then harvested for mycelium or sclerotia. Sclerotia were isolated using sterilized forceps and classified as stage 1, 2, or 3 based on physical characteristics (Figure 5.1). Stage 1 sclerotia were small, white, and easily deformed round structures not fully separated from the originating mycelial tufts. Stage 2 sclerotia were fully rounded, tan, and somewhat resistant to physical deformation. Stage 3 sclerotia were hardened, fully melanized, structures. Mycelium lacking any sclerotial development was isolated at days 2-7 post-inoculation using sterilized forceps. Tissue samples were weighed and immediately frozen in liquid nitrogen, then stored at -80°C.

cDNA library construction. RNA was isolated from tissues using Trizol reagent according to the manufacturer's directions (Invitrogen, Carlsbad, CA). Two grams of each tissue was ground to a fine powder in the presence of liquid nitrogen and added to 15 ml of Trizol reagent. Samples were vortexed then centrifuged at 4°C at 10,000 x g for 15 min. The supernatant was extracted with 3 ml of chloroform, then precipitated with isopropanol. In the precipitation step, the isopropanol was mixed with an equal volume of 0.8 M sodium citrate and 1.2 M NaCl solution to prevent the precipitation of polysaccharides. The resultant pellets were washed with cold 70% ethanol, and resuspended in DEPC-treated water. The resuspended RNA

samples were centrifuged at 4°C at 40,000x g for 45 minutes to pellet the remaining polysaccharides, and the supernatant was removed to a sterile tube and stored at -80°C. Samples were run on a 1.6% formaldehyde gel to ensure RNA quality and quantified by measuring the sample absorbance at 260 nm. For subsequent steps, 20 µg of RNA from each sclerotial stage was combined and diluted to a final concentration of 2 µg/µl to ensure that transcripts from each stage were represented in the differential library.

Using a BD SMART PCR cDNA Synthesis Kit (Clontech, Mountain View, CA), cDNA was synthesized from 1.5 µg of total RNA from the mycelial or combined sclerotial tissues using an oligo dT primer according to the manufacturer's directions. A 1 µl aliquot of the first-strand synthesis reaction was used for PCR amplification of the full-length cDNA. Four reactions per tissue sample were combined, ethanol precipitated, then purified using a NucleoTrap PCR Purification Kit (Clontech). The purified cDNAs were then digested with *RsaI* and purified using a NucleoTrap PCR Purification Kit. Samples were ethanol precipitated in the presence of 1 µg/µl glycogen, resuspended in 6.7 µl 1xTNE buffer (10 mM Tris-HCl, 10 mM NaCl, 1 mM EDTA), and quantified by measuring absorbance at 260 nm. Both the mycelial and sclerotial cDNA samples were adjusted to a final concentration of 250 µg/µl. Digested samples were then used in a BD SMART PCR cDNA Subtraction Kit (Clontech) following the manufacturer's instructions to produce a pool of cDNA fragments upregulated during sclerotial development and a pool of cDNA fragments upregulated during mycelial growth. The SSH pools were cloned into the pCR2.1topo plasmid using a TOPO cloning kit (Invitrogen, Palo Alto, CA). Bacterial colonies were isolated and maintained on LB-ampicillin plates until roughly 1,000 clones were isolated for each library. For long-term storage, colonies were grown overnight in 96-well

microtiter plates with LB amended with 50 µg/ml of ampicillin and 15% glycerol and then frozen at -80°C.

Individual bacterial colonies for both libraries were arrayed on Hybond-XL nylon membranes (GE Healthcare Bio-Sciences, Piscataway, NJ) using a Bio-Grid robot (Bio Robotics Inc., Woburn, MA). Nylon membranes were placed on 22 cm x 22 cm plates containing 250 ml low-sodium (1 g/L) LB-agar with 100 µg/ml ampicillin and stamped with six copies of each library. The plates were incubated for 12 h at 37°C, and then the nylon filters were removed from the media and cells lysed in preparation for colony hybridization (Sambrook et al 1989). DNA was fixed to the membranes by baking at 80°C for 2 hours.

Differential screening of subtracted libraries. The arrayed libraries were probed with subtracted and unsubtracted PCR products. DNAs for probe labeling were purified using a QIAquick Nucleotide Removal kit (Qiagen, Valencia, CA) and quantified by measuring absorbance at 260 nm. For each probe, 90 ng of double-stranded cDNA was labeled with 50 µCi (5 µl of 3000 Ci/mmol aqueous solution) of a [α -³²P]-dCTP as described in the instruction manual for the PCR-Select Differential Screening kit (Clontech). Labeled products were purified by filtration through Sephadex G50 (Sigma, St. Louis, MO) columns and roughly quantified using a Geiger counter. Prehybridization and hybridization of the membranes were performed at 68°C for 4 hours and overnight, respectively, in Church buffer (5 mM EDTA, 0.25 mM Na₂HPO₄, 0.17% H₃PO₄, 1% casein hydrolysate, and 7% SDS) (Church and Gilbert, 1984). Membranes were washed at 68°C as follows: 4 times in 2x SSC, 0.05% SDS for 20 min each, then twice in 0.2x SSC, 0.5% SDS for 20 min each. Membranes were then exposed to X-ray film (Kodak, Rochester, NY) for variable lengths of time. For reuse, filters were stripped of

probes by immersion in boiling fresh 0.5% SDS for 10 minutes twice, air dried, and stored at room temperature.

Sequencing of differential clones. One hundred and seventy-two differential clones were identified and sequenced. Clones were sequenced by the Sequencing and Synthesis Facility at the University of Georgia (Athens, GA). Sequencing data were reviewed and aligned to identify unique sequences using the Seqman tool in the LaserGene software suite v6.0 (DNASar, Madison, WI). Unique EST sequences were compared to the non-redundant GenBank protein database compiled by the National Center for Biotechnology Information (NCBI) using the BlastX algorithm (Altschul, et al 1997). An arbitrary cut off value of E value $> 10^{-5}$ was interpreted as insignificant similarity. Clone sequences that had a higher similarity ($E \leq 10^{-5}$) with known or deduced function were tentatively assigned the similar function.

Northern expression analysis. Five micrograms of total RNA from the different developmental stages of *S. rolfsii* (mycelial, each sclerotial developmental stage, and from the mixed pool of all the sclerotial stages described during the library preparation) were fractionated in a denaturing gel containing 1% agarose and transferred to a positively charged nylon membrane using an Ambion NorthernMax kit (Austin, TX). Prior to blotting, the gel was stained with ethidium bromide and viewed under UV illumination to confirm equivalent loading. RNA was fixed to the membrane by UV cross-linking. RNA probes were prepared by *in vitro* transcription of 0.5 μ g linearized plasmid DNA with the EST sequence of interest in an antisense orientation to the T7 polymerase start site. Probes were labeled with 16-UTP-biotin (Ambion) using a Maxiscript kit (Ambion) following the manufacturer's directions. Probes were treated with DNase and purified using NucAway spin columns (Ambion). RNA concentration of probes was measured at 260 nm. Membranes were prehybridized in 10 ml ULTRAhyb buffer for 30

minutes at 68°C. Labeled probe was added to a final concentration of 0.1 μM and hybridized overnight at 68°C. The membrane was washed using reagents provided in a BrightStar BioDetect kit (Ambion) as directed by the manufacturer. The membrane was blotted gently dry and exposed to X-ray film (Kodak, Rochester, NY).

Real-time PCR analysis. Total RNA was extracted from 50-70 mg of sclerotial or mycelial tissues using a Plant RNEasy kit (Sigma). RNA samples were subsequently DNase-treated and quantified by measuring sample absorbance at 260 nm. One microgram of each sample was run on a 1.6% formaldehyde agarose gel to ensure sample integrity. For each tissue sample, 1 μg RNA was reverse transcribed to cDNA using a RT kit (Invitrogen). Real-time PCR was used to measure relative gene expression using the Syber Green system (Applied Biosciences) using a cyclophilin homolog as a normalization reference. The cyclophilin (peptidylprolyl isomerase; *ppi*) gene has been previously used as a normalization control in qRT-PCR in the basidiomycete model *U. maydis* (Scherer et al 2006; Nadal and Gold, unpublished results). The *ppi* gene in *S. rolfsii* was identified by amplifying genomic DNA with degenerate primers designed from a protein alignment of basidiomycete homologs. The degenerate PCR product was cloned into the pCR2.1 plasmid using a TOPO cloning kit (Invitrogen) and multiple clones were sequenced. The ct value of the *ppi* gene was observed to be highly similar in all tissues and biological replications. Table 5.3 lists all real-time PCR primer pairs and expected product sizes. All reactions were run in an ABI 7300 real-time machine with the following thermal cycling parameters: an initial denaturation step of 94°C for 4 min followed by 40 cycles of two-step PCR, 94°C for 30 s, 60°C for 30 s. Data were collected during the 60°C annealing step and analyzed by the ABI software program. The relative expression level of each target

gene was calculated as the ratio of expression in each sclerotial stage to the expression in mycelium using the Pfaffl equation (Pfaffl, 2001).

RESULTS

Library construction and sequence analysis. Total RNA was extracted from mycelium and stage 1, 2, and 3 sclerotia from *S. rolf sii* strain Wm98-01 (Figure 5.1). RNA from the sclerotial stages was pooled together to represent gene expression during the course of sclerotial development. cDNA synthesized from the mycelial and sclerotial RNA was subjected to Suppressive Subtraction Hybridization PCR (SSH) to produce two cDNA libraries. The two libraries were predicted to contain genes expressed during sclerotium formation and development but not during mycelial growth (S) and genes expressed in mycelium but not during sclerotial development (M), respectively. The 1,017 S and 1,050 M clones were arrayed on a nylon membrane and screened with subtracted PCR products to identify 200 clones with differentially expressed sequences (Figure 5.2). Of the 200 clones, high-quality sequence data were obtained from 143 clones.

Clone sequences were assembled into contigs to identify overlapping clones using the SeqMan assembly program (Lasergene). The 53 resultant contig sequences were designated EST-contigs and used to search the non-redundant GenBank nucleotide and protein databases. EST-contigs were classified as strongly similar if they had a fungal homolog in Genbank with an E value $\leq 10^{-10}$ or weakly similar if the E value ranged between 10^{-10} and 10^{-5} . EST-contigs were assigned putative functions based on sequence homology to fungal proteins in the NCBI databases or protein domains in the Conserved Domain Database (Marchler-Bauer et al, 2005).

The 83 high-quality sequences from S library clones combined to form 29 EST-contigs. Nineteen of the EST-contigs were at least weakly similar to conserved proteins identified in other fungal systems (Table 5.1). Six EST-contigs had no similarity to any protein or nucleotide sequence in GenBank. Four EST-contigs, comprised of 45 clone sequences, were not similar to any protein sequence, but were very similar (an E value $\leq 10^{-88}$) to the nucleotide sequence of the mitochondrial rRNA 28S subunits of *Suillus sinuspaulianus* and *Laccaria bicolor*.

The 60 high-quality sequences from M library clone sequences combined to form 24 EST-contigs. Twelve of the EST-contigs were at least weakly similar to conserved proteins identified in other fungal systems (Table 5.2). Eleven EST-contigs had no similarity to any protein or nucleotide sequence in Genbank, and one EST-contig was most similar to the nucleotide sequence of the *S. sinuspaulianus* mitochondrial 28S rRNA sequence.

Verification of differential expression. The relative expression of 15 genes was estimated using quantitative real-time PCR (Figures 5.3 and 5.4). The qRT-PCR analysis was replicated three times with RNA prepared from independently isolated tissue samples.

Eight genes identified as upregulated during sclerotial development were confirmed to have higher expression in sclerotia than in mycelium (Figure 5.3). The two genes with the greatest number of clones in the S library, lectin and phosphatidylserine decarboxylase, are both highly upregulated in each stage of sclerotium development. On average, expression levels of these genes are over 1,000 times greater in sclerotia than in mycelium. The genes encoding unknown proteins 1 and 2 and threonine aldolase are at least 5 times more highly expressed in each stage of sclerotia. The remaining genes (encoding an aspartic peptidase, vesicular transport protein, and unknown protein 3) have greater than twofold higher expression during stage 1

sclerotia, but fall to levels similar to mycelium (less than twofold difference in expression) in later stages of development.

Relative gene expression was estimated for seven genes identified as downregulated during sclerotial development (Figure 5.4). Transcripts for the unknown protein 4 and potassium transporter beta subunit genes, each represented by multiple clones in the M library, are at least twofold less expressed in all three sclerotial stages (Figures 5.4 and 5.5B). Four genes have differential expression between sclerotial stages. Cytochrome-c oxidase (cox1), cpc2, and S8 gene expression is two times greater in stage 1 sclerotia than in mycelium, but expression levels are four times less in stage 3 sclerotia than in mycelium. S12 expression is similar to mycelium during stage 1 sclerotial development, but decreases in mature stage 3 sclerotia.

The relative expression of the mitochondrial 28S rRNA subunit was assayed, but PCR product was only detected in 3 of the 9 sclerotial cDNA samples, and was undetected in any of the mycelial cDNA samples.

To verify differential expression of the EST-contigs identified in our library screen, we chose a subset of genes and performed northern blot analysis (Figure 5.5). The lectin transcript was highly abundant in the sclerotial RNA samples, but was undetectable in the mycelial RNA samples (Figure 5.5a). Conversely, the beta subunit transcript was more abundant in the mycelial RNA sample than in any of the sclerotial RNA samples (Figure 5.5b). The mitochondrial rRNA sequence was undetected by blot analysis in any RNA samples (data not shown).

DISCUSSION

Numerous studies have identified the physical and/or chemical means to initiate or halt production of sclerotia in *S. rolfsii*, but none have addressed the underlying molecular pathways that control this process. We chose to begin investigating this process by identifying genes that are differentially expressed in sclerotia and mycelium to get a broad idea of the cellular and genetic events involved in differentiation.

In this study, we identified 33 EST-contigs with fungal homologs present in the NCBI databases (Tables 5.1 and 5.2), and 19 EST-contigs representing *S. rolfsii*-specific genes that do not have homologs in sequenced fungal genomes. Future investigation into these sequences may identify sclerotia- or mycelia-specific proteins with intriguing roles in cellular morphology of sclerogenic fungi.

The most highly differentially expressed gene identified in our study encodes a lectin (Figures 5.3 and 5.5a). This finding correlates with a previous report that the lectin is produced abundantly during sclerotium formation and has a 1,000-fold higher specific activity in immunological tests than compared to mycelium (Swamy et al, 2004). Another highly differential gene, phosphatidylserine decarboxylase, encodes an enzyme that catalyzes the formation of phosphatidylethanolamine from phosphatidylserine (Voelker, 1997). This enzyme may be upregulated during sclerotial development to take part in the elaborate cell membrane remodeling that accompanies sclerotium development (Zarani and Christias, 1997).

We identified several EST-contigs that are most similar to enzymes involved in oxidation/anti-oxidation pathways. Several studies have indicated a positive correlation between oxidative stress and sclerotial differentiation (Georgiou, 1997; Georgiou et al, 2006). ROS-forming NADPH oxidase encoding genes are required for sclerotium formation in *S.*

sclerotiorum (Segmüller et al, 2008). Although no NADPH oxidase genes were identified in this study, we did identify an amine oxidase gene in the sclerotium upregulated library (Table 5.1).

Additionally, a cytochrome P450 gene was also identified in the upregulated library.

Cytochrome P450 enzymes are crucial for the oxidation of a variety of substrates in all eukaryotic organisms (Meunier et al, 2004) and are upregulated in fruiting body tissues in the basidiomycetes *Letinula edodes* and *Agaricus bisporus* (Hirano et al, 2004, Eastwood et al, 2001), suggesting that cytochrome P450 may have a conserved role in tissue differentiation in basidiomycetes.

Cellular respiration and energy production appear to be downregulated in sclerotia. Two genes, a putative cytochrome c oxidase and 2-hydroxy-acid dehydrogenase, were identified as downregulated in sclerotia (Table 5.2). The cytochrome c oxidase enzyme is a multi-protein complex involved in aerobic cellular respiration and may be partially regulated by transcription levels in *S. cerevisiae* (Fontanesi et al, 2006). 2-hydroxy-acid dehydrogenase enzymes catalyze oxidation/reduction reactions involved in cellular metabolism (Taguchi and Ohta, 1991). The genes may be downregulated in sclerotia due to the low metabolic activity of the resting structures. Consistent with their roles in metabolically active tissues, both 2-hydroxy-acid dehydrogenase and cytochrome P450 transcripts were enriched in *Magnaporthe grisea* appressoria as compared to conidia (Lu et al, 2005).

Several EST-contigs identified in this study have fungal homologs involved in protein translation, processing, or fate. Sclerotium-upregulated sequences include a putative eukaryotic translation initiation factor (eIF1), Hsp70 chaperone, aspartic peptidase, and vesicular transport protein (Table 5.1). Interestingly, the Hsp70 family proteins are specifically involved in folding newly formed polypeptides (Mayer and Bukau, 2005) and may play a role in the *de novo* protein

synthesis required for sclerotium formation (Okon et al, 1973). Many transcripts related to protein synthesis and/or fate, including Hsp70, eIf1, and aspartic peptidase, were more abundant in differentiating cells than in mycelium of the human dimorphic pathogen *Paracoccidioides brasiliensis*, suggesting that transcriptional regulation of these components occurs in a variety of fungal systems (Parente et al, 2008).

EST-contigs corresponding to the S8 and S12 ribosomal proteins and a translation initiation factor were identified as upregulated in mycelium (Table 5.2). However, qRT-PCR analysis revealed that these sequences were expressed more highly in stage 1 sclerotia and suppressed strongly in mature (stage 3) sclerotia (Figure 5.4). These findings suggest that protein synthesis increases at the initial stages of sclerotial development and decreases when the sclerotia mature.

Our study reveals that differential gene expression occurs during sclerotial differentiation in *S. rolf sii*. We have described 50 EST-contigs that have been identified as differentially regulated, with more than half being similar to proteins found in public sequence databases. Some genes, such as the lectin, phosphatidylserine decarboxylase, and the potassium channel beta subunit, are highly and consistently up- or downregulated during sclerotium development. Other genes, specifically those that encode factors involved in protein synthesis and/or fate, appear to be differentially expressed during sclerotium development. These findings provide a foundation for future studies into the genetic basis of sclerotium formation and development in *S. rolf sii* and may lead to identification of new targets for better chemical control of sclerotium formation in agricultural systems.

LITERATURE CITED

1. Altschul, S. F., Madden, T. L., Schaffer, A. A., Zhang, J., Zhang, Z., Miller, W., and Lipman, D. J. 1997. Gapped BLAST and PSI-BLAST: a new generation of protein database search programs. *Nuc Acid Research* 25: 3389-3402.
2. Calvo, A. M., Wilson, R. A., Bok, J. W., and Keller, N. P. 2002. Relationship between secondary metabolism and fungal development. *Microbiol Mol Biol Rev* 66: 447-459.
3. Calvo, A. M., Bok, J. W., Brooks, W., and Keller, N. P. 2004. *veA* is required for toxin and sclerotial production in *Aspergillus parasiticus*. *Appl Env Microbiol* 70: 4733-4739.
4. Chet I, and Henis Y. 1968. Control mechanism of sclerotial formation in *Sclerotium rolfisii* Sacc. *Journal of General Microbiology* 54: 231-7.
5. Church, G. M., and Gilbert, W. 1984. Genomic sequencing. *Proc Natl Acad Sci USA* 81: 1991-1995.
6. Duran R. M., Cary, J. W., and Calvo, A. M. 2007. Production of cyclopiazonic acid, aflatrem, and aflatoxin by *Aspergillus flavus* is regulated by *veA*, a gene necessary for sclerotial formation. *Appl Env Microbiol* 73: 1158-1168.
7. Eastwood, D. C., Kingsnorth, C. S., Jones, H. E., Burton, and K. S. 2001. Genes with increased transcript levels following harvest of the sporophore of *Agaricus bisporus* have multiple physiological roles. *Myc Res* 105: 1223-1230.
8. Erental, A., Dickman, M. B., and Yarden, O. 2008. Sclerotial development in *Sclerotinia sclerotiorum*: awakening molecular analysis of a “Dormant” structure. *Fung Biol Rev* 22: 6-16.
9. Fontanesi, F., Soto, I. C., Horn, D., and Barrientos, A. 2006. Assembly of mitochondrial cytochrome c-oxidase, a complicated and highly regulated cellular process. *AJP-Cell Phys* 291: 1129-1147.
10. Georgiou, C. D. 1997. Lipid peroxidation in *Sclerotium rolfisii*: a new look into the mechanism of sclerotial biogenesis in fungi. *Mycol Res* 101: 460-464.
11. Georgiou, C. D, Patsoukis, N., Papapostolou, I., and Zervoudakis, G. 2006. Sclerotial metamorphosis in filamentous fungi is induced by oxidative stress. *Integr Comp Biol* 46: 691-7.
12. Georgiou, C. D., Zervoudakis, G., and Petropoulou, P. K. 2003. Ascorbic acid may play a role in sclerotial differentiation of *Sclerotium rolfisii*. *Mycologia* 95: 308-16.
13. Gerogiou, C. D., Zervoudakis, G., Tairis, N., and Kornaros, M. 2001. β -Carotene production and its role in sclerotial differentiation of *Sclerotium rolfisii*. *Fung Genet Biol* 34: 11-20.

14. Griffin, D. M. and Nair, G. N. 1968. Growth of *Sclerotium rolfsii* at different concentrations of oxygen and carbon dioxide. *J Exp Bot* 19: 812-6.
15. Hadar, Y., Pines, M., Chet, I., and Henis, Y. 1983. The regulation of sclerotium initiation in *Sclerotium rolfsii* by glucose and cyclic AMP. *Can J Microbiol* 29: 21-26.
16. Henis, Y., Okon, Y., and Chet, I. 1973. Relationship between early hyphal branching and formation of sclerotia in *Sclerotium rolfsii*. *J Gen Microbiol* 79: 147-50.
17. Hirano, T., Sato, T., and Enei, H. 2004. Isolation of genes specifically expressed in the fruit body of the edible basidiomycete *Lentinula edodes*. *Biosci Biotech Biochem* 68: 468-472.
18. Kritzman, G., Chet, I., and Henis, Y. 1977. Role of oxalic acid in pathogenic behavior of *Sclerotium rolfsii* Sacc. *Exp Mycol* 4: 280-285.
19. Lu, J. P., Liu, T. B., and Lin, F. C. 2005. Identification of mature appressorium-enriched transcripts in *Magnaporthe grisea*, the rice blast fungus, using suppression subtractive hybridization. *FEMS Microbiol Let* 245: 131-137.
20. Marchler-Bauer, A., Anderson, J. B., Cherukuri, P. F., DeWeese-Scott, C., Geer, L. Y., Gwadz, M., He, S., Hurwitz, D. I., Jackson, J. D., Ke, Z., Lanczycki, C. J., Liebert, C. A., Liu, C., Lu, F., Simonyan, V., Song, J. S., Thiessen, P. A., Yamashita, R. A., Yin, J. J., Zhang, D., and Bryan, S. H. 2005. CDD: a Conserved Domain Database for protein classification. *Nuc Acid Res* 33: D192-6.
21. Martinez, A. 2008. Georgia plant disease lost estimates. *Coop. Ext. Ser. Bull.* 41-10, University of Georgia, Athens.
22. Mayer, M. P. and Bukau, B. 2005. Hsp70 chaperones: cellular functions and molecular mechanism. *Cell Mol Life Sci* 62:670-84.
23. Meunier, B., de Visser, S. P., and Shaik, S. 2004. Mechanism of oxidation reactions catalyzed by Cytochrome P450 enzymes. *Chem Rev* 104: 3947-3980.
24. Miller, M. R., and Limberta, E. A. 1977. The effects of light and tyrosinase during sclerotium formation in *Sclerotium rolfsii* Sacc. *Can J Microbiol* 23: 278-87.
25. Okon, Y, Chet, I., and Henis, Y. 1973. Effects of lactose, ethanol, and cyclohexamide on the translocation pattern of radioactive compounds and on sclerotium formation in *Sclerotium rolfsii*. *J Gen Microbiol* 74: 251-258.
26. Parente, J. A., Borges, C. L., Bailao, A. M., Felipe, M. S., Pereira, M., and Soares, C. M. 2008. Comparison of transcription of multiple genes during mycelia transition to yeast cells of *Paracoccidioides brasiliensis* reveals insights to fungal differentiation and pathogenesis. *Mycopathologia* 165: 259-273.

27. Pfaffl, M. W. 2001. A new mathematical model for relative quantification in real-time RT-PCR. *Nuc Acid Res* 29: 2003-2007.
28. Rawn, C. D. 1991. Induction of sclerotia in *Sclerotium rolfsii* by short low-temperature treatment. *J Gen Microbiol* 137: 1063-1066.
29. Rui, O., and Hahn, M. 2007. The *Slr2*-type MAP kinase *Bmp3* of *Botrytis cinerea* is required for normal saprotrophic growth, conidiation, plant surface sensing and host tissue colonization. *Mol Plant Path* 8: 173-184.
30. Scherer, M., Heimel, K., Starke, V., and Kämper J. 2006. The *Clp1* protein is required for clamp formation and pathogenic development of *Ustilago maydis*. *Plant Cell* 18: 2388-2401.
31. Segmüller, N., Ellendorf, U., Tudzynski, B., and Tudzynski, P. 2007. *BcSAK1*, a stress-activated mitogen-activated protein kinase, is involved in vegetative differentiation and pathogenicity in *Botrytis cinerea*. *Euk Cell* 6: 211-221.
32. Segmüller, N., Kokkelink, L., Giesbert, S., Odinius, D., van Kan, J., and Tudzynski, P. 2008. NADPH oxidases are involved in differentiation and pathogenicity in *Botrytis cinerea*. *MPMI* 21: 808-819.
33. Swamy, B. M., Bhat, A. G., Hegde, G. V., Naik, R. S., Kulkarni, S., and Inamdar, S. R. 2004. Immunolocalization and functional role of *Sclerotium rolfsii* lectin in development of fungus by interaction with its endogenous receptor. *Glycobiol* 14: 951-957
34. Taguchi, H., and Ohta, T. 1991. D-lactate dehydrogenase is a member of the D-isomer-specific 2-hydroxyacid dehydrogenase family. Cloning, sequencing, and expression in *Escherichia coli* of the D-lactate dehydrogenase gene of *Lactobacillus plantarum*. *J Biol Chem* 266: 12588-12594.
35. Voelker, D. R. 1997. Phosphatidylserine decarboxylase. *Biochem Biophys Acta* 1348: 236-244.
36. Zarani, F., and Christias, C. 1997. Sclerotial biogenesis in the basidiomycete *Sclerotium rolfsii*: A scanning electron microscope study. *Mycologia* 89: 598-602.

Table 5.1. ESTs upregulated during sclerotium formation and development in *S. rolf sii*

EST-contig	Number of clones	Most similar sequences	E value	Putative function/biochemical categorization
S1	4	<i>S. rolf sii</i> lectin	e-58	Sclerotium germination
S2	5	Phosphatidylserine decarboxylase	e-31	Phospholipid biosynthesis; cell membrane synthesis
S3	3	Unknown Protein 1: Predicted protein in <i>Laccaria bicolor</i> , <i>Coprinopsis cinerea</i> , and <i>Cryptococcus neoformans</i>	e-32	Unknown function
S4	2	Unknown Protein 2: <i>C. cinerea</i> hypothetical protein CG1G_01071	e-85	Unknown function
S5	1	Conserved fungal protein: vesicular transport	e-25	Protein sorting and vesicular transport
S6	1	Conserved sporulation-related fungal protein	e-50	Unknown function; <i>Saccharomyces cerevisiae</i> homolog is upregulated during sporulation
S7	1	Threonine aldase	e-47	Amino acid metabolism
S8	1	Hsp70	e-44	Protein folding; stress response
S9	1	Peroxisomal copper-containing amine oxidase	e-39	Metabolism; oxidation of primary amines, diamines and histamine
S10	1	Hypothetical <i>L. bicolor</i> aspartic peptidase A1	e-36	Protein fate; protein processing, protein/peptide degradation
S11	1	Eukaryotic Initiation Factor 1 (SUI1/eIF1)	e-34	Protein synthesis; translation initiation
S12	1	Unknown Protein 3: <i>C. cinerea</i> hypothetical protein containing Sec7 domain	e-32	Unknown function
S13	1	Cytochrome P450	e-24	Metabolism; oxidation
S14	1	Glutamine amidotransferase class-II	e-28	Metabolism; nitrogen metabolism
S15	1	Tryptophan synthase	e-15	Amino acid synthesis

Table 5.2. ESTs downregulated during sclerotium formation and development in *S. rolfsii*

EST-contig	Number of clones	Most similar sequences	E value	Putative function/biochemical categorization
M1	5	Unknown Protein 4: <i>Coprinopsis cinerea</i> hypothetical protein CC1G_00256	e-08	Unknown function
M2	3	Cytochrome c oxidase (cox1)	e-79	Cellular respiration; required for reduction of oxygen in the electron transport chain
M3	4	<i>C. cinerea</i> hypothetical protein CC1G_05109	e-40	Calcium binding protein; possible signaling sensor or signal modulator
M4	3	Potassium channel beta-2 subunit	e-39	Reduces aldehydes and ketones to primary/secondary alcohols
M5	2	S12e/L7Ae ribosomal protein	e-38	Protein synthesis
M6	1	Cpc2 homolog (<i>Ustilago maydis</i>)	e-57	Protein synthesis; signal transduction, translation initiation
M7	1	Unknown Protein 5: <i>C. cinerea</i> hypothetical protein CC1G_09175	e-41	Unknown function
M8	1	D-isomer specific 2-hydroxyacid dehydrogenase	e-15	Oxidoreductase with NAD(P) binding domain
M9	1	S8e ribosomal protein	e-40	Highly conserved ribosomal protein, involved in protein synthesis
M10	1	FKBP-type peptidyl-prolyl cis-trans isomerase	e-33	Protein fate; protein folding
M11	1	<i>C. cinerea</i> hypothetical protein CC1G_02037	e-11	Protein fate; protein degradation
M20	1	<i>L. bicolor</i> hypothetical protein XP_001878154	e-43	Unknown function

Table 5.3. Primers used for Real-Time PCR analysis		
Gene		Primer sequence
Aspartic peptidase	F	5'-GCCTAATCAGGCATTTGGTGCTGT-3'
	R	5'-TGAGCTAAGGTTGCGAAGAACGGA-3'
Beta subunit	F	5'-AATACCACTATGACCGCTCTGGCT-3'
	R	5'-ATTTTCGGGAGAACCTCGATTGCCT-3'
Calcium binding	F	5'-TACGCCAATTCGGCTACAACCTCT-3'
	R	5'-AAGGCCTCCGTCATCTGCTTGATA-3'
Cox1	F	5'-TTCTTCTTGGCATTCCGGCCAATC-3'
	R	5'-TGCAGGATTCTATTTCTGGACACC-3'
Cpc2	F	5'-ACGGGCATACCGGCTACATTAACA-3'
	R	5'-TTGACGATGTCACCAGCCTCAAGA-3'
Cyclophilin (normalization reference)	F	5'-CTATGGTGAGAAATTCGCAGAC-3'
	R	5'-CCATCAAGCCAGGAGGTG-3'
Lectin	F	5'-AGCACGTTCTTATCATGGGCGGTA-3'
	R	5'-ACACCAAATGTGGCAGTGAAGCTC-3'
Phosphatidylserine decarboxylase	F	5'-ACCGCTCAGCTATTCCAAAGAGGA-3'
	R	5'-AGATAAGGAGACGCGTTGCAGTGT-3'
S8	F	5'-ACTATGGCCAACCTGTGACCAAGA-3'
	R	5'-ATTGTGTCTCCAGGAGCGTGTCAA-3'
S12	F	5'-AGACTTGCACGGAAGCCGAATACA-3'
	R	5'-GTG CCAAGCACTTTAGCATCACCA-3'
Threonine aldolase	F	5'-AGGCAACAACACCCTCCGATCATA-3'
	R	5'-AGGTCCAGGCAAACCGTATCGAAT-3'
Vesicular transport	F	5'-GGCCATTGCGTCTGACTTTGTTC-3'
	R	5'-ATCTTTCGGACCAGATGACACGCT-3'
Unknown 1	F	5'-GGGAAAGTGTTGGTTCAAGGGTGA-3'
	R	5'-AGTGGCAGGTAATGGTGA CT CGAA-3'
Unknown 2	F	5'-ATTGTCTTCTTCAGGGAGCCAGGCTTA-3'
	R	5'-TTGCCTCCGTGTTTCGTGATGAGT-3'
Unknown 3	F	5'-GACCACGTCTGTCAAACGGCAAAT-3'
	R	5'-ATAAAGTGAGACTGGTGCCTTGCG-3'
Unknown 4	F	5'-ACCACCCGATTCCGACTGCATTAT-3'
	R	5'-ACGCTCCCTGGGACTTTATGTTGA-3'

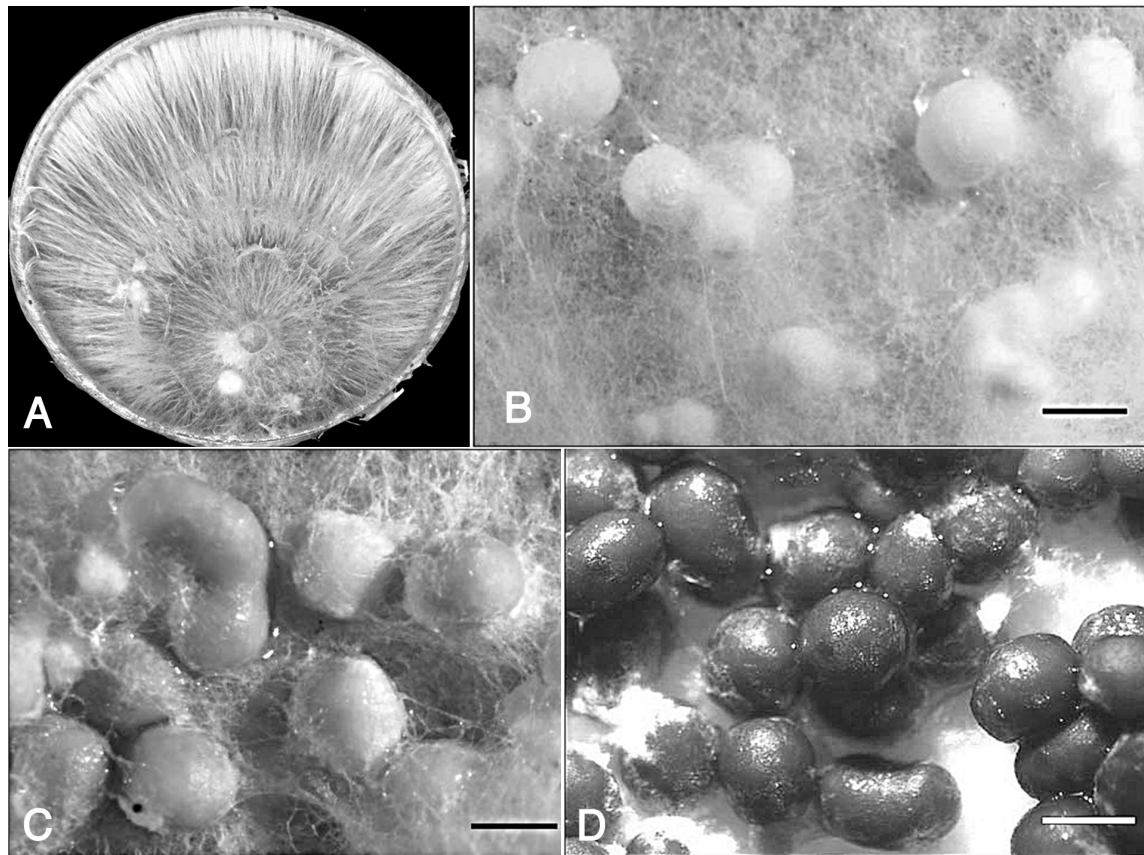


Figure 5.1. Mycelial and sclerotial development in *S. rolfsii*. A: Mycelium 3 days post-inoculation (dpi). B: Stage 1 sclerotia produced 6 dpi. C: Stage 2 sclerotia produced 14 dpi. D: Stage 3 sclerotia produced 20 dpi. All samples were grown on Petri plates of potato dextrose agar (PDA). Bar = 1 mm.

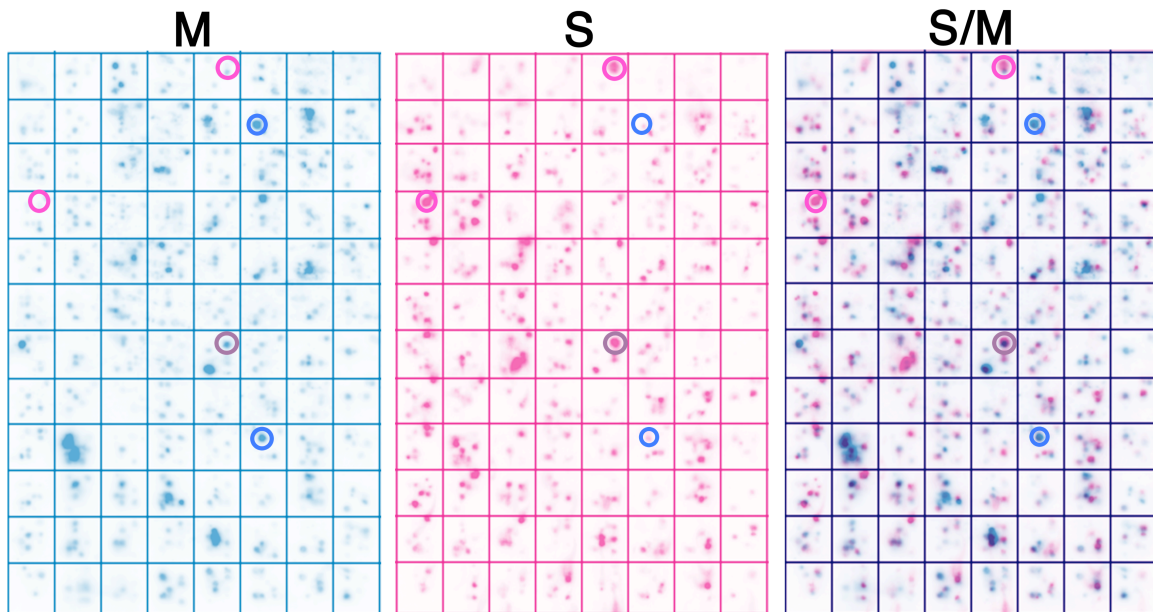


Figure 5.2. Identification of clones containing differentially expressed sequences. Two SSHP cDNA libraries, representing genes up- and downregulated during sclerotium formation and development, were arrayed on nylon membranes and probed with subtracted cDNA to identify differentially expressed sequences. S: Libraries probed with subtracted cDNA derived from sclerotia. M: Libraries probed with subtracted cDNA derived from mycelium. S/M: An overlay of panels S and M. Panels are false colored for ease of differential clone identification. Circles are used to indicate examples of sclerotium-upregulated clones (pink), sclerotium-downregulated clones (blue), and the rare clones with sequences present in both subtracted samples (purple).

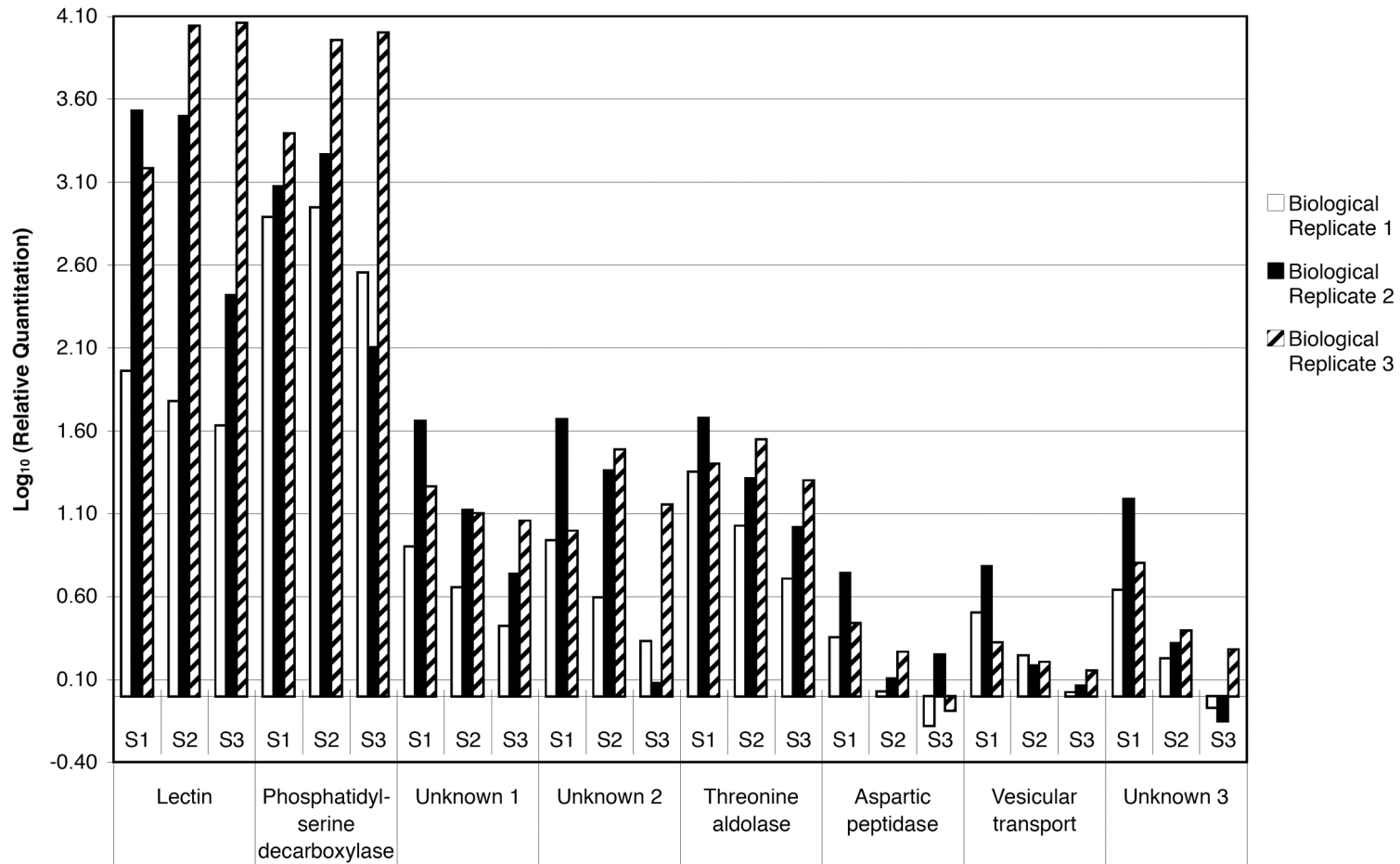


Figure 5.3. Quantitative Real-time PCR analysis of selected genes identified in the sclerotium-upregulated (S) library. Gene names on the x-axis correlate to the name or function of the most similar homologs as listed in Table 5.1. Relative expression of each gene was calculated for each sclerotial stage as compared to the expression level in mycelium and is measured in Log₁₀ on the y-axis. The values for each of three biological replications are included.

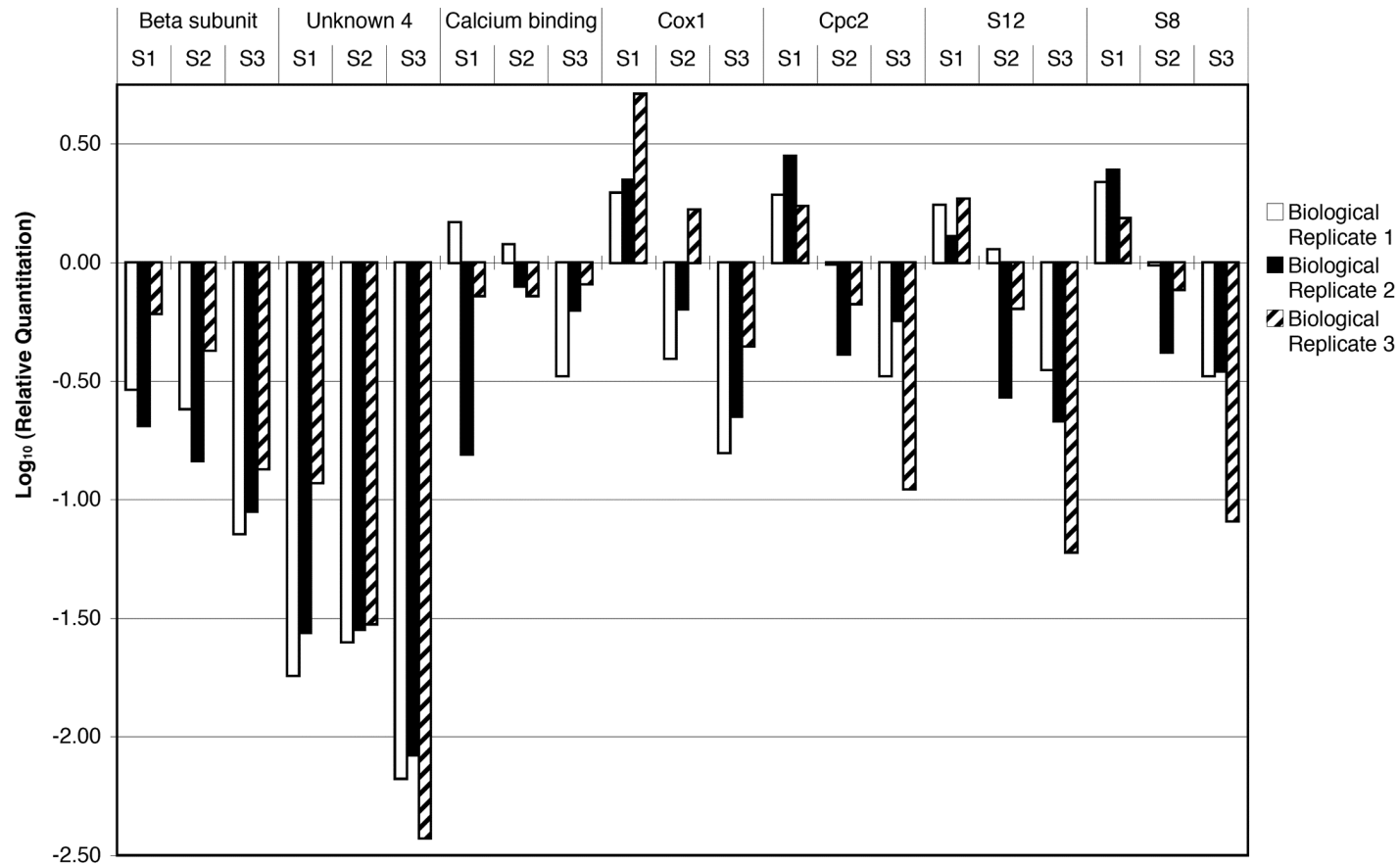


Figure 5.4. Quantitative Real-time PCR analysis of selected genes identified in the sclerotium-downregulated (M) library. Gene names on the x-axis correlate to the name or function of the most similar homologs as listed in Table 5.2. Relative expression of each gene was calculated for each sclerotial stage as compared to the expression level in mycelium and is measured in Log_{10} on the y-axis. The values for each of three biological replications are included.

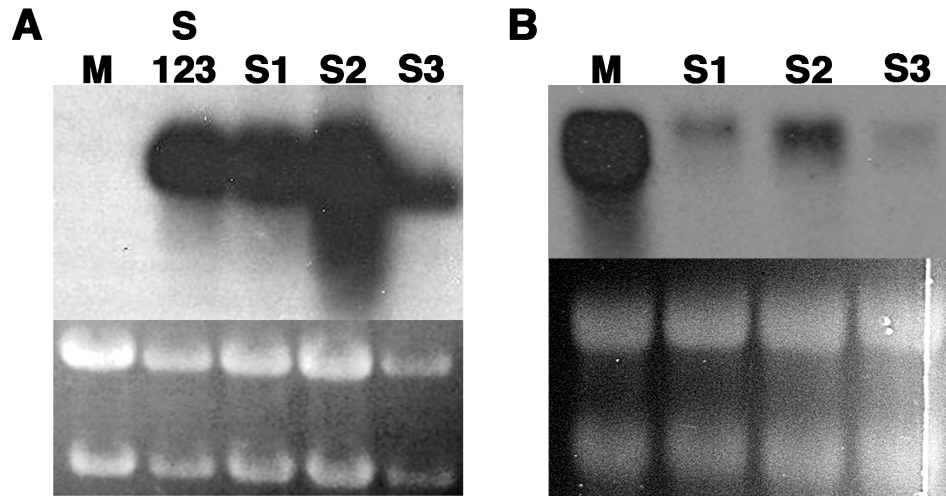


Figure 5.5. Northern blot analysis of selected *S. rolf sii* genes. A: *S. rolf sii* RNA from mycelium and sclerotia was probed with biotin-labeled probe for lectin mRNA. B: *S. rolf sii* RNA from mycelium and sclerotia was probed with biotin labeled probe for the potassium channel beta subunit mRNA. Lanes contain 10 μ g total RNA according to spectrophotometer readings at 260 nm. M: Mycelium. S: Sclerotia. 1, 2, or 3: Stage of sclerotia from which the RNA was extracted. 123: Pooled sclerotial RNA from all 3 stages of development.

CHAPTER 6

CONCLUSIONS

The research presented in this dissertation addresses gaps in current knowledge of the genetic factors involved in developmental and morphological change in basidiomycetous fungi. These changes are critical for the completion of fungal life cycles and host infection of plant pathogenic fungi. To better understand the mechanism and processes that underlie these significant physical changes, the molecular components required for these transformations must be identified and characterized.

To this end, two distantly related plant pathogenic fungi, *Ustilago maydis* and *Sclerotium rolfsii*, were used to identify and characterize genes involved in cellular morphology and sclerotium development, respectively. These fungal systems were chosen because both species undergo dramatic changes in morphology during their life cycles. *U. maydis*, the causal agent of corn smut, requires a dimorphic switch from haploid budding to dikaryotic filamentation for plant infection and subsequent sexual reproduction. *U. maydis* is also a model organism for the study of genetics, fungal mating determinants, fungal dimorphism, signaling pathways and pathogenesis. *S. rolfsii* causes stem rot of peanut and many other crops and produces sclerotia as a means of protection and spread. Prior to this study, little was known about the genetic basis of this process.

In the *U. maydis* model system, the cyclase-associated protein (CAP) homolog was identified and characterized as component of the cAMP/PKA pathway. Deletion of *cap1* resulted in haploid cells growing as short filaments instead of cigar-shaped budding cells. This

phenotype was rescued by the addition of exogenous cAMP to the growth medium, suggesting that Cap1 functions upstream of adenylate cyclase (Uac1) and is a positive regulator of cAMP production. Yeast-two hybrid experiments indicate that Cap1 can interact directly with the C-terminal portion of adenylate cyclase. Prior to this investigation, the only component known to function upstream of Uac1 was the G protein α subunit (Gpa3). The phenotype of $\Delta gpa3$ strains is similar to the $\Delta cap1$ phenotype, and neither strain fully mimics the long filamentous phenotype of *uac1*-mutants. These results support the hypothesis that Gpa3 and Cap1 coordinate cAMP production by Uac1 to affect cellular morphology.

A neuropathy target esterase (NTE) homolog was identified as a potential cAMP binding protein in *U. maydis*. Deletion of *cab1* (cAMP binding) did not affect cellular morphology, and $\Delta cab1$ strains produced normal budding cells with a growth rate similar to wild type in PDB. The mating ability of $\Delta cab1$ strains was not impaired, and compatible $\Delta cab1$ strains were able to infect and cause disease in maize seedlings. $\Delta cab1$ strains do have a significantly reduced growth rate in media enriched with yeast extract, but do not appear to be defective in cAMP signaling. It is unlikely that *cab1* is a component of the cAMP signaling cascade, and future studies will be necessary to identify other possible downstream targets of cAMP signaling to fill the remaining gaps in knowledge of this important signaling pathway.

Although a great deal is known about the physical factors that can stimulate or suppress sclerotium formation and development in *Sclerotium rolfisii*, prior to this report, little was known about the genetic factors involved. To get a broad understanding of the cellular and genetic events involved in sclerotium differentiation in *S. rolfisii*, two cDNA libraries were constructed using Suppressive Subtractive Hybridization PCR (SSH). Of the 54 unique sequences identified as differentially expressed during sclerotium differentiation, 25 had fungal homologs

in the NCBI databases and were assigned similar (putative) functions. Relative expression of 15 genes was measured by real-time PCR analysis. A subset of these genes was also verified by northern blot analysis. Two patterns of differential expression were observed. Some genes were upregulated in all stages of sclerotial development, such as the *S. rolfsii* lectin gene, or downregulated in all stages of development, such as the potassium beta subunit gene. Some genes, however, were differentially expressed between sclerotial stages. For example, three “mycelium-upregulated” genes that encode protein synthesis factors were expressed at high levels during the earliest stage of sclerotial development but were suppressed in mature sclerotia. Additionally, several “sclerotium-upregulated” genes encoding factors related to protein processing are expressed more during the early stages of sclerotial development than at maturation. These results suggest that protein synthesis increases during the earliest stage of sclerotium development but decreases as the sclerotia mature. This research provides a foundation for future studies into the genetic basis and molecular process of sclerotium formation and development in *S. rolfsii*.

APPENDIX

APPENDIX A

GenBank Accession Numbers for Sequences Identified in Chapter 5

EST-Contig number	Clone ID	GenBank Accession Number	Sequence similarity/E value
M1	M1.B07_M9-A11	GR972306	Predicted fungal protein/ e-08
M1	M1.K07_M9-E12	GR972307	Predicted fungal protein/ e-08
M1	M1.J09_M11-G2	GR972308	Predicted fungal protein/ e-08
M1	M1.O03_M11-F3	GR972309	Predicted fungal protein/ e-08
M1	M1.I03_M7-G10	GR972310	Predicted fungal protein/ e-08
M2	M2.J01_M2-H9	GR972311	Cytochrome c oxidase/ e-79
M2	M2.D09_M10-G7	GR972312	Cytochrome c oxidase/ e-79
M2	M2.N09_M10-B9	GR972313	Cytochrome c oxidase/ e-79
M3	M3.H05_M8-B11	GR972314	Calcium binding protein/ e-40
M3	M3.M01_M10-F4	GR972315	Calcium binding protein/ e-40
M3	M3.H03_M5-G11	GR972316	Calcium binding protein/ e-40
M3	M3.K05_M9-H5	GR972317	Calcium binding protein/ e-40
M4	M4.B03_M4-D3	GR972318	Potassium channel subunit/ e-39
M4	M4.B01_M1-E12	GR972319	Potassium channel subunit/ e-39
M4	M4.D03_M5-B11	GR972320	Potassium channel subunit/ e-39
M5	M5.F01_M2-H2	GR972321	S12 ribosomal protein/ e-38
M5	M5.O11_M11-G5	GR972322	S12 ribosomal protein/ e-38
M6	M6.G05_M11-G6	GR972323	<i>U. maydis</i> Cpc2/ e-57
M7	M7.K11_M10-G3	GR972324	Hypothetical protein/ e-41
M8	M8.M05_M10-C10	GR972325	2-hydroxyacid dehydrogenase/ e-15
M9	M9.P01_M4-C6	GR972326	S8 ribosomal protein/ e-40
M10	M10.B09_M10-G10	GR972327	FKBP-type peptidyl-prolyl cis-trans isomerase/ e-33
M11	M11.A05_M2-C1	GR972328	Dipeptidase/ e-11
M12	M12.L03_M6-F5	GR972329	No similarity
M12	M12.K01_M9-G2	GR972330	No similarity
M12	M12.L01_M3-H8	GR972331	No similarity
M12	M12.D07_M9-C3	GR972332	No similarity
M12	M12.F07_M9-E5	GR972333	No similarity
M12	M12.N01_M4-C5	GR972334	No similarity
M13	M13.H01_M2-H5	GR972335	No similarity
M14	M14.E11_M6-C1	GR972336	No similarity
M14	M14.G01_M6-D1	GR972337	No similarity
M15	M15.G09_M6-H10	GR972338	No similarity
M16	M16.C07_M3-G3	GR972339	No similarity
M16	M16.D05_M7-B11	GR972340	No similarity
M17	M17.M11_M11-B1	GR972341	No similarity
M18	M18.E05_M5-H4	GR972342	No similarity
M19	M19.O05_M11-E4	GR972343	No similarity

GenBank Accession Numbers for Sequences Identified in Chapter 5, continued			
EST-Contig number	Clone ID	GenBank Accession Number	Sequence similarity/E value
M19	M19.G03_M6-G1	GR972344	No similarity
M20	M20.E09_M5-H12	GR972345	Hypothetical protein/ e-43
M21	M21.P07_M10-F11	GR972348	No similarity
M21	M21.I05_M8-F1	GR972349	No similarity
M21	M21.J03_M6-E7	GR972350	No similarity
M21	M21.N03_M3-H7	GR972351	No similarity
M21	M21.F05_M7-F4	GR972352	No similarity
M21	M21.O09_M11-D5	GR972353	No similarity
M21	M21.P03_M4-F2	GR972354	No similarity
M21	M21.I07_M8-G2	GR972355	No similarity
M21	M21.A01_M1-D5	GR972356	No similarity
M21	M21.A09_M2-H6	GR972357	No similarity
M21	M21.C03_M3-B1	GR972358	No similarity
M21	M21.K03_M9-B5	GR972359	No similarity
M22	M22.C05_M3-E2	GR972346	No similarity
M23	M23.A11_M2-A7	GR972347	No similarity
S1	S1.B13_S5-B10	GR972360	<i>S. rolfsii</i> lectin/ e = 0
S1	S1.L11_S4-G9	GR972361	<i>S. rolfsii</i> lectin/ e = 0
S1	S1.C23_S3-H5	GR972362	<i>S. rolfsii</i> lectin/ e = 0
S1	S1.I15_S6-A6	GR972363	<i>S. rolfsii</i> lectin/ e = 0
S2	S2.H11_S4-C7	GR972365	Phosphatidylserine decarboxylase/ e-31
S2	S2.A17_S1-G10	GR972366	Phosphatidylserine decarboxylase/ e-31
S2	S2.D23_S11-C7	GR972367	Phosphatidylserine decarboxylase/ e-31
S2	S2.A13_S1-G2	GR972368	Phosphatidylserine decarboxylase/ e-31
S2	S2.B19_S9-C7	GR972369	Phosphatidylserine decarboxylase/ e-31
S3	S3.L21_S11-A5	GR972372	Hypothetical protein/ e-20
S3	S3.E13_S3-C7	GR972373	Hypothetical protein/ e-20
S3	S3.C13_S2-C7	GR972374	Hypothetical protein/ e-20
S4	S4.M19_S8-C7	GR972375	Hypothetical protein/ e-85
S4	S4.F23_S11-D3	GR972376	Hypothetical protein/ e-85
S5	S5.F13_S6-C3	GR972377	Vesicular Transport/ e-25
S6	S6.O17_S8-B9	GR972378	Sporulation protein/ e-50
S7	S7.G21_S6-E1	GR972379	Threonine aldolase/ e-47
S8	S8.P09_S2-E6	GR972380	Hsp70/ e-44
S9	S9.C19_S3-A3	GR972381	Copper amine oxidase/ e-39
S10	S10.B23_S11-B8	GR972382	Aspartic peptidase/ e-36
S11	S11.B21_S10-C6	GR972383	Eukaryotic Initiation Factor/ e-39
S12	S12.O15_S8-A9	GR972384	Predicted protein/ e-28
S13	S13.E15_S9-A3	GR972385	Cytochrome p450/ e-24
S14	S14.F11_S4-B5	GR972386	Glutamine amidotransferase/ e-28
S15	S15.K17_S9-G7	GR972396	Tryptophan synthase/ e-15

GenBank Accession Numbers for Sequences Identified in Chapter 5, continued			
EST-Contig number	Clone ID	GenBank Accession Number	Sequence similarity/E value
S16	S16.N13_S11-G3	GR972387	No similarity
S16	S16.L23_S11-F3	GR972388	No similarity
S17	S17.J23_S11-E5	GR972389	No similarity
S18	S18.J15_S7-G12	GR972390	No similarity
S18	S18.L15_S7-G9	GR972391	No similarity
S19	S19.C15_S2-A10	GR972397	No similarity
S20	S20.A21_S2-A4	GR972392	Hypothetical protein/ e-08
S21	S21.O21_S8-F9	GR972393	Amidase/ e-06
S22	S22.O23_S11-B4	GR972394	No similarity
S23	S23.L09_S1-D5	GR972395	No similarity
S24	S24.D11_S3-G10	GR972364	<i>S. rolfsii</i> lectin, e-18
S25	S25.M13_S9-A2	GR972370	Phosphatidylserine decarboxylase, e-07
S25	S25.M15_S8-B4	GR972371	Phosphatidylserine decarboxylase, e-07